MODELING SEDIMENT DYNAMICS IN THE ZHUJIANG (PEARL RIVER) BASIN, CHINA

BY

WEN XIANYUN

(M.Sc.)

A THESIS SUBMITTED FOR THE DEGREE OF MASTER OF SOCIAL SCIENCE

DEPARTMENT OF GEOGRAPHY

NATIONAL UNIVERSITY OF SINGAPORE

2013

DECLARATION

I hereby declare that the thesis is my original work
and it has been written by me in its entirety.

I have duly acknowledged all the sources of information
which have been used in the thesis.

This thesis has also not been submitted for any degree
in any university previously.

_____

Wen Xianyun
15 July 2013

ACKNOWLEDGEMENT

I am truly grateful to everyone who has helped me along the way but first and foremost among them, I would like to thank my supervisor Professor David Higgitt and co-supervisor Professor Lu Xixi, for their support and advice. Their pursuit of scientific excellence and clarity of thoughts have opened my mind to what excellent scientists are. I would like to express my sincere appreciation to them for their guidance into my current research field, and for always trying their best to provide me the most ideal study and research environment. Without their insights and encouragement, this thesis could not have been possible.

I would also like to take this opportunity to convey my thanks to the faculty members, graduate students and the administrative staff at the Geography department for their generous help during my stay here. Special thanks go to Ms Pauline Lee for her patience and her assistance in student administrative issues; Nick and Xiankun for their advice in data processing and GIS techniques; Swe Hlaing and Lishan for their suggestions on my research. I would also thank A/P Zhang Shurong in the Beijing Normal University for sharing data with me and for her valuable comments.

I would like to thank all my friends in Singapore for accompanying me along this journey. In particular, I would like to give credit to Dr. Huang Dejiang for his encouragement and generosity in offering me accommodation. His wise and timely advice has eased my may through the graduate study. Many thanks to Zhang Beiyu, Lin Jinbin, You Mingliang, Qi Yingjie, Zhu Ruolei, Sun Hongyu, Hu Xiyuan, Zhang Yiwen, with whom I have spent the enjoyable and difficult moments of these two years; Song Lixia, for her warm welcome and assistance when I first came to Singapore and Lisa Zheng for taking care of me like my family. I would also like to say thank you to Guo Jiongcan, Zheng Xianyu, Zhang Mei, Dr. Alvin Lum and Rosalind Sim, and all the other friends for their help. Thanks are extended to my friends and former classmates in China. Especially, I am obliged to Zhang Jingjing, Xu Wenxi, Qi Jiaoying, Zhang Jing, Wen Junya, Wu Huiqing for sharing joys and trials with me.

Finally, special thanks are given to my parents and grandparents, who have offered unconditional love in my life. I could not have finished my study without their support.

Wen Xianyun

1st July, 2013

TABLE OF CONTENTS

SUMMARY

Soil erosion in river basins and sediment delivery by rivers have become a great concern worldwide. The current study aims to investigate the sediment dynamics of the Zhujiang (Pearl River) basin at a basin-wide scale. Spatially distributed soil erosion rates and sediment yields are modeled using global environmental datasets and GIS in the Zhujiang basin with coupled models of erosion and sediment delivery.

Erosion rates were calculated with the Thornes erosion model and Carson and Kirby's surface runoff model. The annual mean surface runoff for the entire basin is 21.21 mm in 1984, 19.35 mm in 1990 and 7.07 mm in 2004. Basin-wide surface runoff in June, July and August are generally higher than in other months in response to the temporal variation in rainfall. Greater surface runoff is generated in the lower reaches, with the highest value in the eastern and southeastern part. Annual mean erosion rates for the entire basin in 1984, 1990 and 2004 are 0.65 mm a^{-1}, 0.75 mm a^{-1} and 0.52 mm a^{-1}, respectively. The erosion rates in each sub-basin ranges from 0.11mm a^{-1} to 1.49 mm a^{-1}. High erosion rates are concentrated in area with steep slope and high precipitation, including the Nanpanjiang and Hongshuihe basin in the upper reaches and the high-gradient mountains and hills in the middle reaches. Lower erosion rates are mostly found in the central area like Liujiang basin. The model estimates a gross erosion of approximately twice as much as the measured sediment load. The monthly erosion rates are negatively correlated with the vegetation cover and positively correlated with the surface runoff. In addition, the erosion rates are found to be associated with the underlying geology.

Sediment delivery ratio (SDR) is modeled using a travel time based model. The overall SDR for the Zhujiang basin is 0.184. High delivery ratios (SDR>0.6) are found in 12.1% of the basin, mostly located in the steep sub-basins. The sediment delivery ratio is lower than 0.2 in 71.0% of the basin area, mostly found in the low-relief, flat-terrain area. The sediment yield in 1984, 1990 and 2004 calculated by coupling sediment delivery ratios and annual erosion rates is 168 t km^{-2} a^{-1}, 201 t km^{-2} a^{-1}, 138 t km^{-2} a^{-1}, respectively. The modeled annual sediment yield exhibits an overall trend of

decreasing downstream along the Zhujiang, suggesting the predominance of slope erosion as compared to channel erosion. Correlation analysis indicates that the modeled sediment yields are influenced by various factors, with topography being a dominant controlling factor, rainfall and vegetation cover being the second-order influences. The sediment loads generated in the upper reaches are higher than those in the lower reaches, suggesting that the basin may be supply-limited rather than transport-limited.

Model evaluation suggests good performance in modeling sub-basin sediment yields in 1984 and 1990 but unsatisfactory for 2004. The bad performance in 2004 is largely due to the limitation in modeling delivery process and disturbance by human activities. Future work on modeling a wider range of processes, obtaining finer resolution and reliable datasets and more field work for calibration and validation is expected to improve model accuracy.

LIST OF TABLES

LIST OF FIGURES

LIST OF ABBREVIATIONS

ARIMA	Autoregressive Integrated Moving Average
ISRIC	International Satellite Land Surface Climatology Project
AVHRR	Advanced Very High Resolution Radiometer
DEM	Digital Elevation Model
FAO	Food and Agriculture Organization
GIMMS	Global Inventory Modeling and Mapping Studies
GIS	Geographic Information System
GLC	Global Land Cover
GLDAS	Global Land Data Assimilation System
HWSD	Harmonized World Soil Database
ISLSCP	International Satellite Land Surface Climatology Project Initiative
ISSCAS	Institute of Soil Science of Chinese Academy of Sciences
IWMI	International Water Management Institute
JAXA	Japan Aerospace Exploration Agency
LE	Land under Erosion
LUCC	Land use and land cover changes
MODIS	MOderate Resolution Imaging Spectroradiometer
MWRC	Ministry of Water Resources of China
NASA	National Aeronautics and Space Administration
NDVI	Normalized Difference Vegetation Index
NOAA	National Oceanic and Atmospheric Administration
PRWRC	Pearl River Water Resources Committee
SCS	South China Sea
SDR	Sediment Delivery Ratio
SOTER	Soils and TERrain Digital Data Base
SRTM	Shuttle Radar Topography Mission
TRMM	Tropical Rainfall Measuring Mission
USDA	U.S. Department of Agriculture
USGS	United States Geological Survey

Chapter 1 Introduction

1.1 Background

1.1.1 Soil erosion in river basins

Soil erosion is a complex natural process that can be strongly affected by human activities. Excessive erosion affects soil productivity by destroying topsoil structure, reducing water storage capacity and infiltration, increasing run-off and washing away organic matter and nutrients needed for plants, such as nitrogen and phosphorous (Oyedele, 1996; Meyer et al, 1985). It has been estimated that 75 billion tons of soil is lost at a global scale annually, affecting 85% of the world's agricultural soils and costing about US$400 billion per year (Eswaran et al., 2001). The erosion is even more severe in mountainous regions due to high relief and extreme weather conditions (Jain et al., 2001; Yang et al., 2003; Marston, 2008). Therefore, soil erosion has been recognized as one of the most critical environmental problems. In addition to the on-site consequences mentioned above, soil erosion has off-site effects. It directly adds to sediment load (Renschle et al., 1999). Milliman and Syvitski (1992) estimated that the modern global sediment flux is at least 100% higher than that of 2000 years ago. Increased sediment transported to rivers has a variety of effects. For example, increased sediment reduces the capacity of rivers and retention ponds, thus enhancing the risk of downstream flooding (Clark, 1985; Boardman et al., 1994; Verstraeten and Poesen, 1999). It may adversely affect water quality by carrying chemical pollutants into rivers. High concentrations of contaminated sediments are harmful to ecosystems and can ultimately impact nutrient supply to coastal area and cause eutrophication (Lancelot et al., 2002; Garnier et al., 2002). Other major off-site consequences include disruption of the ecosystems of water bodies, siltation of water bodies especially reservoirs, damage to turbines and morphological changes in the coastal and nearshore zones (Walling and Webb, 1996; Syvitski, 2003a; Syvitski and Saito, 2007; Yan et al., 2013). Not surprisingly, soil erosion and sediment delivery by rivers have become great concern worldwide. There is an increasing demand for more information about soil erosion process and sediment dynamics for better watershed management.

Rivers play a critical role in transporting eroded sediment from mountains to lowlands and the oceans. In the Anthropocene era, when the influence of mankind on the Earth's environment is at least equal to that of natural factors (Crutzen and Stoermer, 2000; Meybeck, 2001), the hydrological regimes in a catchment are determined by four interrelated sets of factors, including climate, catchment physical characteristics, land use and resource management system (Arnell, 1996). Water discharge and sediment load are influenced by changes in these natural and anthropogenic factors.

Climate plays significant role in the mobilization and relocation of sediments in river basins (Macklin et al., 2006; Piégay et al., 2004). Climate change in terms of temperature and precipitation has been observed in the past decades (Folland et al., 2001). Research shows that climate change can affect water discharge (Nijssen et al., 2001; Zhang et al., 2012), soil erosion rate (Pruski and Nearing, 2002) and sediment flux (Syvitski et al., 2005). Temperature influences sediment flux by controlling the chemical weathering of rocks, freeze-thaw cycles, snow melt and canopy growth ((McCarney-Castle, 2011). For example, Harrison (2000) estimated that an increase of 10℃ in average temperature could raise the rate of erosion by approximately 4.5 times. Syvitski et al. (2003) studied the relationship between temperature and soil erosion based on data from global rivers in different climatic zones. They found that erosion rates in warm and humid regions are basically higher than those in cooler continental climates, with the highest rates of erosion occurring in areas of high altitude and relief. The most direct reason for change in soil erosion rate in response to climate change is the change in the erosive power of rainfall (Nearing, 2001; Pruski and Nearing, 2002a). Precipitation can alter evaporation, soil moisture groundwater availability and the amount of energy available in rainfall to detach and carry sediments, thus influencing the erosion rate and sediment flux (Xu, 2005; Zhang and Nearing, 2005; Maeda et al., 2010). Nearing and Pruski (2004) suggested that erosion and runoff will increase at an even greater rate where rainfall amounts increase: the ratio of erosion increase to annual rainfall increase is on the order of 1.7. Where precipitation decreases occur, the result may be more complex largely due to interactions of plant biomass, runoff and erosion, and either increases or

decreases in overall erosion may be expected (Pruski and Nearing, 2002a). Other researchers argue that no clear relationship exists between precipitation amount and sediment flux (e.g. Walling, 2006). Moreover, rainfall intensity and frequency of storm events causing large floods have been found to cause differences in soil loss and sediment yields (Knox, 1985; Meade et al, 1990). Studies on the 183 rain events in Ohio demonstrated a positive relationship between rainfall intensity and soil loss in Ohio (Fournier, 1972), but the role of intensity is not always obvious, as indicated in other studies (e.g. Morgan et al., 1987).

Catchment-scale studies concerning natural factors show that the effects of a given climate change scenario vary with catchment physical and land-cover properties (IPCC, 2007). Extensive studies have been conducted to explore the impact of catchment characteristics, including elevation, area of the drainage basin, gradient, soil properties, lithology and vegetation cover (e.g. Mohammad and Adam, 2010; Dai and Lu, 2013). Sediment yields are found to be inversely correlated to basin area as larger watersheds have greater capacity to store sediment that would move quickly into the ocean (Milliman and Syvitski, 1992). An opposing view indicated that the main reason for higher sediment yield in small watersheds is the steeper slopes of the basin rather than its size (Harrison, 2000). Many studies show that soil erosion is an integrated result of various physical attributes. For example, Dedkov and Moszherin (1992) indicated that erosion in mountain regions depends on vegetation, relief, tectonic activity and underlying geology.

Although natural erosion occurs slowly, it has been accelerated by human activities dramatically. The history of human modification of Earth's surface spans thousands of years (Ruddiman, 2003). Human activities are estimated to cause 10 times more erosion of continental surfaces than all natural processes combined (University of Michigan, 2004). For sediment yield, Syvitski et al (2005) estimated that at the global scale humans have increased the riverine transport of sediment through soil erosion by 2.3±0.6 billion tons per year but reduced the sediment flux to the coastal ocean by 1.43±0.3 billion tons due to retention in reservoirs. Activities that speed up soil erosion include deforestation, overgrazing, unskilled irrigation, mining and use of chemical fertilizers and pesticides (e.g. García-Ruiz, 2010; Atucha et al., 2012). Among

the activities, land-use change is the most significant one that contributes to soil erosion (Walling, 1999; Walling, 2006). Land use changes have various effects, such as variations in surface roughness, the soil structure and infiltration rate, and the hydraulic connectivity within a catchment (Wei et al., 2009; Fiener et al., 2011). The effects of different vegetation types on runoff generation were investigated using five treatments by Mohammad and Adam (2010) who found that the lowest runoff soil erosion rates were associated with the forest and with natural vegetation dominated by Sarcopoterium spinosum. Deforestation has a direct increasing effect on soil losses. Land cultivation and deforestation create conditions that are favorable for surface runoff and soil erosion, and therefore have a negative impact in terms of increased runoff and soil erosion. Deforestation for cropland is the leading cause for intensive erosion because croplands contribute to soil erosion ten times faster than forests and pastures (Meade, 1982; Meade et al, 1990). Land use change from any type of vegetated land to cultivated land will increase soil erosion rates by an order of magnitude (Walling, 1999). Studies show that transition of other land use/cover types to cropland was the most detrimental to watershed in terms of soil loss while forest acted as the most effective barrier to soil loss (Sharma et al, 2011). Research in the Upper Nam Wa watershed in Nan province of Thailand showed that an absolute majority of the total soil loss (approximately 70%) can be attributable to the shifting cultivation along the steep slopes (Krishna Bahadur, 2009). In fact, through agriculture alone, humans have displaced something on the order of 20,000 Gt of soil through cropland erosion over the history of civilization (University of Michigan, 2004). Poor land management practices accelerate soil erosion, leading to increased sediment inflow into streams (Pimentel and Kounang, 1998). Sediment load is also a function of land use, since the sediment transport capacity is influenced by land cover type (Van Oost et al., 2000).

Many studies on the loess plateau of the Yellow River basin have reported the effects of soil and water conservation practices at the local scale (Li et al., 1992; Zhao et al., 1992). Activities decreasing soil erosion rate include reforestation and improved irrigation schemes. A simulation of erosion response to land-use change in European during the last 50 years showed that de-intensification of land use in marginal agricultural areas have strongly

reduced erosion and sediment export to rivers (Bakker et al., 2008). A similar conclusion has been reached in the Lushi basin in China, where Wang et al. (2012) used a grid-based distributed model to simulate the soil erosion. The modeling results indicate that regional soil erosion rates and sediment transport to rivers are relatively sensitive to land use changes. The average erosion rate increased from 1989 to 1996, in response to the transformation of forest to farmland. Other human activities that strongly alter erosion are sediment extraction (dredging), urban development (Wolman and Schick, 1967) and road construction (Kao and Liu, 1996). The effect of land-use changes within the past 50 years on soil erosion has been well-documented in densely populated area of the world. However, little research has been done in early times due to lack of records. Therefore, population density is sometimes used as a proxy to estimate human impact on the soil erosion (Houghton, 1999; Ramankutty et al, 2006).Regarding the spatial scales of existing studies, the impact of intense land clearance and changing sediment budgets at a regional scale due to accelerated soil erosion has been investigated (Trimble and Crosson, 2000) while a more comprehensive overview of the impact of humans on continental erosion and sedimentation at a global scale has been done by Wilkinson and McElroy (2007). Syvitski's studies (e.g. 2003; 2005; 2007) mainly focus on the temporal variation of sediment flux to global oceans and the influence of humans.

It should be noted that soil erosion and sediment transport is an integrated result from mutual interaction of natural and anthropogenic factors, as shown in Figure 1-1 (Kirkby et al., 2000). Among all the influencing factors, the intensity, duration and frequency of rainfall affect the soil loss amount and the characteristic of precipitation is controlled by the climate, an external factor (Tian et al, 2009). Vegetation cover is a natural factor that can be affected by human activities such as tillage, deforestation and tree planting. One example of combining impacts of both climate change and human activities on soil erosion in river basin is the Yellow River in China, where the pristine erosion rate was about 500 million tons per year in the early and middle Holocene (Zhu, 1990). A natural accelerated soil erosion occurred around 3,000 years BP, when the climate turned cooler and dryer, leading to natural forest degradation. With the rapid population growth, the erosion rate reached a

peak: it is four times greater than the geological norm (He et al., 2006). Over the last decade, implementation of soil and water conservation measures has decreased sediment load in the Yellow River by 25% (Zhang, 1999). The slow-down of soil erosion process is the result of reduced precipitation, soil and water conservation practices and water abstraction for irrigation (He et al., 2006). The contrasting effects of the interrelated factors stated above make it more difficult to gain an explicit understanding of the sediment dynamics in river basins. A slight change in one factor is likely to induce changes in other factors and subsequent feedbacks can be expected.

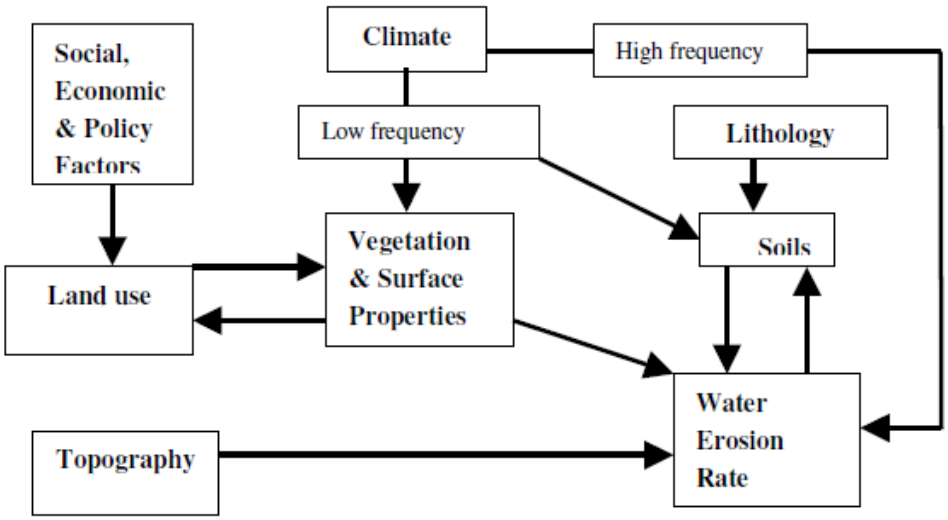

Figure 1.1 Factors influencing water erosion rates (Kirkby et al., 2000)

1.1.2 Modeling soil erosion in river basins: A literature review

Traditional methods to assess soil erosion severity have been focused on quantifying soil erosion from experiments and extrapolation to wider landscape (Evans, 2002). However, the traditional methods have been criticized for limited applicability at a larger spatial scale (Herweg, 1996). Field-based methods to estimate the erosion rate are more suited to small scale drainage basins (e.g. Trimble, 1999; Bartley et al., 2007).The quantification of soil erosion rate at the catchment scale involves the determination of sediment load at the catchment outlet. Ongoing measurements of sediment load at the outlet are limited, covering less than 10% of the Earth's rivers (Syvitski et al., 2005).

Modeling of erosion process in catchments was discussed as early as the 1940s(Foster, 1982) and since then a wide range of soil erosion models in catchments have been published. With the increased computing powers in the last decades, substantial progress has been made in the investigation of catchment erosion using computer models. Integration of Geographical Information Systems (GIS) and Remote sensing techniques have emerged as a useful tool for studying the spatial variation in large basins (e.g. Lu and Higgitt, 1999; Gupta and Chen, 2002; Yazidhi, 2003). Soil erosion is influenced by the spatial heterogeneity in various factors. Estimation of erosion rates and their spatial distribution have been made feasible at large spatial scales by GIS and high solution global environmental datasets are made available, such as the land use data derived from remote sensing images

(Nearing et al., 2000; Ali and De Boer, 2003). GIS and Remote Sensing have been shown to be an effective approach to estimate the magnitude of erosion and spatial distribution of sediment yield (Fernandez et al., 2003). The advantages of linking soil erosion models with GIS include: firstly, the possibility of rapidly producing input data to simulate different scenarios (Sharma et al., 1996), secondly, the ability to use very large catchments with many pixels, so the catchment can be simulated with more detail (De Roo, 1996) and finally, the facility to visualize (Tim, 1996).

Various aspects of the modeling of soil erosion and sediment dynamics have been reviewed in the literature. Zhang et al. (1996) reviews modeling approaches to predict soil erosion in catchments but it is limited to very well-known models only. They concluded that the spatially distributed models can be extended to three-dimensional terrain and incorporate spatial indices and thus are efficient predictors of potential erosion following a variety of disturbances within the catchment. Bryan (2000) performed a review on the water erosion modeling on hillslope and concluded that stochastic modeling might be more effective than physically based modeling in prediction hillslope response to erodibility dynamics. A synthetic review that analyzed specific models was done by Merritt et al. (2003) based on the model input-output, model structures, runoff, water quality modeling and limitations of models. Models vary in terms of complexity, processes included, data requirement for calibration and validation, and hardware requirements. These factors, together with the objectives of model users influence the choice of a model for a specific application (Merritt et al., 2003). According to Wheater et al. (1993), soil erosion models can be categorized as empirical, conceptual and physically-based models, based on different criteria that may encompass process description, scale and model algorithms. Over the last decades, commonly used soil erosion models have been shifting from empirical and conceptual in the 1970s to physically based and conceptual recently. Despite these classifications the distinction between models is not always evident and some models include elements of two or three. A brief review of the three types of soil erosion models will be given. Table 1.1 shows some commonly used empirical, conceptual and physically based models.

Table 1.1 Soil erosion models

Model	Types	Input and Output	Scale	Reference
USLE	Empirical	Input requirement: low Output:erosion	Hillslope	Wischmeier and Smith (1978)
MUSLE	Empirical	Input requirement: low Output:erosion	Hillslope	Kinnel and Risse (1998)
RUSLE	Empirical	Input requirement: low Output:erosion	Hillslope	(Renard et al., 1997)
USPED	Empirical	Input requirement: moderate Output: erosion, deposition	Hillslope/catchment	Mitasova et al. (1996)
Thornes	Conceptual	Input requirement: moderate Output: erosion	Hillslope/catchment	Thornes et al. (1990)
AGNPS	Conceptual	Input requirements: high Output: runoff, peak rate, erosion, sediment yield	small catchments	Young et al. (1987)
HSPF	Conceptual	Input requirement: high Output: runoff, flow rate, sediment load, nutrient concentration	Catchment	Johanson et al. (1980)
LASCAM	Conceptual	Input requirement: high Output: runoff, sediment, salt fluxes	Catchment	Viney and Sivalapan (1999)
SEDD	Conceptual	Input requirement: low Output: erosion, sediment yield	small catchment	Ferro t al. (2002)

Table 1.1 Soil erosion models (continued)

Model	Types	Input and Output	Scale	Reference
SedNet	Conceptual	Input requirement: moderate Output: erosion, sediment yield	Hillslope and catchment	Prosser et al. (2001)
SWAT	Conceptual	Input requirement: high Output: runoff, peak rate, erosion, sediment yield	Catchment	Eckhardt and Ulbrich (2003)
ANSWERS	Physically based	Input requirement: high Output: sediment, nutrients	small catchments	Beasley et al. (1980)
CREAMS	Physically based	Input requirement: high Output: erosion, deposition	plot/field	Knisel (1980)
EROSION2D	Physically based	Input requirement: high Output: runoff, sediment	Catchment	Schmidt (1991)
EUROSM	Physically based	Input requirement: high output: runoff, erosion, sediment	small catchments	Morgan et al, 1998
KINEROS	Physically based	Input requirement: high Output: runoff, erosion, sediment yield	Hillslope/small catchments	Woolhiser et al. (1990)
LISEM	Physically based	Input requirement: high Output: runoff, sediment	Hillslope/Small catchment	De Roo et al. (1996)
MIKE SHE	Physically based	Input requirement: high Output: rainfall, runoff, sediment	Catchment	Andersen et al. (2001)

Table 1.1 Soil erosion models (continued)

Model	Types	Input and Output	Scale	Reference
TOPMODEL	Physically based	Input requirement: high Output: runoff, erosion	catchment	Beven (1997)
TOPOG	Physically based	Input requirement: high Output: water logging, erosion hazard, solute transport	Hillslope	Gutteridge et al. (1991)
WEPP	Physically based	Input requirement: low Output: runoff, sediment characteristics, form of sediment loss	Hillsope/catchment	Laflen et al. (1991)

Empirical models are the simplest of all the three model types. Some models are quite similar because they are based on the same assumptions. The parameters of empirical models have usually been calibrated. The computational and data requirements for empirical models are the lowest of the three model types, and are capable of being supported by coarse measurements (Merritt et al., 2003). Empirical models are generally applied to a restricted area and based on unrealistic assumptions of the physics of the system, ignoring inherent non-linearities in the catchment system (Wheater et al., 1993). The most widely used empirical models are Universal Soil Loss Equation (USLE) (Wischmeier and Smith, 1978). The equation was developed from erosion plot and rainfall simulator experiments to predict the long-term average soil loss in agricultural fields. It provides guidance for soil conservationists to develop catchment management practices for soil erosion control. The equation is given by:

$$E=R\times K\times S\times L\times C\times P \tag{1.1}$$

where E is average annual soil loss (tonnes/acres), R is rainfall erosivity index, K is soil erodibility index, S is slope, L length of the slope, C cropping management factor and P supporting conservation practice factor. The USLE has been updated by a number of researchers. MUSLE (Williams, 1975), its modified version, has been an attempt to compute soil loss for a single storm event. The changes to the USLE incorporated into Revised Universal Soil Loss Equation (RUSLE) (Renard et al., 1997) include a new equation to account for slope length and steepness, new conservation practice values, improved isoerodent maps and time-variant soil erodibility. The greatest limitation of the USLE family of models is the ineffectiveness in applications outside the range of conditions for which they were developed (Nearing et al., 1994).

Estimates of eroded sediments delivered to rivers are essential for water resources management and engineering (Lane et al., 1997). Despite the development of many physically based soil erosion and sediment equations, sediment yield at regional scale are basically estimated by simple empirical models. Sediment yield has been found to relate to basin characteristics, including drainage area, topography, climate, land use/cover change (e.g.

Walling, 1983). Empirical sediment delivery ratio (SDR) equations are often combined with the USLE to estimate the sediment yield. According to Karydas et al. (2009), RUSLE estimates soil loss from a hill slope caused by raindrop impact and overland flow, plus rill erosion. However, it does not estimate gully or stream channel erosion. In addition, the USLE/RUSLE fails to consider the interdependence of controlling factors of soil erosion. However, the conventional linear or non-linear regression approaches can only model the highly sediment flux with limited accuracy because of the simple model structure and mathematical methods.

Conceptual models are based on two criteria: firstly, the structure of the model is specified before modeling work, and secondly, not all of the parameters have a direct physical interpretation (Wheater et al, 1993). In soil erosion studies, conceptual models are based on the representation of the catchment as a series of internal storages. They describe the major processes in the catchment but do not specify the specific details of the process interactions which require more detailed catchment information (Meritt et al, 2003). They are more applicable to answer general questions (Beck, 1987). Compared with empirical models which are usually based on statistics of observed data, conceptual models have more physical information and are more complex in the relationships that define the catchment. Conceptual models play an intermediary role between empirical and physical based models (Beck, 1987). It is a balance between the complexity of the model and available information (Wheater, 2002). These models provide an indication of the qualitative and quantitative processes without requiring large amounts of spatially and temporally distributed input data (Merritt et al., 2003). Commonly used conceptual models include the Sediment Delivery Distributed (SEDD) model, event-based Agricultural Non-Point Source Pollution (AGNPS) model, Large Scale Catchment Model (LASCAM).

Physically based models are based on knowledge of the essential mechanisms controlling soil erosion and takes into account physical characteristics. This type of models describes the dynamics of detachment, transport and deposition and is governed by the law of conservation of mass. Examples of physically based models include AREA Non-Point Source

Watershed Environment Response Simulation Model (ANSWERS) (Beasley et al., 1980), Limburg Soil Erosion Model (LISEM) (De Roo et al, 1996), Chemical Runoff and Erosion from Agricultural Management Systems (CREAMS), Water Erosion Prediction Project (WEPP) (Nearing et al, 1989), EUROpean Soil Erosion Model (EUROSEM) (Morgan et al., 1998), KINematic EROsion Simulation (KINEROS) (Smith, 1991; Woolhiser et al., 1990).These complex approaches have a relatively high requirement for input data. Physically based erosion models provide explanations for spatial variation of such physical characteristics as topography, slope, vegetation, soil and climate parameters as precipitation, temperature and evapotranspiration (Legesse et al., 2003). Although preparation of the data is a hard task, physically based models have been used extensively. Obviously, physically based models have much more detail than the USLE and its derivatives. So Great attempts have been made to develop physically based erosion models (Aksoy and Lenvent Kavvas, 2005).

There are some other types of classification. Firstly, lumped and distributed models. A lumped model uses single values of input parameters without considering the spatial variation of the input and thus produces single outputs. A distributed model uses spatially distributed parameters and provides distributed outputs. Semi-distributed models combine the advantages of the above two. They discretize the catchment to a degree thought to be useful by the modeler using a set of lumped models and thus representing important features of catchment with lower data requirements and lower computational costs than distributed models (Orellana et al., 2008). Secondly, deterministic and stochastic models. The latter have variables which are regarded as random and have distributions and probability while all variables of the former type are free from random variation. Soil erosion models can be classified as continuous simulation models and single event based models regarding time scale and can be classified into those of small catchments ($<100 km^2$), medium-size catchments (100 -1000 km^2) and large catchments (>1000 km^2) regarding spatial scale.

With more and more models being developed, increasing attention has been paid to model performance and accuracy. One misconception is that

model accuracy can be improved with higher complexity. Actually, simpler models can perform equally well as more complex models (e.g. Perrin et al., 2001). According to Beven (1989), over-parameterisation will lead to error accumulation and this problem cannot be circumvented unless additional parameter observations are available. He stated that many parameters in complex models have to be determined through calibration, resulting in non-uniqueness and difficulties with model identifiability. Overall, physically based, complex models try to cover the complexity of the real world while empirical and part of the conceptual models aim to highly simplify it.

1.1.3 Soil erosion and sediment studies in the Zhujiang basin

Soil erosion affects an area of 3.56×10^6 km^2 or 37% of China's land area, equally distributed over water and wind erosion (Ministry of Water Resources of China (MWRC), 2009). The total area of China account for 6.8% of the world's total, yet the annual soil loss is nearly 20%. Over a third of the seven river basins (including the Amur, Hai, Huai, Liao, Zhujiang, Yangtze and Yellow River) is suffering from soil erosion (Yang et al., 2002). Soil erosion has been a serious hindrance in sustainable development of China (Li et al., 2009; Liu and Yan, 2009). A large population is facing the challenge of water and food security as a result (He et al., 2003).

Among the seven great rivers in China, the Zhujiang River is the second largest river in terms of annual water discharge (336 km^3, Pearl River Water Resources Committee (PRWRC), 1991), playing a key role in water supply to large cities in the Zhujiang Delta Region, including Zhuhai, Guangzhou, Hong Kong and Macau. It extends 2,075 km and the drainage basin located in China is 4.42×10^5 km^2, accounting for more than 97% of its total. It is a compound water system comprised of three principal rivers: the Xijiang (West river), Beijiang (North river), and Dongjiang (East river), and some small rivers draining the Zhujiang (Pearl River) Delta (Figure 1.2). The annual sediment load of the whole basin is about 7.70×10^7 t (Shen and Wang, 2004). The Zhujiang basin lies in the subtropical and tropical monsoon zone, with the Tropic of Cancer running through it. The climate and corresponding vegetation have typical characteristics of subtropical monsoon climate zone:

high temperature and intense precipitation. The basin is characterized by various anthropogenic interventions during the last 50 years, including deforestation/reforestation, agricultural activities, in-channel damming for hydropower generation, road and reservoir construction and mining, just as most river basins in China. Therefore, soil erosion and sediment transport are supposed to be intense under such circumstances. Actually, about 14% of the Zhujiang basin has been affected by soil erosion (erosion rate > 0.37 mm a^{-1}) (MWRC, 2004). The soil erosion associated environmental problems include the loss of soil productivity of farmland and increasing sediment delivered to downstream which blocks canals and reduces the capacity and design life of reservoirs. The upper reach of the river is among the most severely eroded region in China. The Karst area is even more vulnerable to soil erosion due to its fragility.

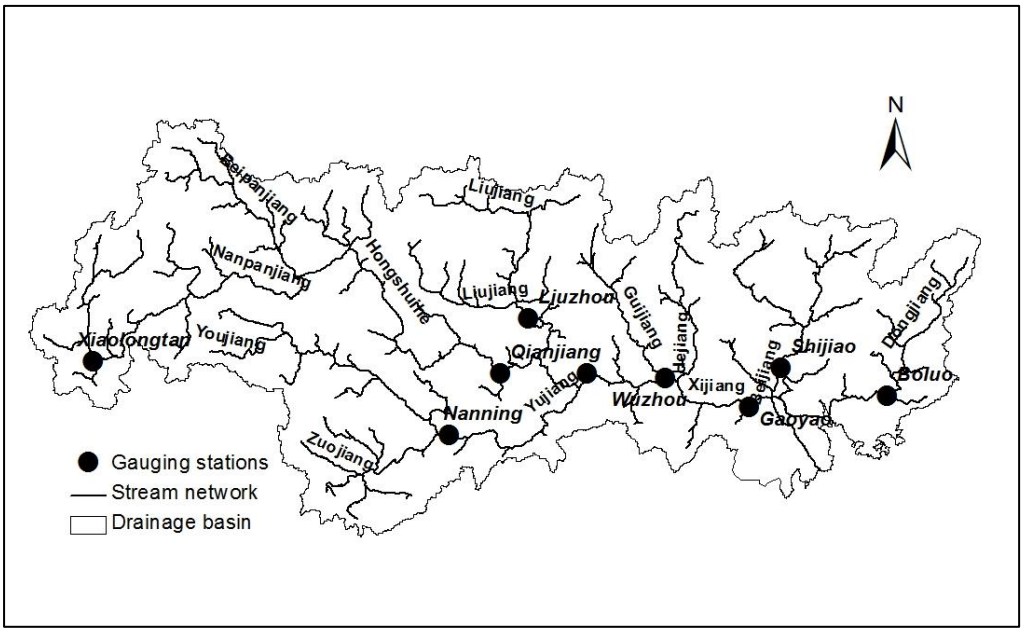

Figure 1.2 The stream network of the Zhujiang River

There have been several studies of river sediment and soil erosion within the large drainage basin of the Zhujiang river. Walling (2006) briefly discussed the sediment load at Gaoyao hydrological station of Xijiang, a tributary of Zhujiang. Dai et al. (2007) studied the variation of sediment discharge of the river basin from 1955 to 2005 based on long time-series data of the water and sediment discharge at the main gauging stations. Beijiang and Dongjiang have been found to show a decreasing trend of sediment discharge while the situation in Xijiang is more complex. They stated that the variation

of precipitation contributed greatly to annual fluctuation of the sediment flux but little to the decreasing trend of sediment into the sea. The influences of soil conservation measures and dam construction have also been analyzed. Zhang et al. (2008) analyzed annual sediment load from the 1950s to 2004 and reached a similar conclusion that dam construction and water discharge induced by climate change were the main cause of the decline in sediment flux. A more detailed and quantitative evaluation of the impacts of the dams was done by Chu et al. (2009) and they found that intensified in-channel sand mining was responsible for 0.8 Gt reduction of sediment in Zhujiang during mid-1990s and 2007. A future decrease in sediment flux into the sea is predicted to result from the construction of new dams. Based on updated data, Zhang et al. (2012) analyzed abrupt changes of the sediment load and water discharge at different scales using a coherency analysis technique. Other studies concerning sediment in the Zhujiang basin are mainly about the biogeochemistry (e.g. Wei and Wang, 2006; Zhang et al., 2007). Although information on sediment load can be used as an indicator of the rate of soil erosion occurring within the catchment (Jain and Kothyari, 2000), direct studies of erosion process have been scarce while most of the above studies focused on the sediment load. With regard to methods used in previous studies, empirical methods, or more specifically, statistical methods have been widely used to investigate the temporal variation of sediment load based on long series data from only nine stations. Conceptual and physically based models have rarely been used. Data from gauging stations, which are usually located at the outlet of each basin, are the summation of the response of its subbasins. Much less is known about the spatial variation and the controlling factors of soil erosion within each sub-basin. In addition, few studies on soil erosion have been done at such a large scale using modeling methods. This research gap points to the need of a modeling approach to gain a better understanding of sediment dynamics of the Zhujiang River at the drainage basin scale. In this study, Thornes erosion model is selected for its simplicity and flexibility of model application on multi-temporal and spatial scales. More importantly, it has moderate data requirements and the data it needs are relatively easy to obtain. Additional advantages include its compatibility with

GIS allowing calculation of erosion rate and sediment yield on a cell by cell basis.

1.2 Aims and objectives

The overall aim of this study is to investigate the sediment dynamic of the Zhujiang (Pearl River) basin at a basin-wide scale. More specifically, this study has three objectives:

- To examine the temporal and spatial variation of overland flow and erosion rate in the catchment;
- To explore the implementation of the Thornes erosion model in the Zhujiang basin and to evaluate its ability to predict erosion rates in a large scale drainage basin.
- To evaluate the suitability of a distributed modeling approach to determine sediment delivery to the stream network and to predict sediment yields by coupling models of soil erosion and sediment delivery.

1.3 Framework of this study

This research consists of five stages. The framework of the overall research methods is shown in Figure 1.2. The first stage is data collection and retrieval, including field data, maps and documents to provide background context on physical characteristics and socio-economic environment of the basin. The second stage involves the establishment of a surface runoff model using GIS and Remote sensing techniques. In the third stage, Thornes erosion model is applied to calculate erosion rate based on surface runoff estimated. The fourth stage focuses on the coupling of the erosion model and Sediment Delivery Ratio (SDR) model to predict sediment yields, and analysis of catchment controls of sediment fluxes. Finally, sediment predictions are evaluated by accuracy statistics using the observed sediment yields and main conclusions will be drawn from the results. Detailed descriptions of methods used for data collection and models are provided in the corresponding chapters.

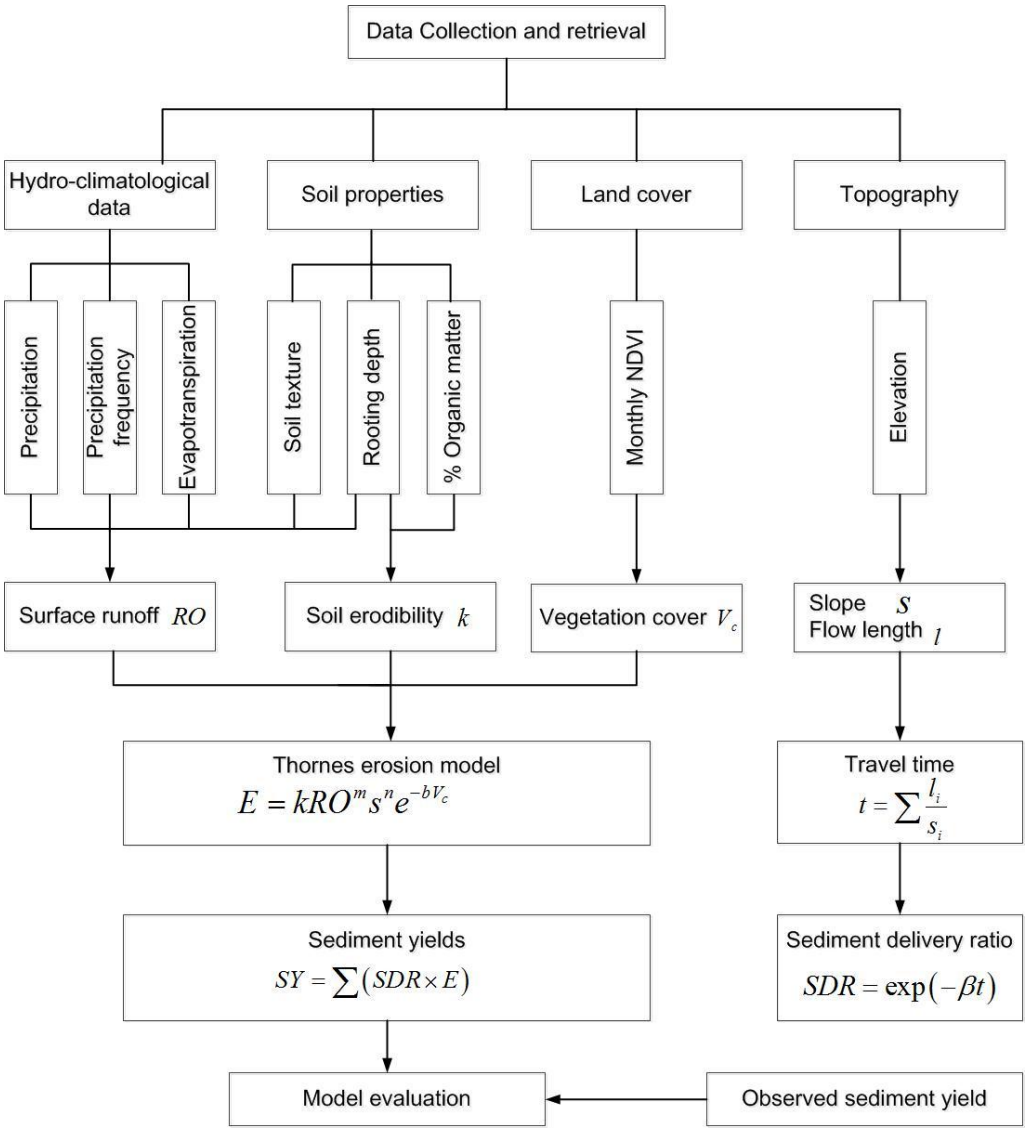

Figure 1.3 Framework of this study (modified from Ali and De Boer, 2010)

1.4 Arrangement and structure of thesis

The structure of this thesis and the main content of each chapter are briefly described below. It should be noted that introductions and literature review about specific topics are presented in the corresponding chapters.

Chapter 1 provides research background, a literature review on erosion models and the objectives of this study;

Chapter 2 involves descriptions of physical and socio-economic characteristics of the study area and the problems in the catchment;

Chapter 3 establishes the surface runoff model. The temporal and spatial variation of precipitation, water discharge and surface runoff are discussed;

Chapter 4 addresses the soil erosion model to estimate erosion rate using GIS and examines the spatial variation of erosion rate with varying climate;

Chapter 5 establishes the SDR model to estimate sediment yields together with the erosion model. The spatial and temporal variation of sediment yields and catchment controls of sediment fluxes are discussed.

Chapter 6 summarizes the main finding of this thesis and provides recommendations for future work based on the limitations of the current study.

Chapter 2 Study area

The Zhujiang (Pearl River) is located between 21.31° - 26.49° N, 102.14° -115.53° E, with a total length of 2,075 km and a drainage area of 4.5×10^5 km^2. It originates on the Yunnan Plateau and drains the Yunan, Guizhou, Guangxi, Guangdong, Hunan and Jiangxi Provinces of China and the northern part of Vietnam before emptying into the South China Sea (SCS). The Zhujiang River is the second largest Chinese river in terms of mean annual water discharge (Pearl River Water Resources Committee (PRWRC), 1991). It is a compound water system comprised of three principal rivers: the Xijiang (West river), Beijiang (North river), and Dongjiang (East river), and some small rivers draining the Zhujiang (Pearl River) Delta. In this study, the whole basin excluding the Zhujiang River Delta is selected as the study area. The location of the Zhujiang basin is shown in Figure 2.1. The physical characteristics, social economic developments and environmental problems of the basin are briefly described in the following sections.

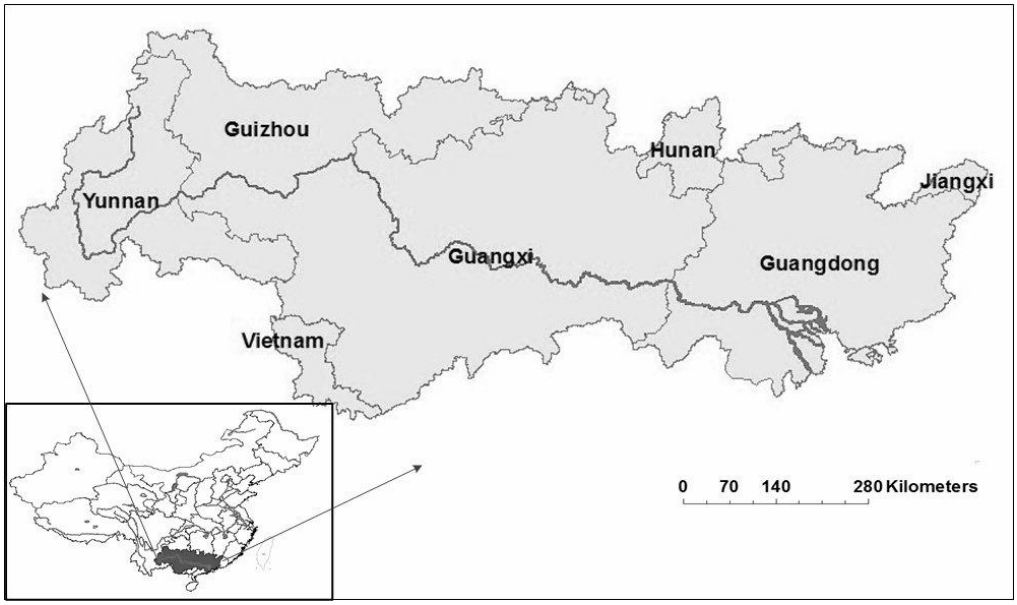

Figure 2.1 Location of the Zhujiang (Pearl River) basin

2.1 Geophysical background

2.1.1 Topography and landforms

The elevation in the Zhujiang basin ranges from 0 m to 2885 m, decreasing from northwest (Yunnan - Guizhou Plateau) to the delta in the

southeast (Figure 2.2). There are three main types of landforms in the basin: mountains (>500 m), hills (80-500 m) and flat. As is shown in Figure 2.3, mountains and hills cover about 94% of the entire basin, while the plains account for only 6%. The western area is characterized by mountains with several peaks above 2500 m. The southwestern area is famous for the well-developed karst landforms in the upper stream (e.g. near Nanning, the capital of the Guangxi Zhuang Autonomous Region). Lower mountain ranges and hills surround the central and southern lowland areas where there are red soil depressions. Along the sea coast lie narrow plains, the largest one being the Chaoshan plain in the lower reaches. Following this topography, the flow directions of rivers are mainly from west and north toward the coast of the South China Sea in the southeast.

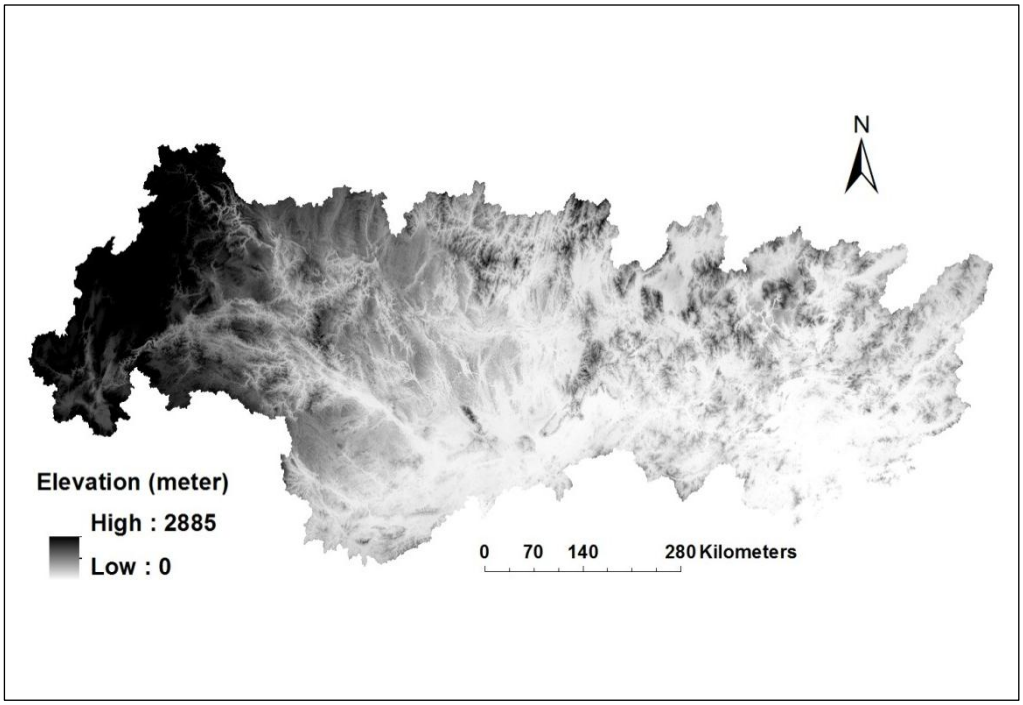

Figure 2.2 Topography of the Zhujiang basin (USGS, 2008)

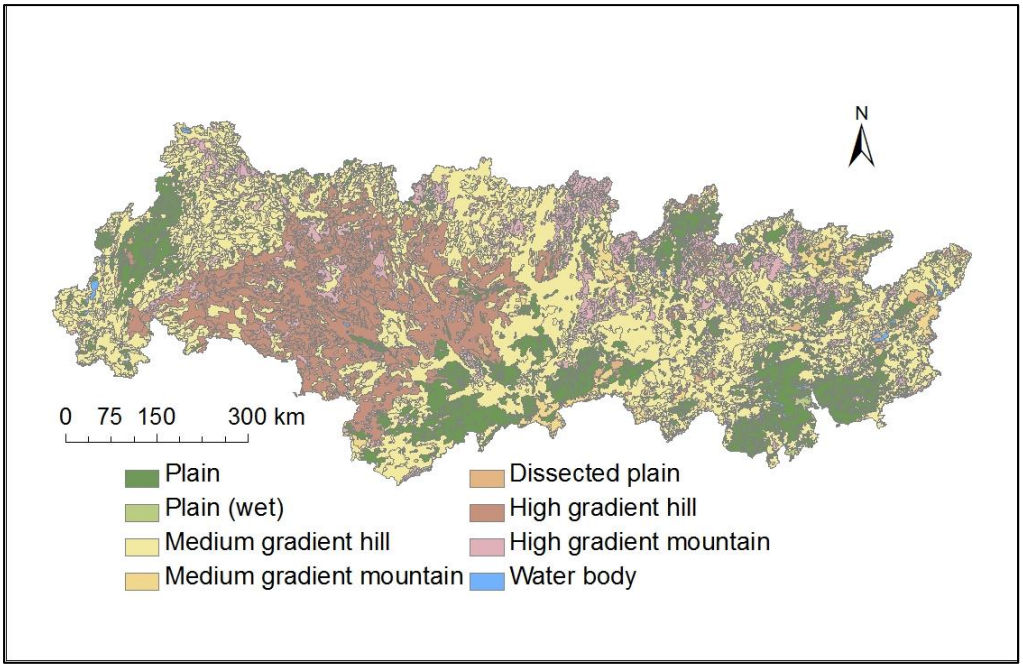

Figure 2.3 Landforms in the Zhujiang basin (FAO, ISRIC and ISSCAS, 2009)

2.1.2 Geology

Geologically, the Zhujiang River basin consists of various source rocks from Precambrian metamorphic rocks to Quaternary fluvial sediments. The lithological units range from the Paleozoic Cambrian to Cenozoic Quaternary alluvial deposits in age. Figure 2.4 is the lithology map from the world Soils and TERrain Digital Data Base (SOTER). Carbonate (including limestones and dolomites) are widely distributed in the Zhujiang basin, accounting for 39% of the total basin area (PRWRC, 1991). Widespread pure and thick Paleozoic carbonate strata provide fundamental conditions for the karst development in the upper reaches. In the headwaters of the Xijiang which is located in the Yunan-Guizhou Plateau (Southeast China), karstification is highly developed, such as in the stone forests in the Guizhou and eastern Yunnan Province. The karst types are very diverse and the karst area is among the largest in the world (Xu and Liu, 2007). The Nanpanjiang River and Beipanjiang River are the upper reaches of the Xijang. The karst area in these two basins accounts for about 60% of their total drainage area. The strata exposed here are mainly pre-Jurassic in age. It also includes large areas of Permian and Triassic carbonate rocks and coal bearing formations. The upper reaches of the Xijiang are distributed detrital sedimentary rocks (including

shales, sandstones and siltstones) and magmatic rocks (basic and ultrabasic rocks) (Zhang et al., 2007). The middle and lower basin mostly consists of Precambrian igneous rocks and metamorphic rocks. The igneous rocks accounted for about 25% of the entire basin, most of which are granites with acid to intermediate composition. Metamorphic rocks are mainly schist, slate and phyllite, accounting for 9.1% of the basin. Sedimentary rocks cover about 31.15% of the basin. Jurassic detrital sedimentary rocks (shales and red sandstones) are distributed in the middle basin area. Quaternary fluvial sediments are mostly developed in the lower alluvial plain, the delta plain and the interior river valley plain, accounting for 8.3% of the basin. The Dongjiang is composed of granite, sandstone and fluvial sediments. The dominant lithology of the upper and middle reach of Beijiang basin is granite, shales and clastic rocks. Minor evaporites are mainly scattered in the upper reaches of the Zhujiang. Pyrites can be found concomitant with high sulfur content coal in Yunnan and Guizhou Provinces (Zhang et al, 2007).

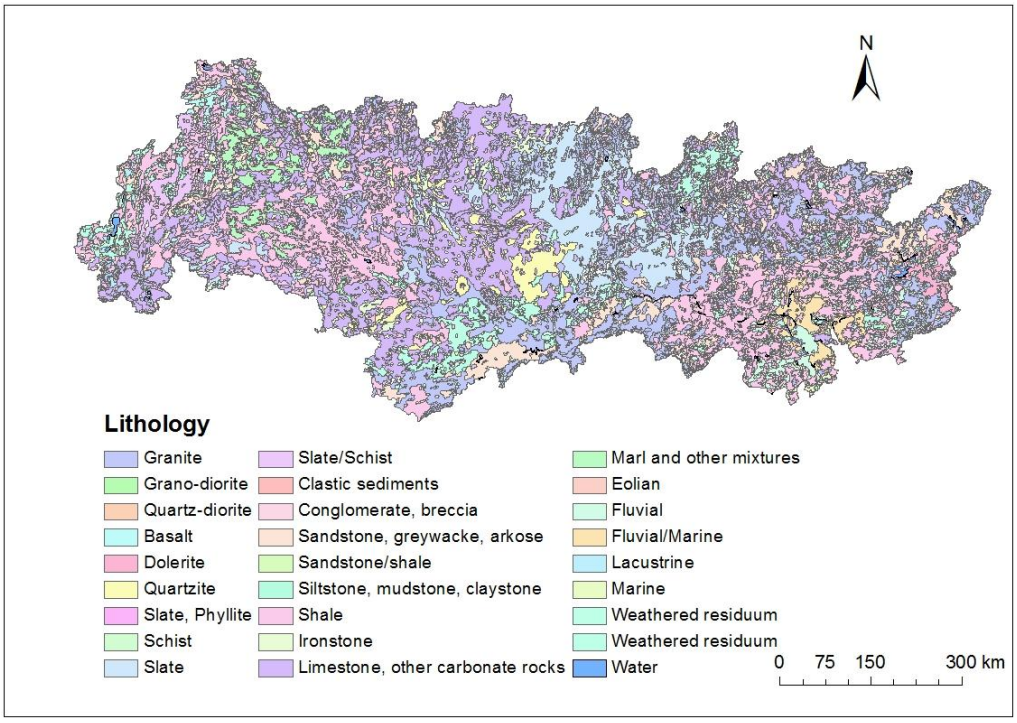

Figure 2.4 Geological map of Zhujiang basin (FAO, ISRIC and ISSCAS, 2009)

2.1.3 Climate

The Zhujiang River basin is located in the sub-tropical monsoon zone, with the Tropic of Cancer going through it. As Figure 2.5 shows, the annual mean temperature of Zhujiang ranges from 13℃in the western and north-western elevated parts of the basin to 24℃ in the coastal lowlands in the south and southeast (Fischer et al., 2011). The highest and lowest monthly mean temperature is 13℃ in July and 28.5℃ in January respectively (Figure 2.5).

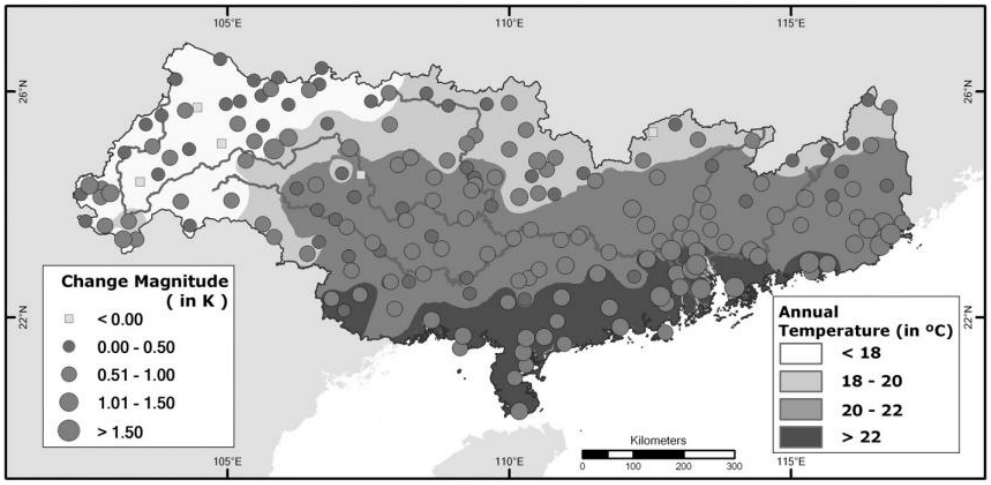

Figure 2.5 Annual mean temperature in the Zhujiang basin, 1961-2007 (Fischer et al., 2011)

The mean annual precipitation from 1961 to 2007 is above 2000 mm along the south-eastern coastline and below 1000 mm in the mountainous western parts of the basin (Figure 2.6) (Gemmer et al., 2010). The precipitation decreases from southwest to northeast with minimum value in the karst region in the west of the basin. The lowest annual precipitation is 720 mm in Xijang and the highest is 2574 mm in Beijiang (MWRC, 2004). Generally, precipitation is higher in the mountainous area and lower in the lowlands. The seasonal variation is considerable within a year. Precipitation mainly falls during the summer. The winter season is comparatively dry, with around 50 mm of rain per month; compared to around 200 mm in summer months (Fischer et al., 2011). Strongly influenced by East Asian monsoon, the study area has approximately 80% of annual precipitation occurring between April and October (Gemmer et al., 2010).

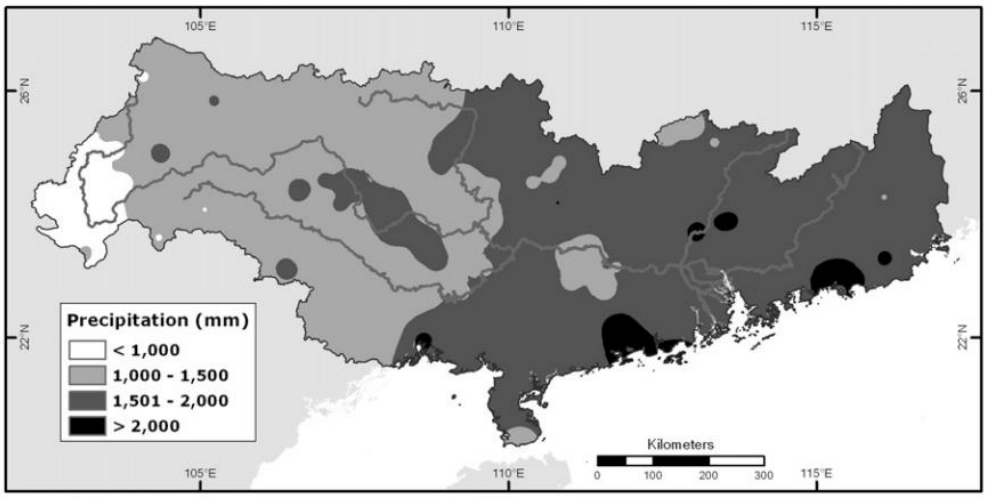

Figure 2.6 Annual mean precipitation in the Zhujiang basin, 1961-2007 (Gemmer et al., 2010)

2.1.4 Soil

There are a total of 12 soil types (which can be further classified into 35 soil units) in the Zhujiang basin based on the classification standards of Food and Agricultural Organization (FAO, 1998) (Figure 2.7). Major types are Acrisols (35%), Anthrosols (25%) and Alisols (11%). Acrisols are characterized by subsurface accumulation of low activity clays and low base saturation. Specifically, Acrisols in the study area consist of red soils and yellow soils which are rich in iron hydroxides. They are widely distributed in the basin, mainly in the area with limited human modification, such as mountains, hills and barren land. Latosols (Alisols) lie in the northern and northwestern part of the basin, where the elevation and gradient are relatively high. Another type that dominates the upper reaches of the basin is weakly to moderately developed Cambisols which accounts for 8.82%. Anthrosols, as its name indicate, are soils in which human activities have resulted in profound modification of soil properties. Most of the paddy soils (Anthrosols) are distributed in the hills, valleys and plains at the lower reaches of the Zhujiang and the delta, with small coverage in the Beipanjiang and Nanpanjiang basin. Regosols (3.13%) (mainly purple soils) are highly susceptible to soil erosion and are concentrated in the Sichuan Depression.

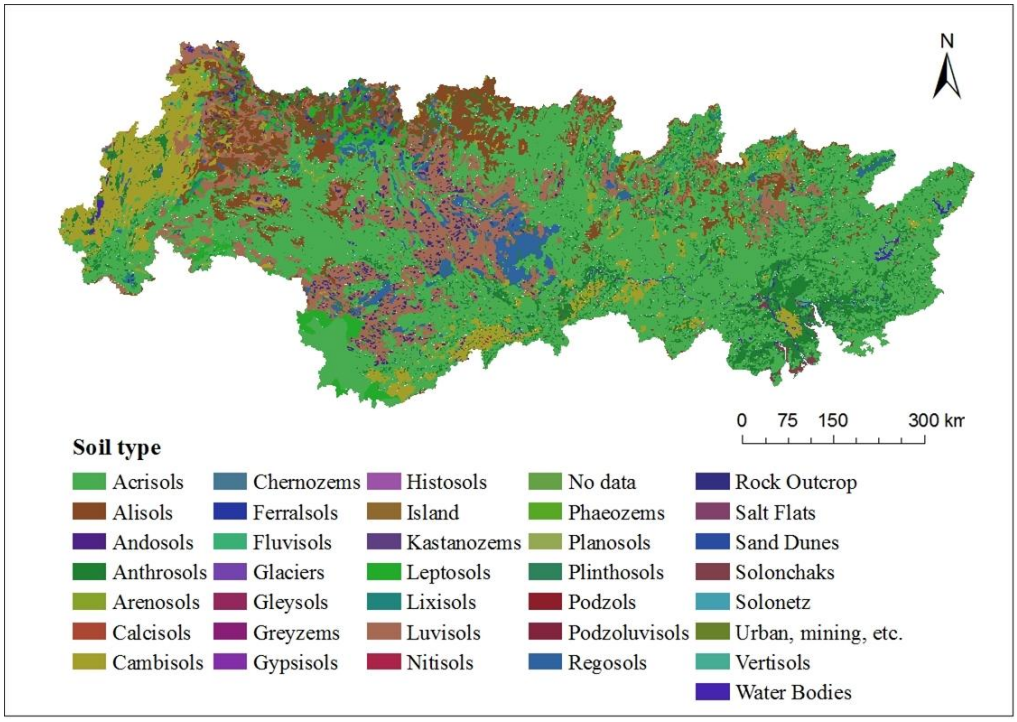

Figure 2.7 Soil units in the Zhujiang basin (FAO, ISRIC and ISSCAS, 2009)

2.1.5 Land cover

The typical vegetation in the study area is tropical to subtropical forest due to its geographical location. Currently, cropland and natural vegetation are the dominant land cover type in the catchment, occupying 41 % and 39 % of the basin, respectively (Figure 2.8). Natural vegetation is predominantly evergreen rainforest, broadleaved forest and shrubland.

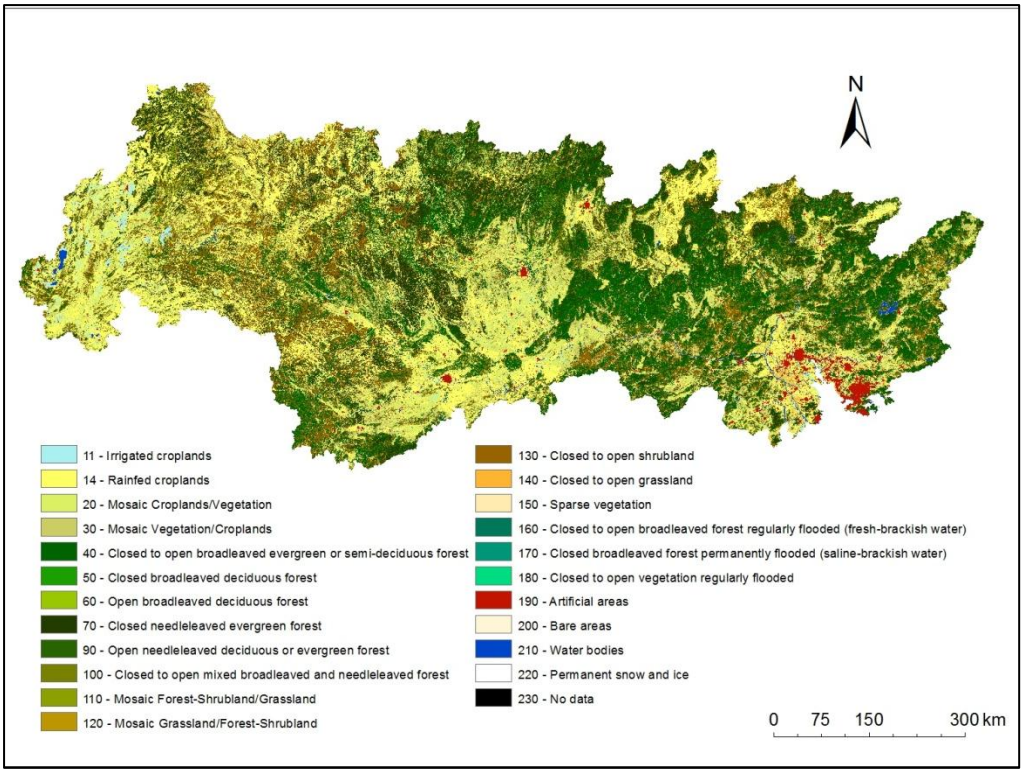

Figure 2.8 Land cover map of the Zhujiang basin, 2009 ((FAO, ISRIC and ISSCAS, 2009; UCLouvain team and ESA team, 2010)

Vegetation cover (in percentage) varies between different areas, generally with higher vegetation cover in the lower reaches. The upper reaches of the Nanpanjiang and Beipanjiang are covered by mid-subtropical evergreen oak forest and pine forest. Cork oaks have developed as secondary forests after deforestation (Wei, 2003). Crops grown in this area include rice and wheat. The lower reaches of the Nanpanjiang and Beipanjiang and hilly area in the Hongshuihe basin are covered by tropical and subtropical vegetation. The former is distributed in area with an elevation lower than 800m, where the tropical rainforests have been removed and replaced by grassland. The subtropical plants are mostly deciduous oak forest, pine-oak mixed forest, shrub and grass. At the middle reaches of Xijiang, the Guangxi basin is covered by two types of vegetation: subtropical broadleaved evergreen forest and northern tropical evergreen forest. Paddies, corn and sweet potatoes are grown in the middle reaches. The natural vegetation at the lower reaches of the Xijiang, Beijiang and Dongjiang are largely subtropical broadleaved evergreen forest and subtropical rainforest, needleleave forest being the secondary vegetation (Wei, 2003). A major part of the land in the Zhujiang River Delta is

for urban use.

The most serious deforestation occurred in the Great Leap Forward Movement (1958-1960) and Cultural Revolution period (1966-1976). The forest coverage in Guangdong Province, for example, decreased from 38% to 27% during this period (Xia, 1999). The soil and water conservation practices started in 1983, since when the vegetation cover began to rise. The rural settlement, the need for more agricultural and urban land has significantly changed the land use/cover in the basin. For example, the Xijiang drainage basin, especially at the lower stream, is highly populated, cultivated and industrialized and has been drastically affected by anthropogenic activities. As a result, in recent years the forests have been replaced by grassland and cropland (Wei et al., 2010).

2.1.6 River system

The Zhujiang River is a compound water system with a drainage area of 4.54×10^6 km^2, 97.4% of which belongs to China and the rest to Vietnam. There are three main rivers: the Xijiang (West River), Beijiang (North River) and Dongjiang (East River) as well as some small rivers draining the Zhujiang Delta (Figure 1.2). The Xijiang River is the largest and drains the western and central parts of the basin while Dongjiang and Beijiang drain the eastern part.

The Xijiang River originates from the Maxiong Mountain in Yunnan Province in southwest China, and flows 2,214 km southeastward to enter the South China Sea through the Pearl River Delta in Guangdong Province. The main channel of the Xijiang is composed of different sections: Nanpanjiang, Hongshuihe, Qianjiang, Xunjiang and Xijiang (in a downstream direction).There are five principal tributaries of Xijiang, namely, Beipanjiang, Liujiang, Yujiang, Guijiang and Hejiang. The Beijiang River is the second largest river system in the Zhujiang basin, originating in the Damao Mountain in the Jiangxi Province. The total length is 520 km. Main tributaries include the Wushui, Lianjiang and Suijiang River. The Donjiang River originates from the Yahuanbo Mountain in the Jiangxi Province and has a length of 562 km. Principal tributaries are the Xinfeng and Xizhi River. Hydrological data of annual discharge and sediment load are provided by nine stations (Figure 1.2).

Table 2.1 shows the general information about the main rivers and tributaries, and about the stations. Out of the total water discharge of Zhujiang (336 km^3), 238 km^3 is from the Xijiang, 39.4 km^3 from the Beijiang, 23.8 km^3 from the Dongjiang, and 34.8 km^3 from the delta region (Pearl River Water Resources Committee (PRWRC), 1991). The annual sediment load is 7.5×10^7 t/a. The seasonal runoff is unevenly distributed, with 80% of the annual runoff between April and September (the flood season) and more than 50% between July and September (Zhang et al., 2007).

Table 2.1 General information of rivers and stations in the study area (Zhang et al., 2009)

River system	River	Station	Drainage area (10^3km^2)	Discharge (10^9m3/a)	Sediment load (10^6t/a)
Xijiang's main channel	Nanpan-jiang	Xiaolongtan	15.4	3.8	4.9
	Hong-shuihe	Qianjiang	128.9	66.6	42.2
	Xunjiang	Dahuangjiangkou	288.5	171.3	57.8
	Xijiang	Wuzhou	327	204.0	63.3
	Xijiang	Gaoyao	351.5	219.9	67.5
Xijiang's tributary	Liujiang	Liuzhou	45.4	39.9	5.1
	Yujiang	Nanning	72.7	37.1	9.2
Beijiang	Beijiang	Shijiao	38.4	41.7	5.4
Dongjiang	Dong-jiang	Boluo	25.3	23.0	2.4
The Zhujiang[a]			415.2[a]	285.2[a]	75.0[a]

Note: The Zhujiang is the sum of the Xijiang at Gaoyao, Beijiang at Shijiao and Dongjiang at Boluo, excluding the delta region.

2.2 Social and economic developments

The Zhujiang River basin flows through six provinces and the two autonomous regions of Hong Kong and Macao. It has been among the most rapidly developing and economically prosperous regions in China since the adoption of the reform and opening-up policy in the late 1970s. Many foreign firms are attracted to locate their factories as village-township enterprises. Those labor-intensive industries have transformed the spatial economy of the delta, bringing fundamental changes in land use and cover patterns (Weng, 2002). The total population in the Zhujiang basin (excluding Hong Kong and Macao) increased from 244 million in 1979 to 315 million in 2011 (National Bureau of Statistics of China, 2001; 2011). Rural population accounts for 44% and urban 56%. The population is unevenly distributed, with 22.6% in the

Zhujiang River Delta where Special Economic Zones and the Economic Open Zone have been established. The Zhujiang Delta is the third biggest river delta in China, consisting of three sub-deltas formed by sediments from Xijiang, Beijiang and Dongjiang. Under the influence of the economic development and population growth over the past decades, the delta has become more and more vulnerable to natural hazards such as flood and storm surges (Chen et al., 2010).

The Zhujiang basin has many natural resources such as coal and manganese ore. Agriculture holds a significant role in the economic development in the basin. The main agricultural products include rice, wheats, peanuts and soybean. The secondary sector of industry has been highly developed in the basin, including manufacturing and construction. Water resources in the basin are about 4700 m^3 per capita, 1.7 times as much as that of China. Water resources have been highly developed and heavily committed for a variety of uses such as water supply, hydropower, navigation, irrigation and suppression of seawater invasion (Chen et al., 2011). Ever since the 1950s, many water conservancy projects, such as diversion ditches, reservoirs and ponds have been built in the catchment to meet the increasing irrigation demand. Approximately 14,000 reservoirs with a total storage capacity of 706 km^3 have been constructed (PRWRC, n.d.). Nearly 8000 hydropower stations have been built or are under construction since the first one in 1970s, with a generating capacity of 46450 MW (PRWRC, n.d.). The Longtan hydropower station, China's third-largest, started operation in the upper reaches of the Hongshuihe River in 2008.

2.3 Problem statement in the study area

Due to significant inter-annual variability, the annual precipitation in wet years is 6-7 times as the amount in dry years (Liu and Chen, 2007). The water discharge, as a result, has significant temporal variability. Floods and droughts have been frequently reported in the Xijiang basin and lower reaches of the Beijiang and Dongjiang, causing large economic loss. Although the sediment concentration of the Zhujiang is relatively low compared to other great rivers of China, the annual sediment load is considerable given the large discharge

(336 km^3/a). Sediment dynamics has become a great concern for researchers and policy makers.

Soil erosion is a major environmental problem in the Zhujiang river basin. The consequences include the loss of soil productivity of farmland and increasing sediment delivered to downstream which block canals and reduces the capacity and design life of reservoirs. Mechanical erosion is severe due to both precipitous relief and high population, which lead to a high ratio of cultivated land. Soil erosion is relatively serious in the Xijiang River. The situation of the Dongjiang River basin is much better, but in the middle and lower reaches, the erosion has increased dramatically because of human activity. The Beijiang River basin has suffered slight erosion only (Wei and Wang, 2006).

The national soil erosion survey in 2000 based on remote-sensing images show that 14.2% of the Zhujiang basin has been under erosion (MWRC, 2004). The MWRC organized field survey teams for each province to set up image interpretation indicators for Landsat TM 5 images and to calibrate the images. Based on the TM images, the national database of land use, DEM, data of soil type, geology, sediment monitoring, soil erosion coverage was set up by inter-human-computer image interpretation and integrated analysis by ArcGIS. Digital erosion map was merged to obtain provincial coverage (Feng et al., 2002; MWRC, 2004). The upper reach of the river is among the most severely eroded regions in China. Actually, sediment concentration in certain section of the river is almost as high as that of the Yellow river and that section is named as “Little Huanghe” by local residents. The population growth in the Zhujiang basin started in 1950s. An increasing need for food and wood induced by population growth enhanced deforestation. The most intense deforestation and slope reclamation activities took place in late 1950s to the 1970s. The area of land under erosion expanded quickly in the basin (Table 2.2). Since the 1980s, particularly during 1986-1995, soil and water conservation projects have been implemented in the basin for better ecological environment. The area of land under erosion decreased in Guangdong Province and Guangxi Autonomous Region by 23% in total and remained stable after 1995. Soil erosion is a result of both physical and anthropogenic

factors. Physical characteristics in the study area, such as high precipitation and gradient, provide favorable conditions for soil erosion. Besides, soil erosion is accelerated by human activity, such as deforestation, slope farming and mining. Although the total area of land under erosion shows a decreasing trend, the increase of human induced soil erosion still exist (PRWRC, 2004).

Table 2.2 Changes of area of land under erosion in the Zhujiang River basin (unit: km^2) (MWRC, 2004)

	1950s and 1960s	1980s	1990s	1995	2004
Guangxi	12,000	30,600	28,100		
Guangdong	7,444	17,070	8,650		
the Zhujiang River basin				62,700	62,730

Figure 2.9 shows a time series of precipitation, water discharge and sediment load in the basin. The data is from the Ministry of Water Resources, China (MWRC). A change point for water discharge and sediment load has been detected using the two-phase linear regression scheme (Zhang et al., 2012). Abrupt changes of water discharge and sediment load are identified around 1989. There are also differences in the abrupt behavior of water discharge and sediment load variations for different regions. Although the temporal changes of sediment load have been studied from long-term historical data, the temporal and spatial variation of erosion rate and sediment load at basin scale are still unclear.

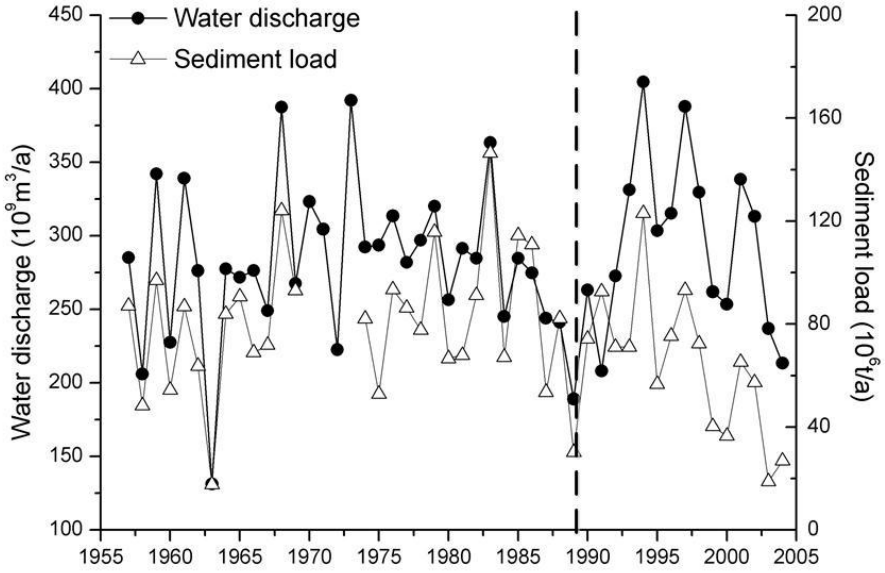

Figure 2.9 Time series of annual water discharge and sediment load in the Zhujiang basin (1957-2004) (Source: Ministry of Water Resources, China (MWRC))

Chapter 3 Hydrological modeling of the basin

3.1 Introduction

Soil erosion by water can be defined as the detachment of soil from land and the transport of vulnerable soil by running waters. When raindrops hit bare soil and their kinetic energy is able to detach and move a soil particle, erosion by rainfall is induced. This process is commonly referred to as rainsplash or raindrop splash (Thornes, 1985). As the rain continues, water will infiltrate into the soil at a rate controlled by the intensity of water arriving at the surface and the soil's infiltration capacity. If rain arrives too quickly or if the soil has already been fully saturated, surface runoff or overland flow will occur whenever excess water cannot be absorbed by the soil or trapped on the surface (McManus, n.d.). The infiltration excess overland flow is referred to as Hortonian overland flow and the saturation excess overland flow is referred to as Hewlett overland flow (Figure 3.1) (Musy, 2001). It is now accepted that and the former more commonly occurs in arid and semi-arid regions while the latter is the dominant overland flow mechanism in humid areas (Davie, 2002). Soil erosion is found to be strongly related to this surface runoff generation process which is caused by rain falling on the land (Govers et al., 2000; Le Bissonnais et al., 2005). The erosion by means of runoff in rills and gullies is the dominant form of soil erosion by water in many parts of the world. Therefore a good knowledge of surface runoff is required for soil erosion modeling. Studies show that the occurrence and quantity of runoff are dependent on the characteristics of the particular rainfall event, i.e. intensity, duration and distribution as well as the characteristics of the particular land (Critchley and Siegert, 1991). The infiltration capacity of a certain type of soil depends on its texture and structure as well as on the initial soil moisture content. The initial capacity of a dry soil is high but it decreases with rain falling until it reaches a steady value referred to as the final infiltration rate (Critchley and Siegert, 1991). The infiltration process is also influenced by vegetation because rainfall is partly intercepted by the leaves and branches of plants. The relationship between rainfall and runoff can be quite complex, as the generation of runoff is highly non-linear, time varying and spatially

distributed.

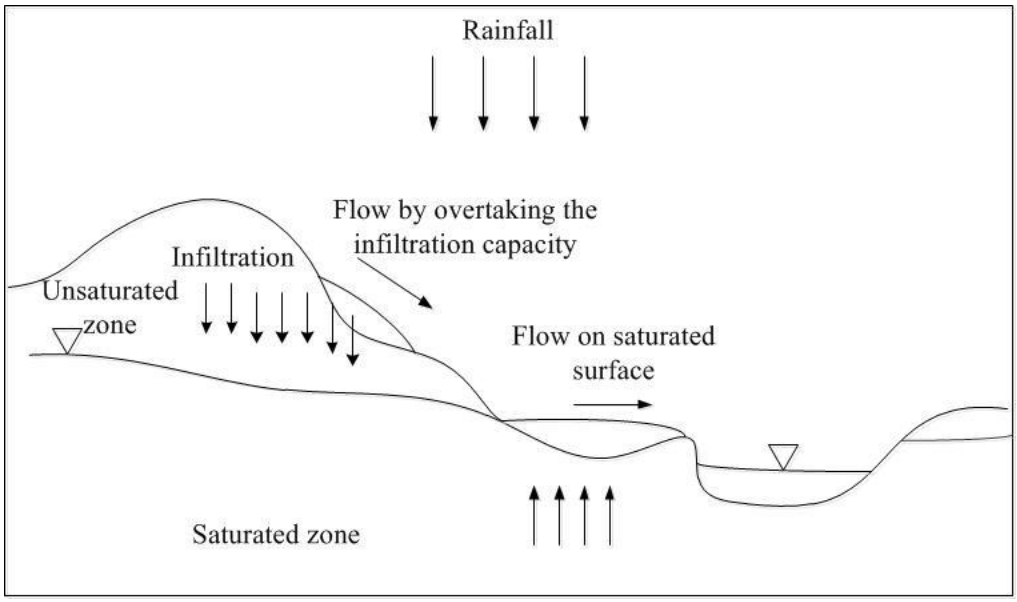

Figure 3.1 Flow processes generated through exceeding the infiltration capacity and through flows on saturated surfaces (adapted from Musy, 2001)

Due to the complex interaction among precipitation, evapotranspiration, infiltration and overland flow, numerous hydrological models have been developed to describe the rainfall-runoff process in various scenarios. Each model uses specific parameters as inputs for runoff estimation. But most of the models are variants of previous ones, with minor adaptations for particular regions or catchments (Chiew, 2010). According to Abbott and Refsgaard (1996), these models can be classified into stochastic and deterministic, the latter of which can be further classified into empirical models, lumped conceptual models and distributed physically based models. Empirical models attempt to use equations to relate rainfall to runoff. Examples include ARIMA (Autoregressive Integrated Moving Average), regression method, artificial neural networks, etc. The most popular empirical model to estimate runoff is Soil Conservation Service-Curve Number methods (SCS-CN) developed by the US Department of Agriculture for use in rural areas. The model structure is simple and has relatively low requirement for data. Lumped models consider the entire catchment as a single hydrologic element with lumped parameters representing average values over the catchment (Chin, 2000). The equations are semi-empirical but still with a physical basis. Examples of lumped conceptual rainfall-runoff models include IHACRES (Croke et al., 2006),

SIMHYD (Chiew et al, 2002) and AWBM (Boughton, 2004). The distributed physically based models involve the concept of water balance and divide the process of precipitation and runoff generation into different components. These models consider runoff process at scales smaller than the catchment size (UNESCO-IHE Institute for Water Education, n.d). This type of models, such as HSPF (Bicknell et al., 1996) and SHE (Abbott et al., 1986), require fine resolution hydro-climate input data and extensive field measurement of soil, vegetation and some other catchment properties (Chiew, 2010).

Considering that the Zhujiang basin is characterized by subtropical and tropical monsoon climate, the most widely used SCS-CN model, which is commonly considered as a Hortonian model and applies to semi-arid and arid regions, will not be used in this study. Additionally, the large area of the Zhujiang basin makes it necessary to derive distributed information about rainfall, soil and vegetation within different segments of the catchment (Abbot et al., 1986). Therefore, lumped models are not applicable to the study area. Another factor to consider in model selection is data availability. The hydrological data from the Zhujiang River basin are scarce apart from some long-term discharge records for the main channel and some of its major tributaries. There are nine major hydrological stations in this large basin, whose general information is provided in Section 2.1.6. In ungauged or poorly gauged areas, the dependence on field measurement for parameter calibration restricts the application of many models. Physically based models can hardly be applied. Previous studies on the hydrology of the Zhujiang are mostly based on statistical analysis of long-term water discharge. The data used for statistical analysis are mostly yearly data while knowledge about the seasonal variations remains limited. Additionally, runoff modeling has rarely been conducted to study the spatial variation of surface runoff at the basin scale. Regarding all these issues stated above and the data availability, this study uses Carson and Kirby's model (1972), an empirical distributed model, to estimate surface runoff within the basin. The requirement for data is low. Key variables include information on the basin's climate, such as precipitation and evapotranspiration, and soil properties.

Recent developments in Geographic Information System (GIS)

techniques enable the description of the heterogeneities in model variables. GIS-based distributed modeling can be used to create a more faithful representation of spatial characteristics of a basin (Vieux, 2003). In this study, an attempt is made to model the spatial and temporal variation of soil erosion and sediment delivery. As a demonstration, three specific years are selected based on the availability of all input data for the model and sediment data. Furthermore, because of the existence of a change point (see section 2.3), years before and after 1989 are selected. The year of 1984 and 1990 were chosen because the observation in these two years is close to long-term average. According the MWRC, more recently the sediment load has been reported to decrease significantly. Therefore year 2004 was selected to represent the latest time and to explore the reasons for such a change.

3.2 Data sources and methods

3.2.1 The Carson and Kirkby model

Carson and Kirkby (1972) developed a simplified model to estimate the surface runoff. This model assumes that under given conditions of soil and vegetation, the surface runoff occurs when the total rainfall exceeds a critical value (r_c) which represents the soil water storage capacity. And it is assumed that the daily rainfall amounts approximate an exponential frequency distribution within each month in a year from the long term point of view. Then the surface runoff is given by an empirical equation (Equation 3.1) using monthly precipitation (mm), mean rainfall amount per rainy day and soil water storage capacity.

$$OF_i = P_i \cdot e^{(-r_c/P_0)} \tag{3.1}$$

where i is the time period (from 1 to 12 for months), OF_i is the surface runoff (mm), P_i is the total monthly precipitation (mm), r_c is the potential water storage capacity (mm) and P_0 is the mean precipitation amount for each rainy day (mm). P_0 is calculated using the following equation:

$$P_0 = P_i / D_i \tag{3.2}$$

where D_i is the number of rainy days per month. The water storage capacity is

influenced by soil texture, structure and vegetation. r_c is estimated to be 10 mm for bare ground, 40 mm for a good grass cover 100 mm for an oak tree (Carson and Kirkby, 1972). To calculate the water storage capacity, an equation by Withers and Vipond (1974) is used. They assume that r_c is a function of bulk density, soil moisture content at field capacity, effective hydrological depth (EHD) and ratio of actual to potential evapotranspiration :

$$r_c = 1000 \cdot MS \cdot BD \cdot EHD \cdot (AET/PET) \qquad (3.3)$$

where MS is soil moisture content at field capacity (w/w), BD is bulk density of the topsoil (g/cm^3), EHD is effective hydrological depth or A-horizon depth (m) which depends on vegetation crop cover, presence or absence of surface crust, and presence of impermeable layer within 0.15 m of the surface. AET is the actual evapotranspiration and PET is the potential evapotranspiration. The AET/PET ratio is commonly used as an indicator of aridity. AET is limited by the availability of water whereas PET is an artificial value based on the assumption that there are no restrictions on the availability of water (Kemp, 1998). In a raster-based GIS, the study area is divided into an array of grids or cells, each of which represents an area with average properties.

3.2.2 Data sources

The data required as input to the Carson and Kirby model are shown in Table 3.1. These data were collected from various sources. A brief description on the data sources and derivation of model parameters is given below.

Table 3.1 Input parameters for the Carson and Kirkby's surface runoff model

Data type	Parameter	Data source	Spatial coverage and resolution	Temporal coverage and res
Climate data	P_i	Global Land Data Assimilation System (GLDAS)	Global, 1.0°×1.0°	Jan 1st, 1979 to prese
		and Tropical Rainfall Measuring Mission (TRMM)	50°S-50°N,180°W-180°E, 0.25°×0.25°	Jan 1st, 1998- presen monthly.
	D_i	International Water Management Institute (IWMI)	Global, 0.25°×0.25°	1961-1990, long-term monthly me
	AET	Global Land Data Assimilation System (GLDAS)	Global, 1.0°×1.0°	Jan 1st, 1979 to present f 1.0 °data, Feb 24, 2000 to present f 0.25°data.3-hourly or mo
	PET	International Water Management Institute (IWMI)	Global, 0.25°×0.25°	
Soil properties	*MS*	Harmonized World Soil Database (HWSD)	Global, 30 arc-second	
	BD	Harmonized World Soil Database (HWSD)		
	EHD	the International Satellite Land Surface Climatology Project (ISRIC),Harmonized World Soil Database (HWSD)		

The precipitation data of the basin is from the Global Land Data Assimilation System (GLDAS) and the Tropical Rainfall Measuring Mission (TRMM). GLDAS is generating a series of land surface state and flux products simulated by four land surface models. Monthly data used in this study are produced through temporal averaging of the 3-hourly products. The Tropical Rainfall Measuring Mission (TRMM) is a joint mission between National Aeronautics and Space Administration (NASA) and the Japan Aerospace Exploration Agency (JAXA) to measure rainfall for weather and climate research using satellites. Launched in late 1997, TRMM provides gridded products in the tropical and sub-tropical regions of the earth at higher resolution than GLDAS. Therefore the TRMM 3B43 dataset was used to model the surface runoff in 2004. The maximum and minimum grid values of the two datasets are slightly different due to scale effect, but the difference in the areal average value is almost negligible, even for an area as small as 1.0°×1.0°. Figure 3.2 shows the precipitation in 1984, 1990 and 2004. The spatial patterns of the rainfall in the basin are generally the same. Rainfall varies from 700 mm to 2100 mm, with an increasing trend from the western area to the eastern coastal area. Among the sub-basins, the Dongjiang basin has a highest rainfall, about 1700 mm/a while the lowest rainfall occurs in Nanpanjiang basin (<1000 mm/a). Figure 3.3 shows the histograms of monthly mean rainfall of the entire basin. The division between dry and wet seasons is evident. January to April experiences low precipitation, typically less than 150 mm per month, whereas rainfall starts to increase from May to September and peaks at nearly 200 mm per month. Afterward, it drops moderately between October and December. The temporal patterns of the precipitation in Zhujiang are a result of the East Asia monsoon.

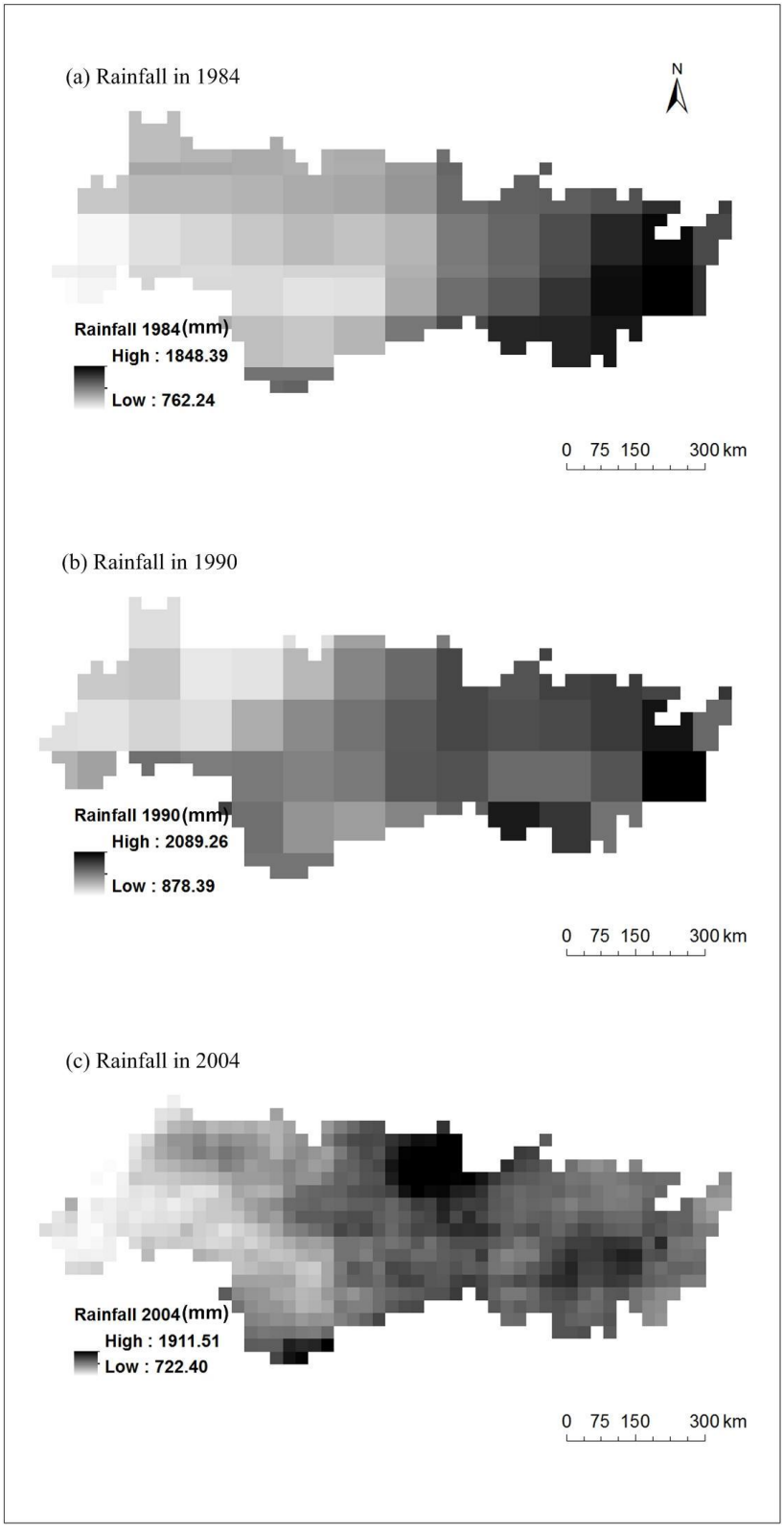

Figure 3.2 Total precipitation of the Zhujiang basin in 1984 (a), 1990 (b) and 2004 (c) (NASA, 2012; NASA and JAXA, 1998)

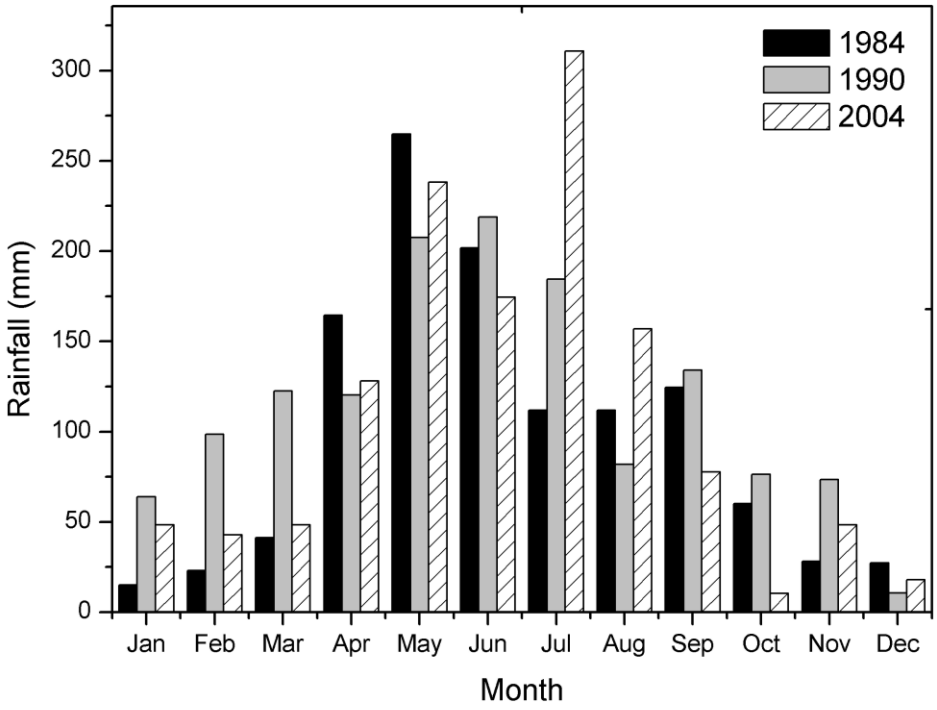

Figure 3.3 Monthly precipitation of the Zhujiang basin in 1984, 1990 and 2004

The rainfall frequency data is obtained from the International Water Management Institute (IWMI). IWMI provides direct access to global water and climate data for water resource management. The Climate Atlas (International Water Management Institute, 2008) provides users with monthly values for precipitation, average temperature, wind speed, humidity and etc. during 1961-1990. Rainy days are defined as those with precipitation higher than 1 mm. The mean number of rainy days per month (D_i) and Penman-Montieth reference evapotranspiration (PET) estimated from daily temperature, wind speed, humidity and solar radiation, are used in this study. The mean number of rainy days in January and July is 11.45 days and 16 days, respectively. As shown in Figure 3.4, the Liu basin has most rainy days (205.4 days) among all the sub-basins and the southwestern and northeastern area has a lower rainfall frequency.

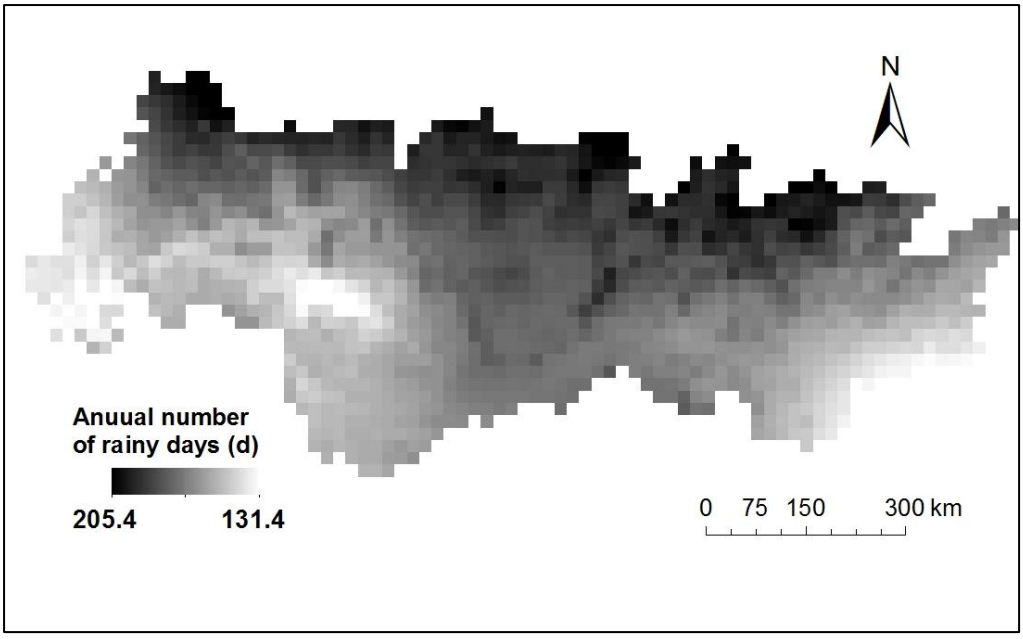

Figure 3.4 Long-term annual number of rainy days in the Zhujiang basin (International Water Management Institute, 2008)

Actual evapotranspiration (AET) is extracted from the GLDAS dataset, averaging 653.9 mm for the whole basin. In general AET increases toward the low latitude area and is higher in summer than in winter. The strongest evaportranspiration occurs in July, when the precipitation is also high. AET/PET ratio of the Zhujiang River basin ranges from 0 to 0.95. Higher ratio tends to occur in humid regions while lower ratio is observed in semi-arid and arid regions. It should be noted that in the southern Dongjiang basin and the Zhujiang Delta, AET/PET ratio data is not available. The Delta is not modeled and analyzed in this study. The surface runoff is assumed to be 0 mm in the Dongjiang basin as is shown in the frame in Figure 3.5.

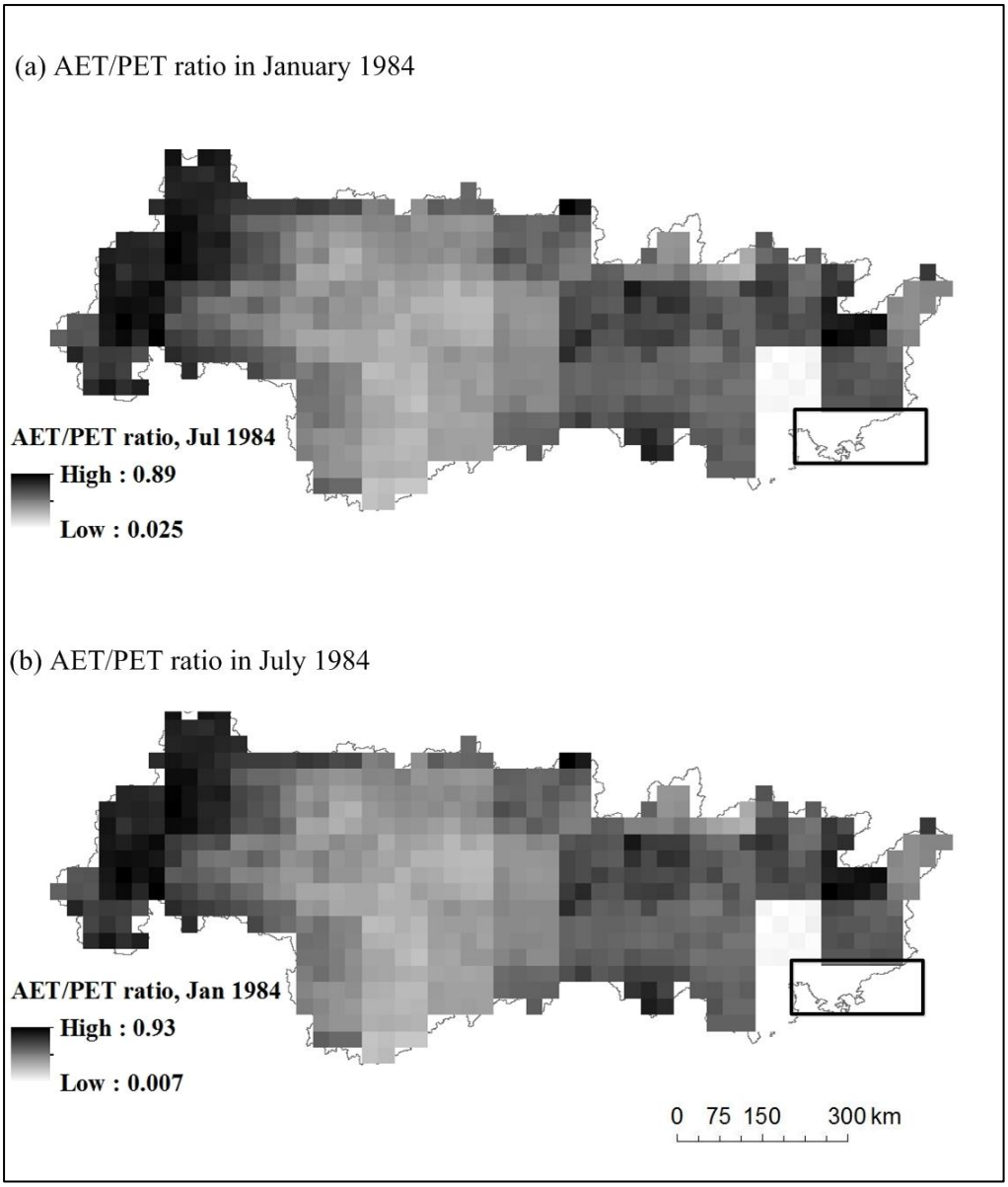

Figure 3.5 Ratio of actual and reference evapotranspiration in the Zhujiang River basin in January (a) and July (b), 1984 (Derived from GLDAS data)

Soil properties are derived from different data sources. The Federal Agriculture Organization of the United Nations (FAO) established a Harmonized World Soil Database (HWSD) in partnership with other organizations and institutes to provide up-to-date information on global soil resources. This database is a 30 arc-second raster database that combines existing regional and national updates of soil information, including a recent 1:1,000,000 scale soil map of China. The major soil types in the Zhujiang basin are Acrisols (35.3%), Anthrosols (25.47%) and Alisols (10.99%). Soil parameters contained in HWSD include pH, salinity, textural class, water

storage capacity of the soil and the clay fraction, reference depth as well as bulk density of the topsoil (*BD*) which is used in this study (Figure 3.6). The bulk density does not show significant spatial variation, ranging from 1.33 g cm^{-3} to 1.54 g cm^{-3}. The density for inland water, rock debris and urban area is 0. Soil moisture content at field capacity (*MS*) is the amount of water remaining in the soil retaining in soil at 1/3 bar of hydraulic head (Veihmeyer and Hendrickson, 1931). It is largely dependent on the soil texture. The main type of texture of the Zhujiang basin is clay (light), loam and sandy clay loam. The soil properties of the basin will be discussed later with more detail in Chapter 4. The soil moisture at field capacity can be determined by joining the following table (Table 3.2) with HWSD attribute data. The soil moisture data for each soil texture class is obtained from field/laboratory measurements (van Lieshout, n.d.). In the Zhujiang River basin, eight types of topsoil texture can be found: silty clay, clay (light), silt loam, loam, sandy clay loam, sandy loam, loamy sand and sand. The average *MS* ranges from 0.22 to 0.3 for each sub-basin. *EHD* data can be found in the International Satellite Land Surface Climatology Project Initiative II data collection (ISLSCP II) at the resolution of 1.0 degree. *EHD* decreases from the highest in the Nanpanjiang River basin in the upper reaches and reaches an even lower value in the middle and lower reaches of the Zhujiang. *EHD* is the depth of soil within which the soil storage capacity controls the generation of runoff. Values of *EHD* can be varied to take account of the different depths of rooting of the vegetation/crop cover and the presence or absence of surface crusting (Morgan and Duzant, 2008). Table 3.3 gives some guide values for *EHD* for use in the Carson and Kirkby model.

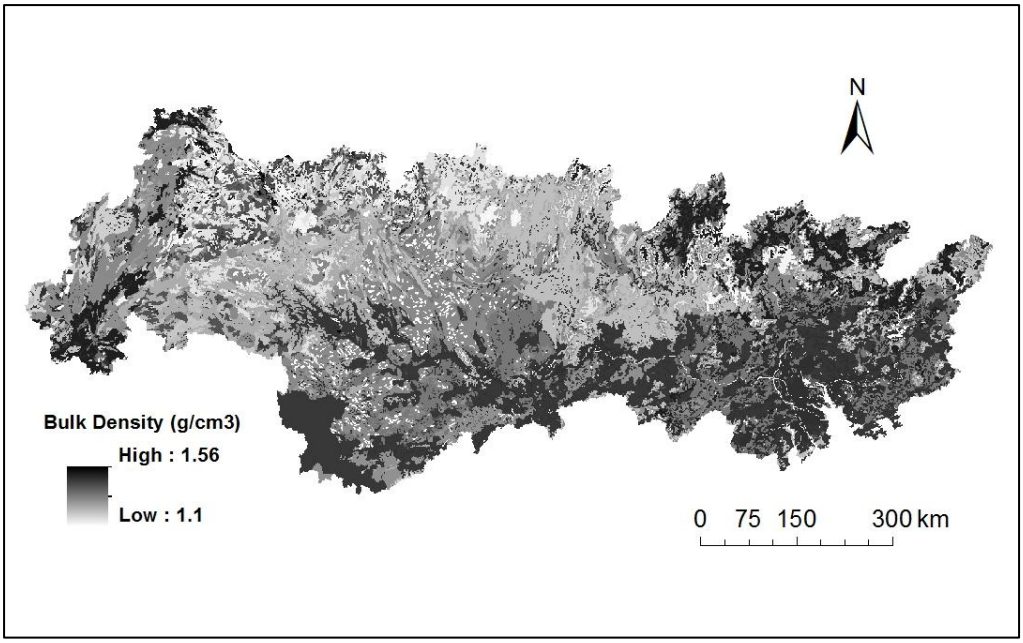

Figure 3.6 Bulk density of the topsoil in the Zhujiang basin (FAO, ISRIC and ISSCAS, 2009)

Table 3.2 Soil parameters used in the model (Shrestha, 1997; Morgan et al., 1984)

USDA[a] code	Topsoil texture	Soil moisture content at field capacity
1	clay(heavy)	0.45
2	silty clay	0.3
3	clay (light)	0.43
4	silty clay loam	0.25
5	clay loam	0.4
6	silt	0.37
7	silt loam	0.35
8	sandy clay	0.25
9	loam	0.2
10	sandy clay loam	0.28
11	sandy loam	0.18
12	loamy sand	0.15
13	sand	0.08

Note: [a] USDA: U.S. Department of Agriculture.

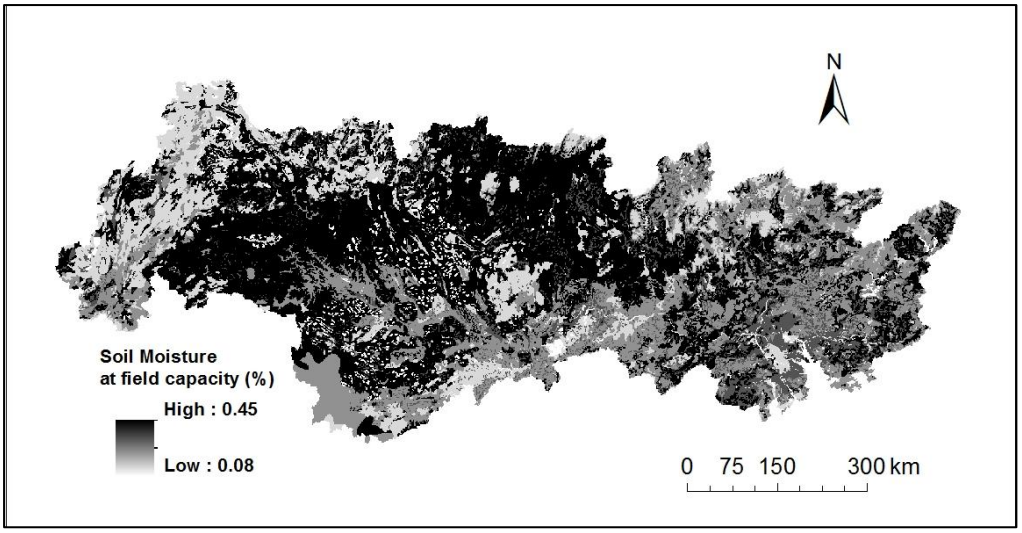

Figure 3.7 Soil moisture content at field capacity in the Zhujiang basin (FAO, ISRIC and ISSCAS, 2009)

Table 3.3 Recommended values for Effective Hydrological Depth (*EHD*)

Condition	*EHD* (m)
Bare crusted soil	0.05
Bare soil (no crust)	0.09
Cropland	0.12
Mature forest, dense secondary forest	0.20
Cultivated grass	0.12
Lowland grass	0.12
Woodland (broad leaved)	0.20
Woodland (coniferous)	0.20

3.3 Results and discussion

3.3.1 Monthly overland flow in 1984, 1990 and 2004

After extracting the required data from the respective databases, format conversions were conducted where necessary and all layers were resampled. Regarding that the resolution of the datasets range from 30 arc-second (approximately 1km) to 1° (approximately 100km), all layers were resampled to 1 km ×1 km grids for best resolution. Soil water storage capacity is estimated to be 20.1-43.4 mm for each sub-basin. Based on this estimation, the surface runoff model was applied at a monthly time step. The Zhujiang River

Delta is excluded from analysis and will not be shown in the following maps. The monthly mean surface runoff for the entire basin ranges from 0.01 to 6.85 mm in 1984, 0 to 4.21 mm in 1990 and 0 to 10.39 mm in 2004 (Table 3.4). The monthly runoff in 2004 is generally lower than those in 1984 and 1990 and has a significant temporal variation. Without much difference in the monthly rainfall and PET, the low surface runoff in 2004 is mainly caused by higher AET. The rate of AET is controlled by several factors, including water availability, wind speed, physical attributes of the vegetation, soil characteristics and temperature. The higher AET in 2004 compared to that in 1984 and 1990 in this study can be partly explained by the increase of vegetation cover caused by the soil and water conservation practices. Forest and crop land cover types contribute more AET than sparse vegetation (Martin and Bourque, 2013). For all months, a significant increase in temperature from 1961 to 2007 has been reported in the entire basin with the coastal area in particular. Therefore, higher AET in 2004 may also be caused by the increasing temperature.

Table 3.4 Modeled monthly mean surface runoff and annual total surface runoff in 1984, 1990 and 2004

Month	Surface runoff in 1984 (mm)	Surface runoff in 1990 (mm)	Surface runoff in 2004 (mm)
January	0.01	0.49	0.17
February	0.01	2.03	0.00
March	0.05	1.46	0.02
April	4.50	1.34	0.32
May	6.85	4.22	1.98
June	1.80	1.69	0.26
July	0.86	2.97	10.39
August	0.42	0.29	0.23
September	1.32	1.08	0.02
October	0.08	0.24	0.00
November	0.08	0.35	0.02
December	0.02	0.00	0.00

The temporal patterns of surface runoff normalized to annual totals in

1984 and 1990 are very similar. Basin-wide surface runoff from May to August are generally higher than in other months, accounting for about 50% of the annual total. In contrast, the winter months have much less surface runoff. The monthly runoff in 2004 has a greater temporal variation, with 94.1% generated in the summer. This is associated with the greater temporal variation of rainfall in 2004, when the standard deviation of rainfall is highest among the three years. The surface runoff maps of the basin in January and in July of the three years are presented in Figure 3.8 In January, there is little runoff in the upper reaches of the basin in response to the variation in precipitation. In July, a large amount of surface runoff is generated in the Nanpanjiang and Hongshuihe basin because of low water storage capacity. The greater runoff in the Xunjiang is mainly caused by higher precipitation. Runoff peaks in the southeastern corner of the Xijiang basin, which is quite close to the Zhujiang River Delta where the AET/PET ratio is low due to large area of urban and built-up land, despite a high temperature.

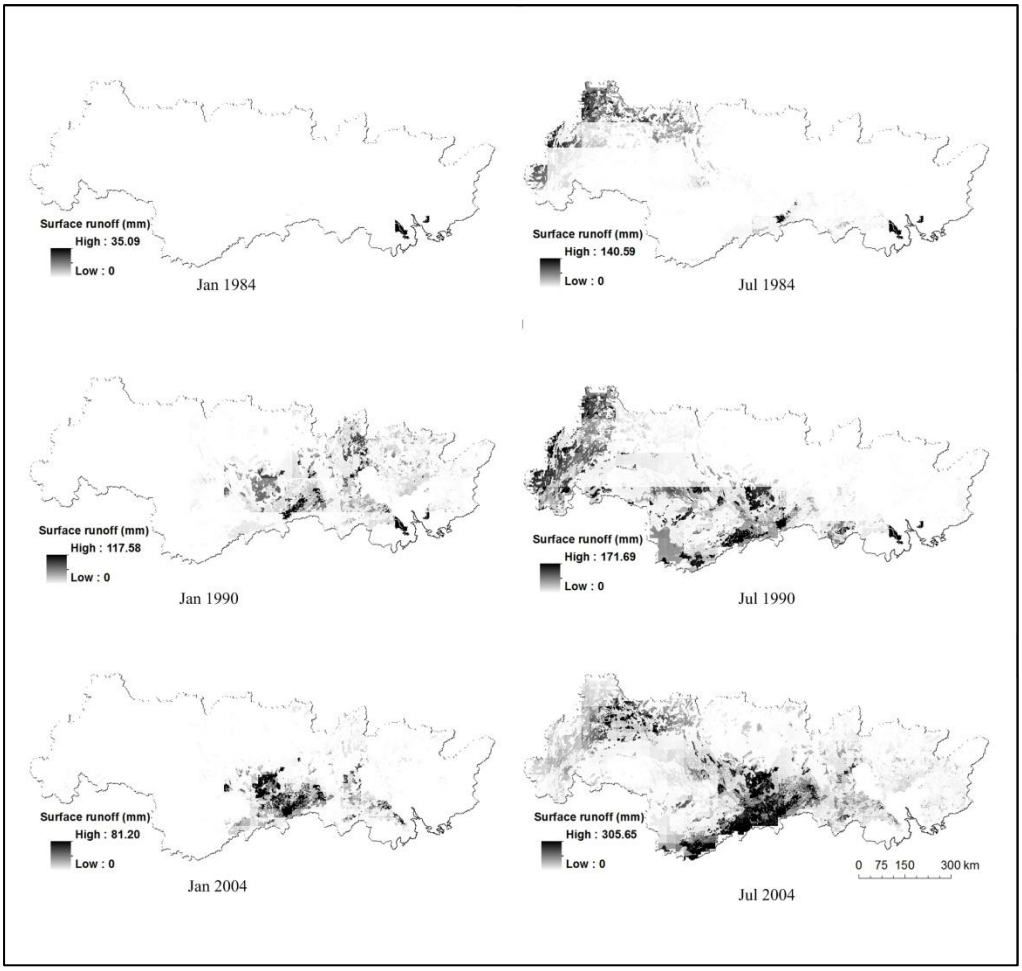

Figure 3.8 Spatial distribution of monthly surface runoff of the Zhujiang River in January and July

3.3.2 Annual surface runoff in 1984, 1990 and 2004

Monthly surface runoff was summed to obtain annual surface runoff. The annual surface runoff for the entire basin is 21.2 mm in 1984, 19.4 mm in 1990 and 7.1 mm in 2004. The spatial pattern of annual surface runoff is similar to that in July, with greatest runoff generated in the delta, followed by those in the eastern and southwestern area (Figure 3.9). Significant spatial and temporal variation of annual surface runoff can be seen for the nine sub-basins and the delta (Figure 3.10). This is mainly due to the sensitivity of surface runoff to the soil water storage capacity in the Carson and Kirkby model. The soil water storage capacity in this study is determined by soil properties and AET/PET ratio only while the influence of actual soil moisture is not considered. If monthly soil moisture is included in the model, then $-r_c$ in Carson and Kirkby model will be substituted by the difference between the actual moisture and the water storage capacity and thus be lowered. So the model sensitivity is likely to be lowered with monthly soil moisture included. This study mainly concerns the areal average value and the runoff coefficient for sub-basins ranges from 0.001 to 0.05, which is acceptable. So it is generally satisfactory to exclude the actual soil moisture. Additionally, the definition and unit of soil moisture from currently available datasets are different from those in Carson and Kirby's model. Since the water storage capacity is influenced by soil structure, organic matter content, carbonate content vegetation and even the presence of stones, reliable approach for unit conversion is yet to be developed. The lack of reliable approach as well as the large amount of time involved in image processing make it difficult to include the soil moisture in estimating the soil water storage capacity in this study.

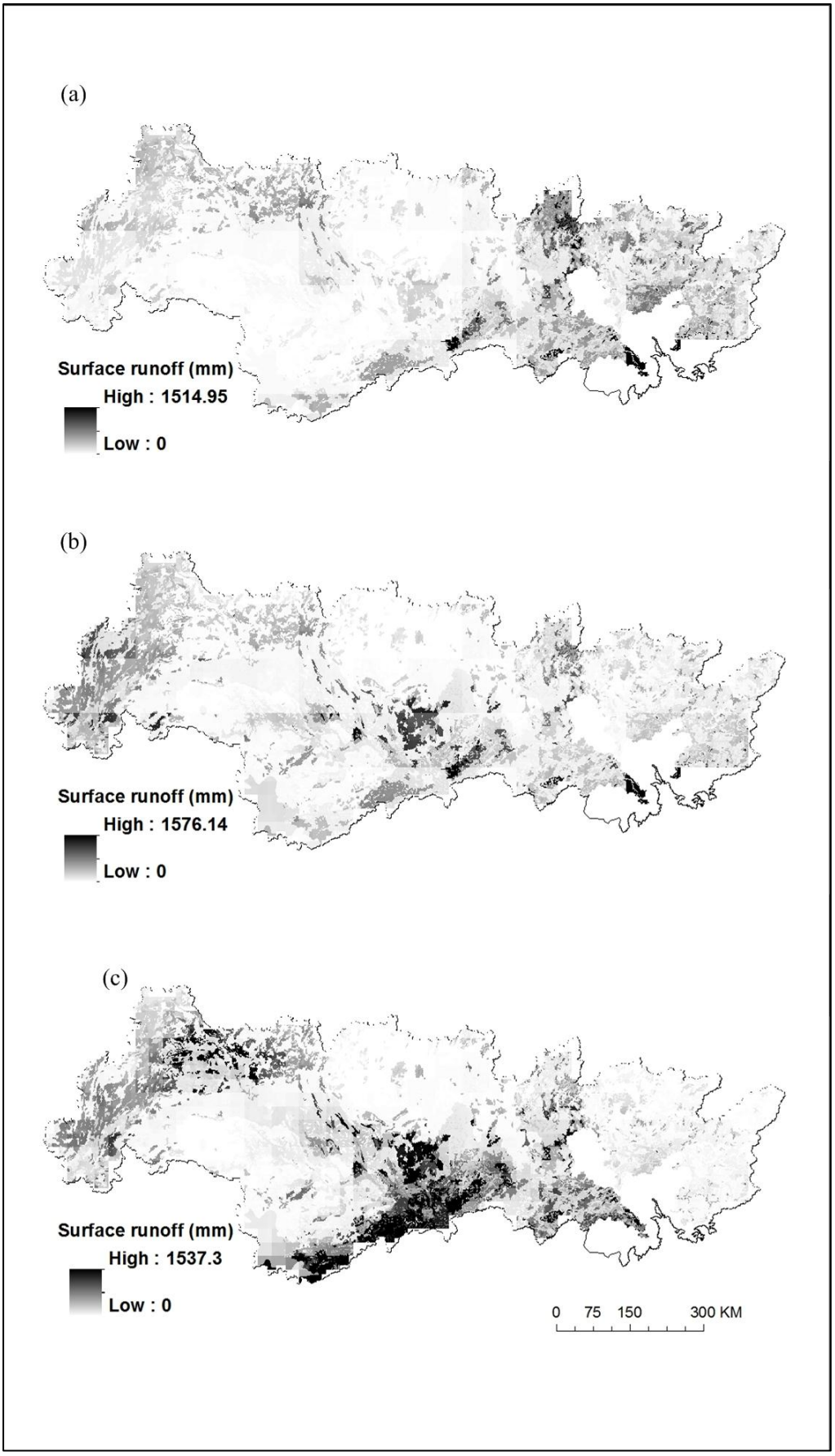

Figure 3.9 Annual surface runoff in 1984 (a), 1990 (b) and 2004 (c)

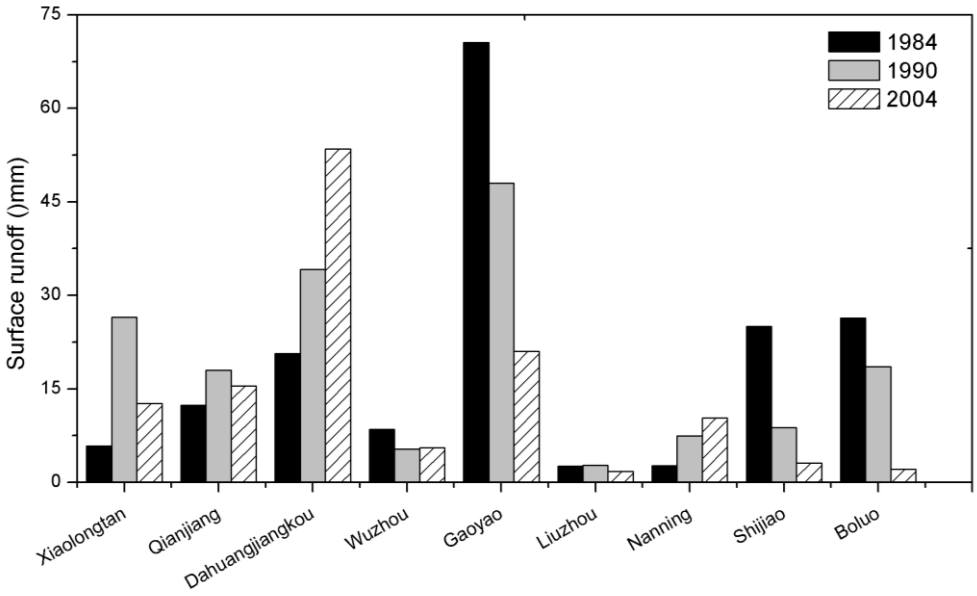

Figure 3.10 Average surface runoff in sub-basins in 1984, 1990 and 2004

3.4 Summary

This chapter investigated the monthly and annual surface runoff in 1984, 1990 and 2004 using Carson and Kirkby model (1972). Basin-wide surface runoff in the summer months of June, July and August is generally higher than in other months in response to the temporal variation in rainfall. The annual mean surface runoff for the entire basin is 21.21mm in 1984, 19.35 mm in 1990 and 7.07 mm in 2004. Greater surface runoff is generated in the lower reaches, with the highest value in the eastern and southeastern part of the basin. The modeling result is satisfactory and will be used as input for soil erosion model in the next chapter.

Chapter 4 Modeling soil erosion in the Zhujiang (Pearl River) basin

4.1 Introduction

Soil erosion can be directly measured in the field. But this traditional method is reliable at a specific site in the landscape and has been criticized for limited applicability at a larger spatial scale. Therefore models have been developed as an alternative way to study soil erosion. Modeling soil erosion is the process of mathematically describing soil particle detachment, transport and deposition on land surfaces (Blaszczynski, 2001). Data availability is another main guiding principle in the selection of an appropriate model. As the aim of this research is to estimate soil erosion rate and sediment yield by using low demanding models at large spatial scale and with a monthly time step, the selected model should fit such temporal and spatial scales. As discussed in the first chapter, the advantage of empirical models is their simplicity and low requirement for data. But most empirical models are derived from field measurement. A purely empirical model will not be suitable for this study because the field measurement needed for model calibration are difficult in such a large basin with complex terrain. Physically based models are usually used in small catchments because they are highly data demanding. On the other hand, modeling results may be often impressive but difficult to interpret (Meyer and Flanagan, 1992) and validate because of model complexity. Beven (1995) and Van Rompaey et al. (2003) argue that the simpler and less data-intensive conceptual models may be able to perform equally well in terms of overall catchment response, with much less time and effort required to apply them compared with detailed distributed process-based models. With regard to all these, the Thornes erosion model (Thornes, 1990), a conceptual model is used in this study to estimate soil erosion in the Zhujiang basin. This modeling approach has been used in soil erosion studies in different geographical settings and at various spatial scales (e.g. Zhang et al., 2002; Saaverdra and Mannaerts, 2005; Anh Luu, 2009; Ali and De Boer, 2010). The objective of this chapter is to explore the implementation of the Thornes erosion model in the data sparse Zhujiang River basin and to evaluate its ability to predict

erosion rates in a large drainage basin setting.

4.2 Method and materials

4.2.1 Thornes erosion model

Erosion is calculated as a function of the indicators of driving forces (e.g. runoff rate and gradient) and resistance to erosion (e.g. soil properties and vegetation cover). Thornes (1985; 1990) put forward a conceptual erosion model that contains a hydrological component based on a runoff storage type analogy, a sediment transport component and a vegetation cover component. The Thornes erosion model requires estimates of the rate of surface runoff production and is based on square grid cells. It is based on the assumption that daily precipitation can be approximated by an exponential frequency distribution within a specified area (Thornes, 1990).The model equation for each grid cell reads:

$$E_i = k \cdot OF_i^2 s^{1.67} e^{-0.07 c_i} \tag{4.1}$$

where E_i = erosion rate (mm month^{-1} or mm year^{-1} depending on the time step),

k = soil erodibility coefficient representing soil susceptibility to erosion,

OF_i = surface runoff (mm) derived from hydrological sub-models,

s = the slope (m m^{-1}),

c_i = the fraction of vegetation cover (%).

Individual GIS layers were built for individual model input parameters stated above. A brief description of the sources, including the spatial and temporal resolution of the dataset required for modeling is given in Table 4.1.

Table 4.1 Input parameters for the Thorne's soil erosion model

Data type	Parameter	Data source	Spatial coverage and resolution	Temporal coverage and resolution
Topography	s	Shuttle Radar Topography Mission (SRTM)	56° S to 60° N, 90m	
Soil properties	k	Harmonized World Soil Database (HWSD)	Global, 30 arc-second	
Land cover	c_i	Global Inventory Modeling and Mapping Studies (GIMMS)	Global, 0.25°×0.25°	July 1981 to December 2006, monthly
		MOderate Resolution Imaging Spectroradiometer (MODIS)	Global, 1 km	February 18, 2000 to present, monthly

4.2.2 Topography data

Topography influences flow paths and determines the effect of gravity on the movement of water and sediment. Slope data in the Thornes model were derived from the 90 meter product of the Shuttle Radar Topography Mission (SRTM) Database Version 4.1, a joint database for Digital Elevation Models (DEM) on a near global scale. The raw data was obtained since 2000 and projected in a Geographic (Lat/Long) projection, with the WGS84 horizontal datum and the EGM96 vertical datum. It was processed following the methods described by Reuter et al. (2007). The first processing stage involves importing and merging the 1-degree tiles into continuous elevational surfaces in ArcGRID format. The second process fills small holes iteratively, and the cleaning of the surface to reduce pits and peaks. The third stage then interpolates through the holes using a range of methods. The method used is based on the size of the hole, and the landform that surrounds it. The SRTM data is currently distributed free of charge and is available for download on USGS website. Slope can be calculated using ArcGIS slope tool and converted from degree to m m^{-1}. Figure 4.1 shows the basin slope of the Zhujiang basin, as derived from the SRTM data. The slope of the basin ranges from 0°to 72.8°, or 0 m m^{-1} to 3.228 m m^{-1}.

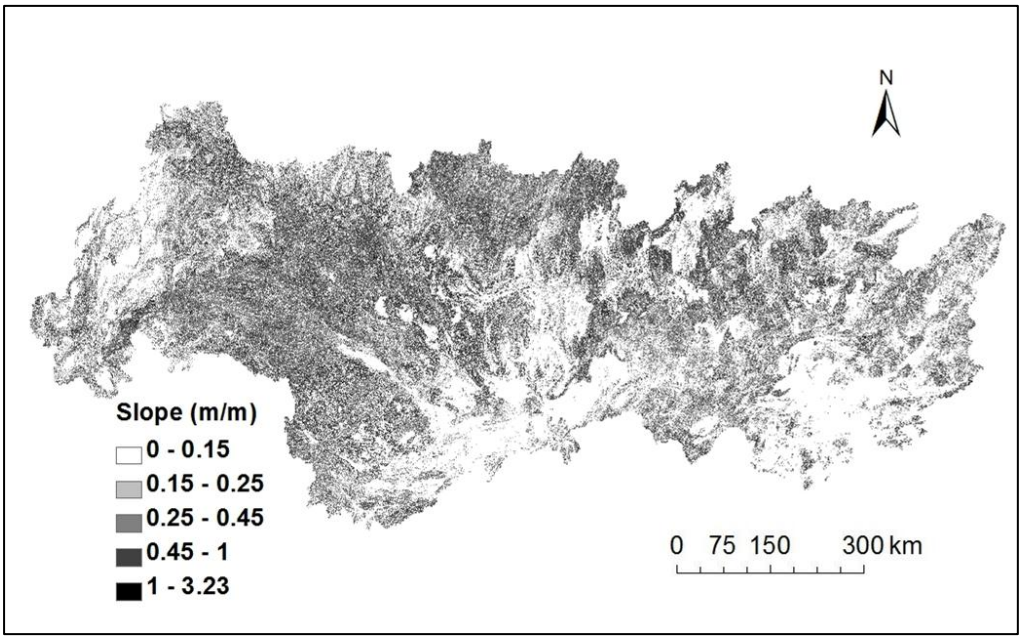

Figure 4.1 Slope map of the Zhujiang basin (USGS, 2008)

The western mountainous area and hills in the central area are characterized by steep slopes. Areas with moderately steep slope (> 0.2 m m^{-1}) account for more than 50% of the total. The southern and southeastern part have more gentle slopes. There are several narrow plains lying in the lower reaches of the Zhujiang. Following this topography, the flow directions of rivers are mainly from west and north toward the coast of the South China Sea in the southeast.

4.2.3 Soil data

Soil resists the forces of erosion to varying degrees based upon its physical and chemical properties. The resistance of a soil to the forces of detachment and transport is referred to as a soil's erodibility (Wischmeier and Mannering, 1969). Relevant soil properties were derived from the Harmonized World Soil Database (HWSD).The dominant soil types in the basin are Acrisols, Anthrosols and Alisols (10.99%). Figure 4.2 is the soil textural classes and their percentages in the Zhujiang basin.

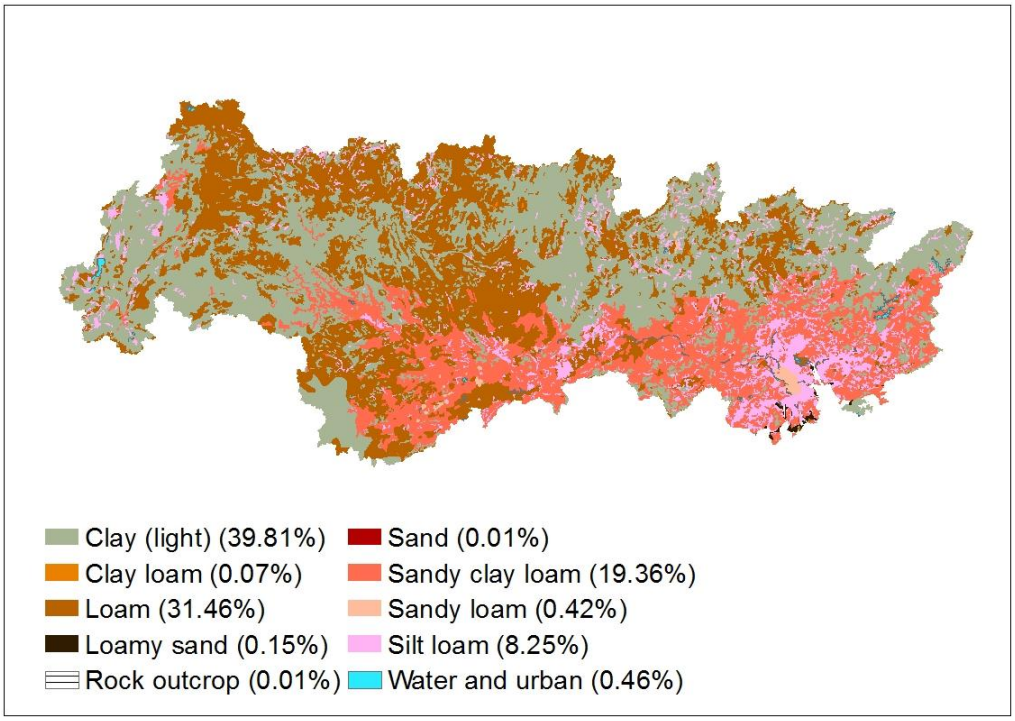

Figure 4.2 Soil texture in the Zhujiang basin (FAO, ISRIC and ISSCAS, 2009)

The soil erodibility k was determined from the organic matter content and soil texture following Stone and Hilborn (2000) (Table 4.3). About 5% of the Zhujiang river basin is characterized by bare rock, urban area and water bodies. To account for these land classes, k values of 0 were adopted for bare rock, urban area and water bodies, respectively. Soil erodibility factors were separately calculated for representative soil polygons and assigned to similar polygons. The polygons were then converted to raster format (Figure 4.3). The average soil erodibility is highest in Liujiang basin and lowest Dongjiang basin.

Table 4.2 Soil erodibility (k) factors, after Stone and Hilborn (2000)

Textural Class	Organic Matter Content (%)		
	Average	Less than 2%	More than 2%
Clay	0.22	0.24	0.21
Clay loam	0.3	0.33	0.28
Coarse Sandy loam	0.07	-	0.07
Fine sand	0.08	0.09	0.06
Fine sand loam	0.18	0.22	0.17
Heavy clay	0.17	0.19	0.15
Loam	0.30	0.34	0.26
Loamy fine sand	0.11	0.15	0.09
Loamy sand	0.04	0.05	0.04
Loamy very fine sand	0.39	0.44	0.25
Sand	0.02	0.03	0.01
Sandy clay loam	0.20	-	0.20
Sandy loam	0.13	0.14	0.12
Silt loam	0.38	0.41	0.37
Silty clay	0.26	0.27	0.26
Silty clay loam	0.32	0.35	0.30
Very fine sand	0.43	0.46	0.37
Very fine sandy loam	0.35	0.41	0.33

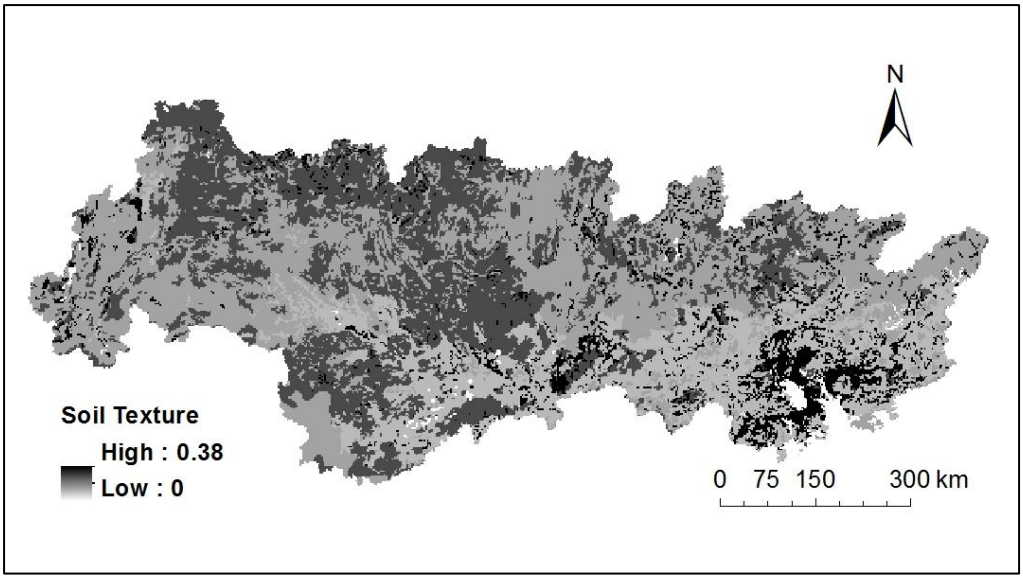

Figure 4.3 Soil erodibility factor (k) in the Zhujiang basin

4.2.4 Vegetation cover

Vegetation parameters account for the protection against erosion provided by the canopy and ground cover. Vegetation characteristics vary in space and time and it is difficult to measure the vegetation change on-site at large scale. Therefore remote sensing techniques are useful tools under these circumstances. The Normalized Difference Vegetation Index (NDVI) is one of the most widely used vegetation indexes and its utility in satellite assessment and monitoring of global vegetation cover has been well demonstrated over the decades (Tucker, 1979; Purevjord et al., 1998; Leprieur et al., 2000). The empirical relationship between NDVI and vegetation cover based on the data has been derived based on data reported in the literature. The fraction of vegetation cover can be calculated using the equation by Drake et al. (1998):

$$c_i = 8.79815 + 93.07466 NDVI_i \qquad 4.1)$$

where c_i is the fraction of vegetation cover for a cell for time period i (%).

There are two sources of NDVI data for this study. One is the Global Inventory Modeling and Mapping Studies (GIMMS) data set spanning from 1981 to 2006. The dataset is derived from imagery obtained from the Advanced Very High Resolution Radiometer (AVHRR) instrument onboard the NOAA satellite. This data set provides improved results based on corrections for calibration, view geometry, volcanic aerosols, and other effects

not related to actual vegetation change (Tucker et al., 2004). The spatial resolution of the GIMMS data set is 8 km. For better modeling result, another dataset at higher resolution is used for 2004. MODIS vegetation indices are designed to provide consistent spatial and temporal comparisons of vegetation conditions. The accuracy of GIMMS and its compatibility with NDVI data from MODIS has been proven to be suitable for a global assessment (Tucker et al., 2005, Brown et al., 2006). Global MOD 13A3 data are provided monthly at 1 km resolution as a gridded product. The original global data from the GIMMS and MODIS product range from -88 to 1 and -2,000 to 10,000 respectively (Figure 4.4). Negative values are mainly generated from water and snow and values near zero are mainly from rock and bare soil (National Aeronautics and Space Administration (NASA), n.d.). In the study area, all the NDVI values derived from the GIMMS are positive except several cells without data in certain months. These cells are either water bodies or a consequence of data quality problems. Cells without data in the nine sub-basins (excluding the Zhujiang River Delta) occupy less than 3% of the total area and were therefore ignored in the subsequent modeling. Since NDVI values range from -1.0 to 1.0, the original data from MODIS were normalized to fall within this range before any calculation can be done. Very low values of NDVI (0.1 and below) correspond to barren areas of rock, sand or snow. Moderate values represent shrub and grassland (0.2 to 0.3) while high values indicate temperate and tropical forests (0.6 to 0.8) (National Aeronautics and Space Administration (NASA), n.d.)

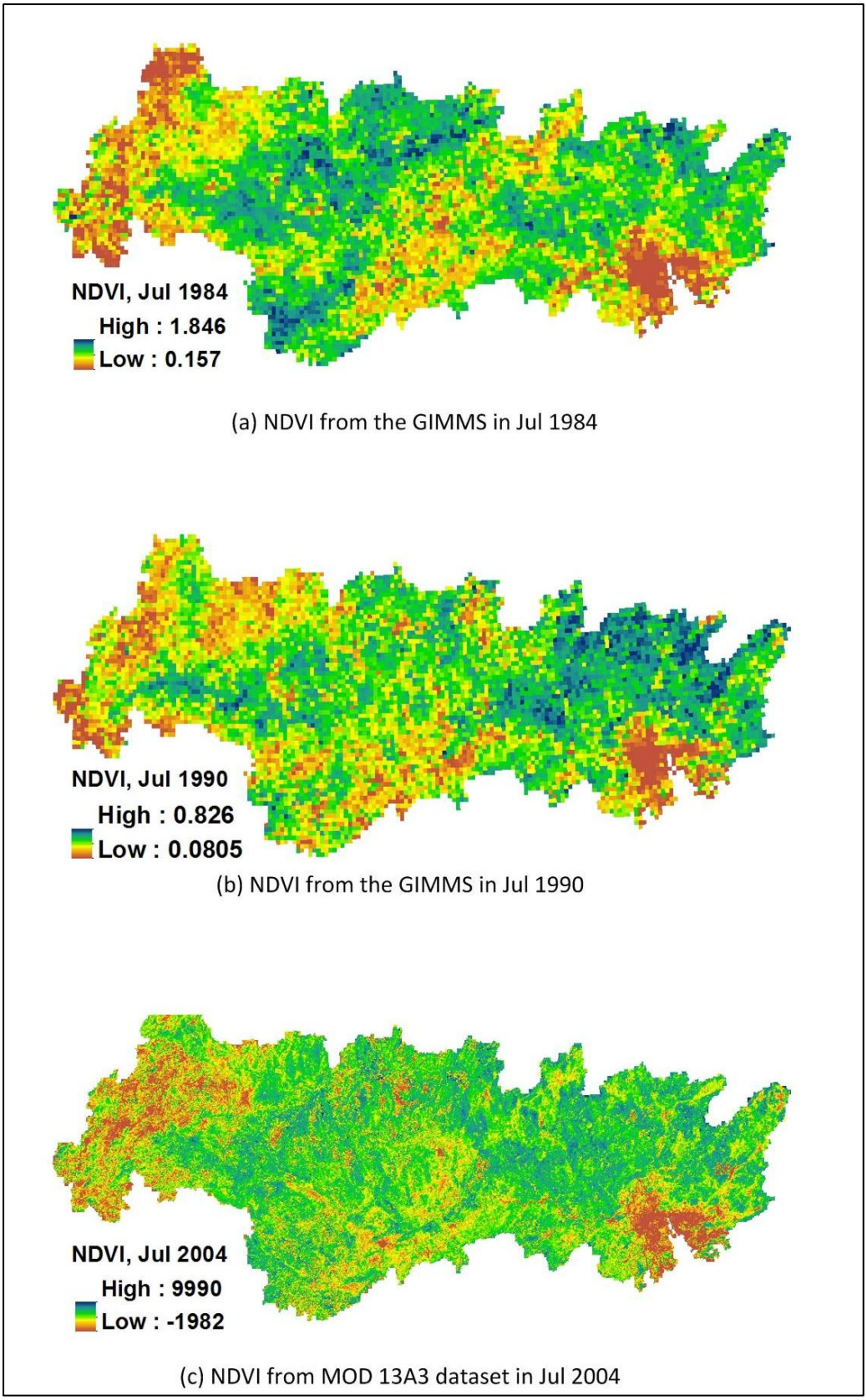

Figure 4.4 Original data from the GIMMS in Jul 1984 (a), July 1990 (b) and MOD 13A3 in Jul, 2004(c)

Normalized data were used to calculate the fraction of vegetation cover for each month in 1984, 1990 and 2004 using equation (4.1). The estimated vegetation cover in January and July is presented in Figure 4.5. As expected, the vegetation cover is denser in July than in January because of greening of deciduous vegetation in summer. Annual vegetation coverage percent can be achieved by averaging the twelve monthly data in each year. The mean vegetation cover was 48.9% in 1984, 50.1% in 1990 and 67.5% in 2004. Change detection was done based on the NDVI data in different years. The vegetation cover can be classified into five categories (Sun et al., 2008): no vegetation cover (NC) for $c_i \le 20\%$, low vegetation cover (LC) for $20\% < c_i \le 45\%$, medium vegetation cover (MC) for $45\% < c_i \le 75\%$, high vegetation cover (HC) for $75\% < c_i \le 90\%$, and full vegetation cover (FC) for $c_i \ge 90\%$. Results show that most of the area remained unchanged from 1984 to 1990 while a more obvious increase of vegetation cover can be observed in many pixels (Figure 4.6). Only a few pixels experienced decrease in vegetation cover from 1984 to 1990 and from 1990 to 2004. During the first period, change from MC to LC occurred mostly in the Hongshui River basin, where the soil and water conservation practice took effect. From 1990 to 2004, 35% of the basin area experienced increase in vegetation cover, including 7.6% from LC to MC, 26.3% from MC to HC and 1.1% from LC to HC. The reasons for such change may partly be the soil and water conservation project staring from early 1980s. But the estimated fraction includes both natural vegetation and crops which cover nearly 60% of the total basin in 2000 according to the statistics from Global Land Cover 2000 Project (GLC 2000), without a detailed map of land cover in the two periods it is difficult to conclude whether the increase in vegetation cover is caused by the efforts on soil and water conservation or by increasing need for agricultural products.

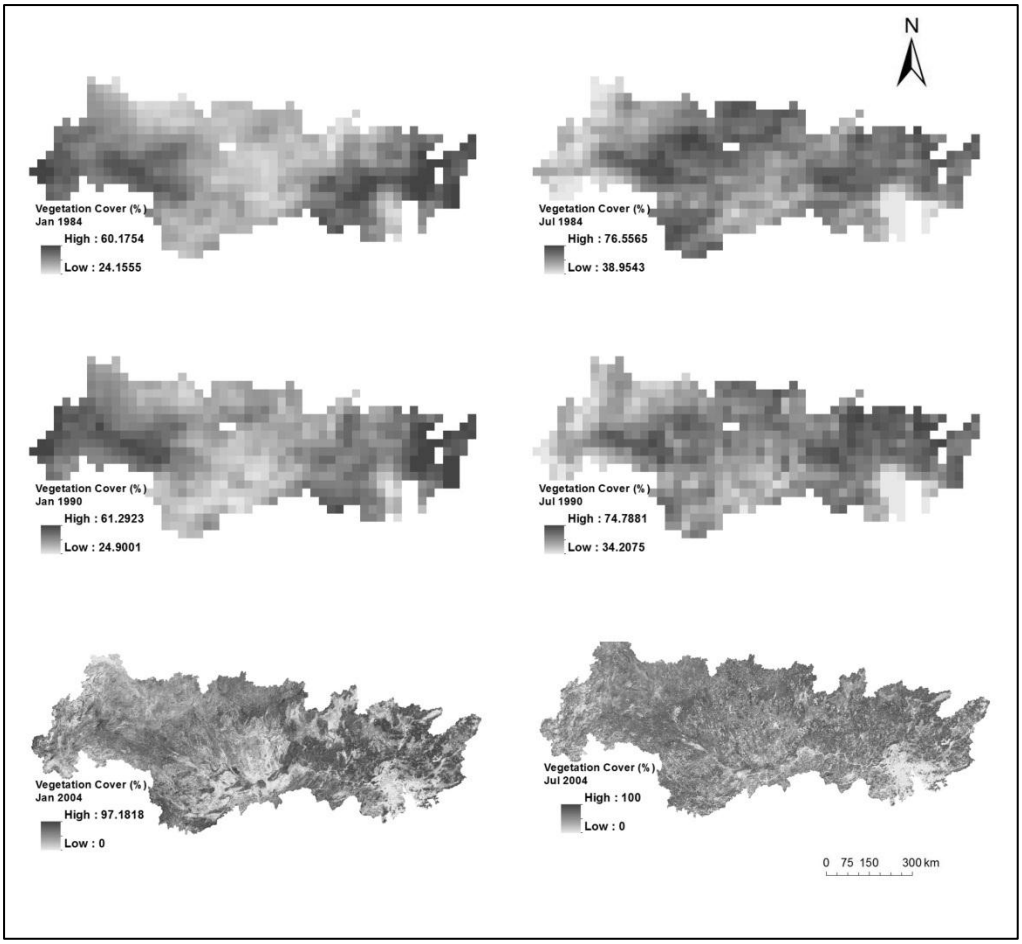

Figure 4.5 Vegetation cover in January and July for year 1984, 1990 and 2004 in the Zhujiang basin

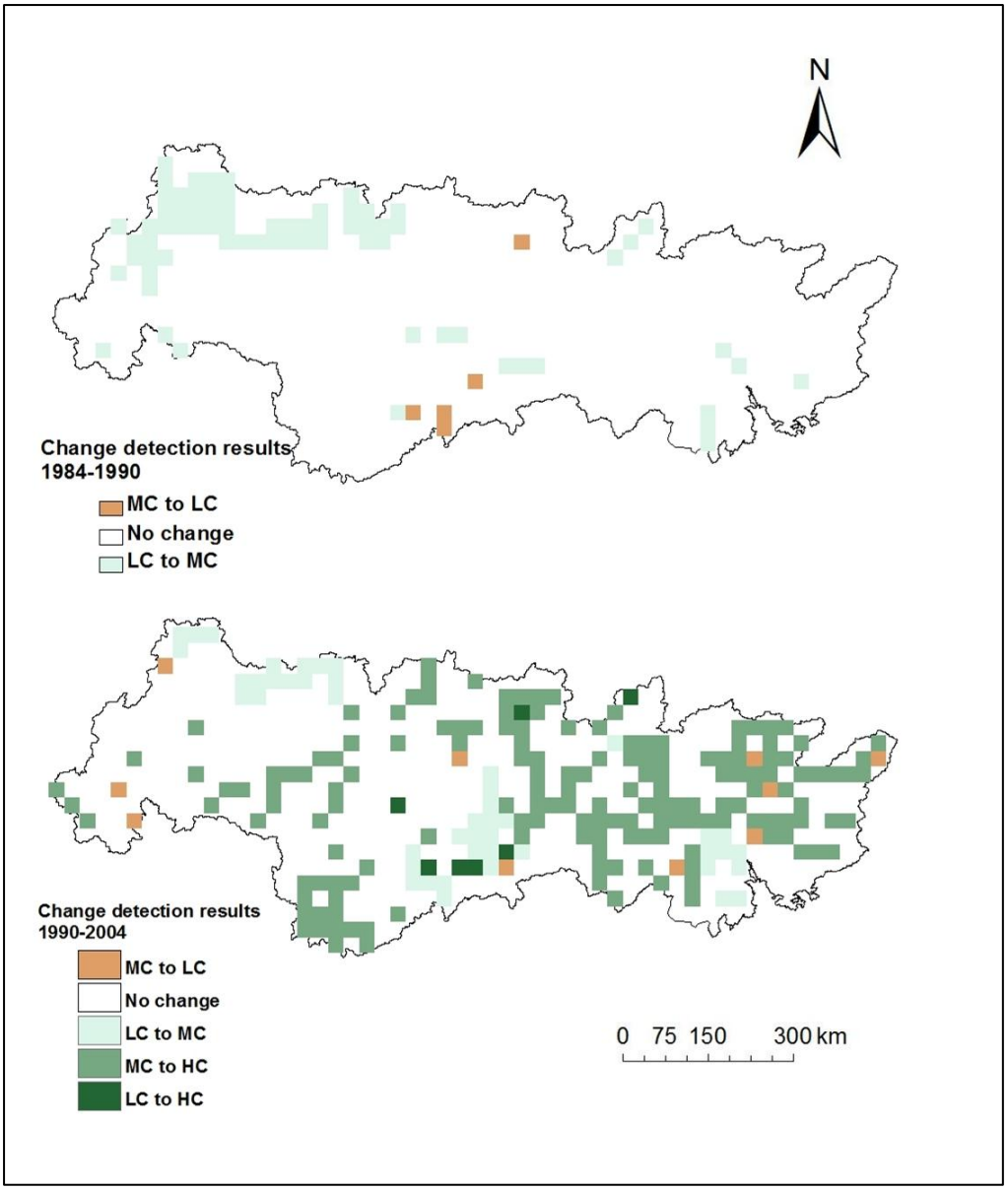

Figure 4.6 Change detection of the vegetation cover in the Zhujiang basin

4.2.5 Sub-basin boundaries

Sub-basin boundaries are necessary for estimating the average erosion rate and sediment yield in different sub-basin. Large river basins consist of a series of hierarchical sub-basins. There are two alternative methods to estimate the average erosion rate and sediment yield for such hierarchical sub-basins. Sediment yield can be estimated by deducting the sediment load at the neighboring upstream station from the load at the gauging station which is then divided by the incremental catchment area (Jansson, 1988; Lajczak and Jansson, 1993; Lu et al., 2003) (Figure 4.7). Sediment yield can also be

calculated as the total load divided by the total catchment area upstream of the gauging station. The latter method is a spatial averaging of hierarchical sub-basins. In order to distinguish the net erosion and sediment generation for a certain river section, this impact of spatial averaging should be reduced. Therefore the former method is adopted in the present study. The incremental area is used for subsequent spatial statistics of soil erosion rate and sediment load.

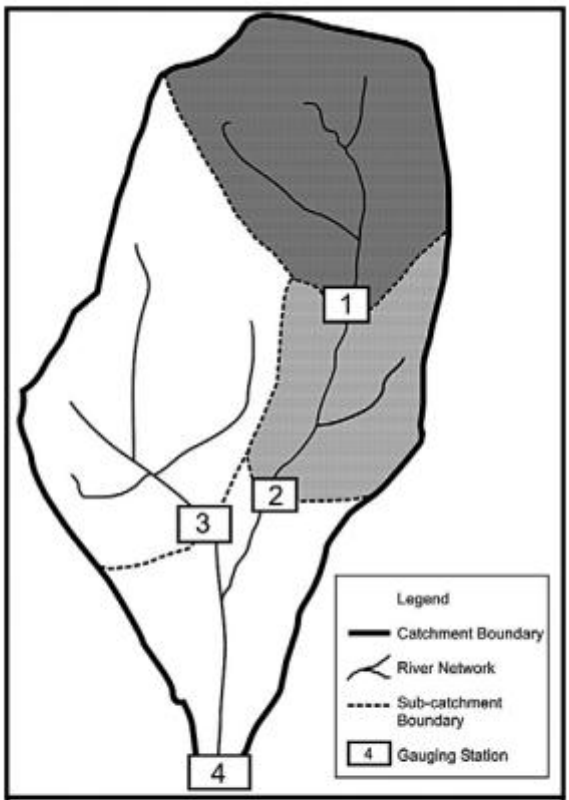

SEDIMENT YIELD CALCULATIONS	
CATCHMENT METHODS (THIS STUDY)	SUB-CATCHMENT METHODS (LAJCZAK AND JANSSON, 1993)
SY1=SL1/DA1 SY2=SL2/DA2 SY4=SL4/DA4	SY1=SL1/DA1 SY2=(SL2-SLI)/(DA2-DA1) SY4=(SL4-SL3-SL2)/(DA4-DA3-DA2)

Figure 4.7 Schematic map showing hierarchical sub-catchments.
SY: sediment yield (t km^{-2} yr^{-1}), SL: sediment load (t yr^{-1}) and DA: drainage area (km^2) (Lu et al., 2003)

The information about the stream network and sub-basin boundaries can be obtained from HYDRO 1k, a global database providing topographically derived datasets. Streams, drainage basins and ancillary layers are derived from the USGS' 30 arc-second digital elevation model of the world (GTOPO

30). HYDRO 1k uses the Pfafstette System to automatically identify all the watersheds upstream and downstream of a given basin. The Pfafstette Coding System is hierarchal and watersheds are delineated from junctions on a river network. Level 1 watersheds correspond to continental scale watersheds and higher levels represent ever-finer tessellations of the land surface into small watersheds, which are sub-watersheds of lower level watersheds. Figure 4.9 shows the level 4 and level 5 watersheds of the Zhujiang River basin extracted from the HYDRO 1k dataset. However neither of them is totally consistent with the classified watersheds from the data of MWRC which provides the measured sediment load data for this study, as can be seen from the drainage area (Table 4.4). Sub-basin boundaries are primarily regenerated based on the hierarchical relationships between streams, which can be seen from the HYDRO 1k dataset. In areas near the gauging stations, it might be difficult to determine whether a particular sub-basin should be included because the gauging stations usually lie at the junctions of river network. In this case, the drainage area data provided by MWRC and data from other researchers (e.g. Shen and Wang, 2009) are used as reference to ensure that the boundaries divide the basin in a way that the sub-basin area can best match those from MWRC and literature.

Table 4.3 Area of level 4, level 5 HYDRO 1k watersheds, sub-basins classified by MWRC and reclassified sub-basins in the Zhujiang basin

River system	River	Station	Level 4 (10^3km^2)	Level 5 (10^3km^2)	sub-basins classified by MWRC (10^3km^2)	Reclassified sub-basins (10^3km^2)
Xijiang main channel	Nanpanjiang	Xiaolongtan	15.53	9.92	15.4	15.53
	Hongshuihe	Qianjiang	53.05	4.35	113.5	116.29
	Xunjiang	Dahuangjiangkou	36.53	4.35	41.5	42.85
	Xijiang	Wuzhou	36.53	0.10	38.5	28.11
	Xijiang	Gaoyao	15.87	15.87	24.5	38.82
Xijiang tributary	Liujiang	Liuzhou	54.31	2.08	45.4	48.73
	Yujiang	Nanning	90.08	1.89	72.7	74.49
Beijiang	Beijiang	Shijiao	4.40	4.40	38.4	39.64
Dongjiang	Dongjiang	Boluo	31.12	2.79	25.3	30.07
The Zhujiang					415.2	434.53

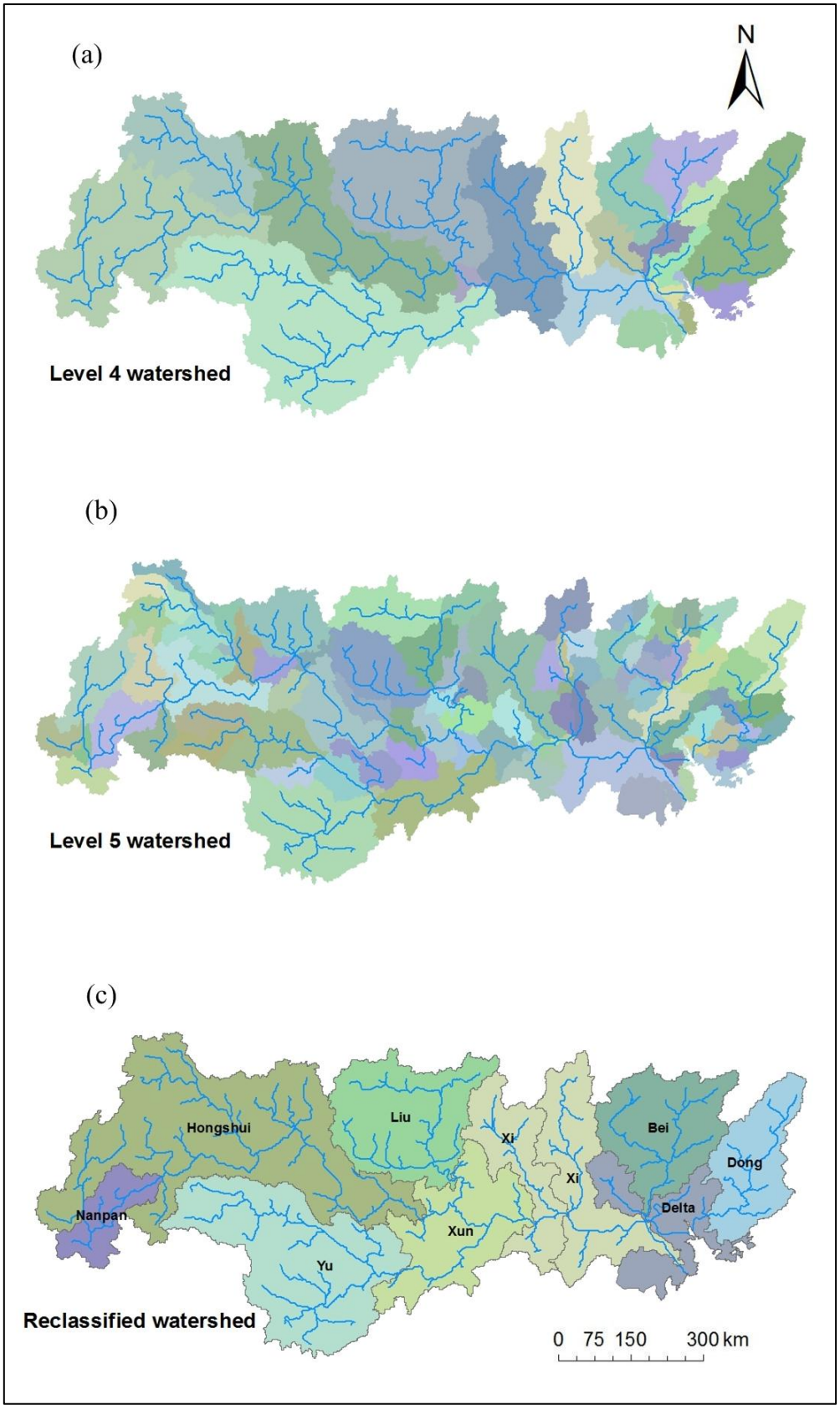

Figure 4.8 Level 4 watersheds (a), level 5 watersheds (b) and sub-basins reclassified for this study

4.3 Results and discussion

4.3.1 Modeled monthly erosion rates

After deriving the required data from the databases, grids of slope, soil erodibility, monthly fraction of vegetation cover and the monthly surface runoff for the years 1984, 1990 and 2004 were geo-referenced and resampled to 1 km×1km. The erosion rates (mm month^{-1}) for the Zhujiang River basin can be calculated using equation 4.1 in combination with the surface runoff sub-model (Equation 3.1) at a 1-km spatial scale and monthly time step. Although the monthly mean surface runoff for the whole basin is less than 10 mm, some cells have extremely large amounts of surface runoff (more than 40 mm) due to the exponential nature of the empirical relations used for surface runoff estimation or data quality problems. This gives a few abnormally high values of erosion rates. Therefore a restriction on the monthly erosion rates in each cell is given. In this study, erosion rates are assumed to be no more than 1mm month^{-1}. Table 4.5 shows the modeled erosion rates.

Basin wide erosion rates in the rainy season (from April to September) range from 0 to 0.34 mm month^{-1}, average 0.09-0.11 mm month^{-1}. Results show that more than 70% of the gross erosion occurred in the rainy seasons, which is substantially higher than that in the dry season. The temporal patterns of monthly erosion rates at the nine sub-basins are generally similar. It indicates that the temporal pattern of erosion is controlled by seasonality. It should be noted that this is not necessarily the case at the long-term scale as the gross erosion may not show a simple relationship (Trimble, 1999; Pistocchi, 2008).

Table 4.4 Modeled monthly mean and annual erosion rates in 1984, 1990 and 2004 for the Zhujiang basin

Month	1984 (mm)	1990 (mm)	2004 (mm)
January	0.00	0.02	0.01
February	0.00	0.09	0.00
March	0.00	0.08	0.00
April	0.19	0.05	0.02
May	0.28	0.20	0.11
June	0.06	0.09	0.02
July	0.05	0.14	0.34
August	0.02	0.01	0.01
September	0.05	0.05	0.00
October	0.01	0.01	0.00
November	0.00	0.01	0.00
December	0.00	0.00	0.00
Annual	0.65	0.75	0.52

4.3.2 Modeled annual erosion rates

Monthly erosion rates were summed to calculate annual erosion rates. The annual erosion rates for the entire basin in 1984, 1990 and 2004 are 0.65 mm a^{-1}, 0.75 mm a^{-1} and 0.52 mm a^{-1}. These were grouped into five classes following the guidelines established by Wall et al. (1997) (Table 4.6).

Table 4.5 Area (%) of modeled annual mean erosion rates classes for the Zhujiang basin (Wall et al. (1997))

No.	Erosion rate (mm a^{-1})	Erosion risk class	Percentage		
			1984	1990	2004
1	0-0.2	Low	58.17%	65.62%	58.45%
2	0.2-1.0	Medium	13.28%	6.60%	13.34%
3	1.0-5.0	High	28.02%	25.95%	28.15%
4	5.0-10	Very high	0.04%	1.70%	0.04%
5	>10	Extreme	0.02%	0.13%	0.02%

According to the classification scheme, about 70% of the basin experienced low to medium erosion (0 - 1.0 mm a^{-1}) and 30% high to severe intensity of erosion (>1.0 mm a^{-1}). The area under high to extreme erosion has decreased slightly by 3.1% over decades. It is hard to tell whether the slight change is caused by the uncertainties of data or a real change. Annual mean erosion rates in the sub-basins are obtained by zonal statistics using the vector map of the basin (Table 4.7). The spatial distribution of modeled annual erosion rates is presented in Figure 4.9. It can be seen that high erosion rates are concentrated in area with steep slopes and high precipitation, such as the mountainous Nanpanjiang basin and Hongshuihe basin in the upper reaches, the high-gradient mountains and hills in the middle reaches. Lower erosion rates are mainly found in the central area such as Liujiang basin (Figure 4.9). Liujiang basin is dominated by medium to high gradient hills and lower vegetation cover but still present lower erosion rates. This may be attributable to a lack of water in landscape, affected by the low precipitation in the area.

Table 4.6 Mean erosion rates in 1984, 1990 and 2004 for the sub-basins of the Zhujiang basin

River system	Station	1984	1990	2004
Nanpanjiang	Xiaolongtan	0.334	1.362	0.739
Hongshuijiang	Qianjiang	0.801	0.984	0.779
Xunjiang	Dahuangjiangkou	0.655	1.115	0.889
Xijiang	Wuzhou	0.463	0.335	0.316
Xijiang	Gaoyao	1.490	1.356	0.950
Liujiang(Tributary)	Liuzhou	0.133	0.176	0.108
Yujiang (Tributary)	Nanning	0.144	0.450	0.322
Beijiang	Shijiao	1.130	0.620	0.221
Dongjiang	Buoluo	0.783	0.551	0.096
Zhujiang (excluding the delta)		0.638	0.750	0.519

The modeled annual mean erosion rate for the Zhujiang River basin is 1.5 - 2 times as much as the overall global average erosion rate of 0.38 mm a^{-1} estimated by Yang et al. (2003). The gross erosion in mass can be estimated by multiplying erosion rate by soil density for each grid. The gross erosion of the basin is approximately 400 Mt a^{-1} in 1984 and 1990, equivalent to 2.3 times the long-term sediment yield of the basin estimated by MWRC (2004). The gross erosion in 2004 dropped significantly to 294 Mt a^{-1} because of denser vegetation.

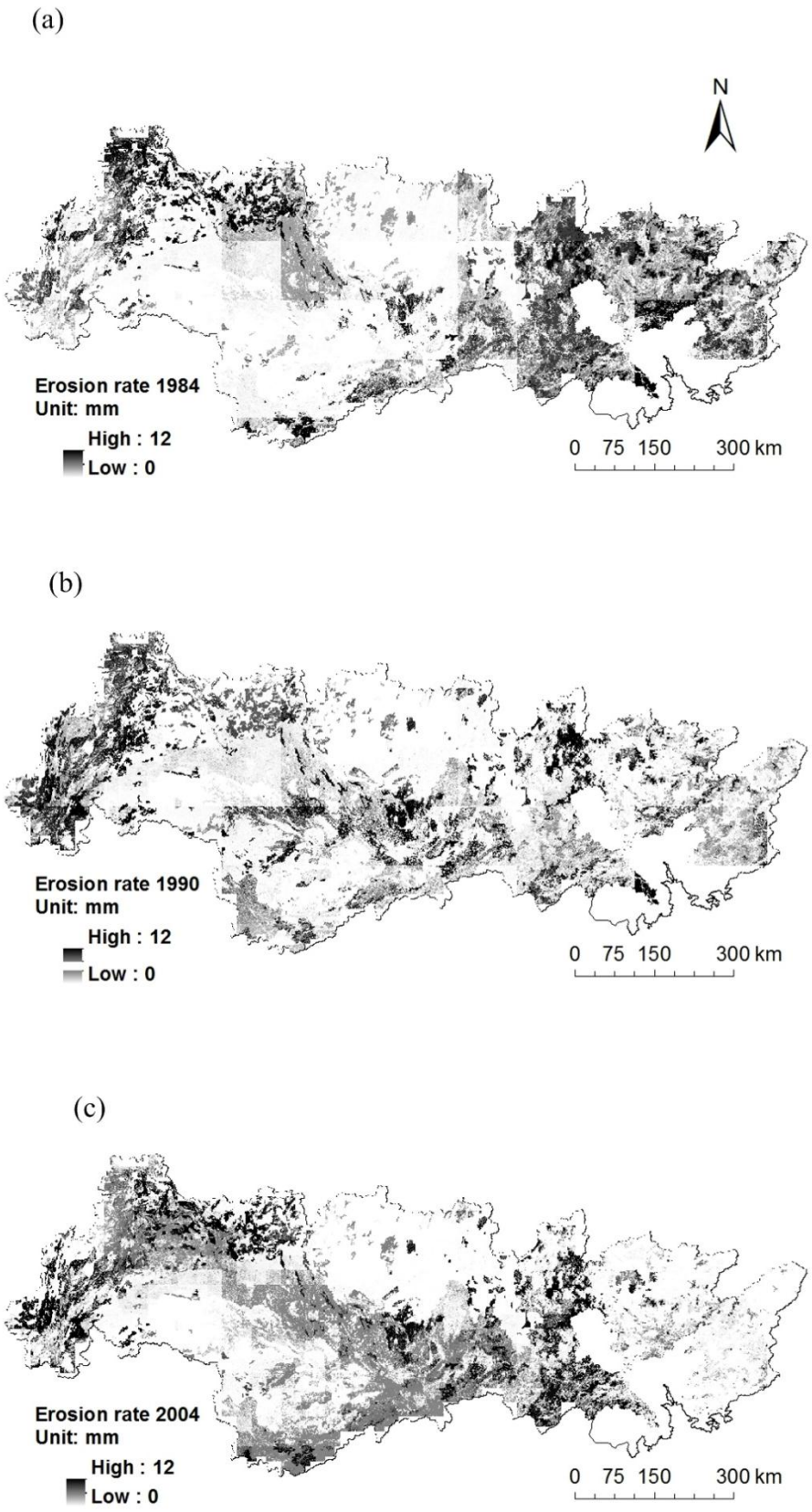

Figure 4.9 Spatial distribution of erosion rates of the Zhujiang River basin in 1984, 1990 and 2004

4.3.3 Validation of modeled erosion rates

Most of previous sediment studies in the Zhujiang river basin focused on the suspended sediment. Direct measurement of erosion rates is scarce and difficult at large spatial and temporal scales. So it is hard to do a fully quantitative validation of soil erosion rates. The model results can be validated semi-quantitatively by comparing modeled erosion rates in the basin to published erosion rates from literature. But it should be noted that the temporal and spatial scales in the literature may vary and the measured erosion rates may be influenced by the techniques used. Erosion rates in the Zhujiang river basin, areas located within the basin and other subtropical monsoon river basin from the literature in the world are presented in Table 4.7. The soil density is assumed to be 1.4 g cm^{-3} for unit conversion. A comparison of these rates to modeled erosion rates shows a generally good agreement. The modeled erosion rate for the entire basin is higher than the global average but lower than the other subtropical monsoon river basins. Wei et al. (2010) analyzed the ^{14}C values of the suspended sediment in the Zhujiang River basin and found that the soil erosion in the Xijiang basin is more severe than that in Dongjiang and Beijang basin and erosion is deeper into the soil profile in the Xijiang. This result is consistent with the modeled annual erosion rate. The high erosion rates measured in the upper reaches have been attributed to the rapid economic development and wide exposure of less erosion-resistant limestone. The modeled erosion rate is consistent with the erosion rate (1.86 mm a^{-1}) reported by MWRC. But there are a few exceptions. For example, the modeled erosion rate in the Dongjiang basin is lower than the rate obtained by USLE (Pan et al., 2010). This may be caused by the lack of data in the southern part of Dongjiang basin. As is mentioned in Chapter 3, surface runoff is this area is assumed to be 0 mm, so the mean erosion rate of Dongjiang basin is underestimated.

Table 4.7 An overview of erosion rates reported for the Zhujiang river basin, area within the basin and other subtropical monsoon basins

Location	Erosion rates (mm a^{-1})	Method or technique	Source
Zhujiang basin			
Zhujiang basin	0.519-0.750	Spatially distributed modeling	This study
Sub-basins of Zhujiang	0.096-1.356	Spatially distributed modeling	This study
Upper reaches	1.86	Suspended sediment yield	MWRC (2003)
Dongjiang basin	1.34	USLE	Pan et al. (2010)
Areas within the basin			
Guangdong Province (Red soil)	5.4-5.6	Field experiment	Li and Yao (1998)
Yunnan province (including both Yangtze River basin and Zhujiang basin)	1.0	Suspended sediment yield	Wan et al. (2005)
Red soil in southern China	4.67±2.65	Field experiment	Huang et al. (2010)
Other subtropical monsoon basins			
Maotiao River basin	2.05	RUSLE	Xu et al. (2008)
Bata river basin (India)	2.87	USLE	Mohamed Rinos et al. (1997)

Table 4.7 An overview of erosion rates reported for the Zhujiang river basin, area within the basin and other subtropical monsoon basins (continued)

Location	Erosion rates (mm a -1)	Method or technique	Sources
Dafukou Watershed	2.2-2.7	USLE	Lin et al. (2002)
Dongxi River basin	1.6-10.4	^{137}Cs technique	Pu et al. (1998)
Liao Watershed	1.3	USLE	Li et al. (2010)
Yangtze River	1.16	Suspended sediment yield	Dai et al. (1996)
South China (nine provinces)	0.22-0.43	Suspended sediment yield	Chen (1993)
China	14.7	Modeling	Yang et al. (2003)
Global average	0.38	Modeling	Yang et al. (2003)

4.3.4 Erosion rates and basin characteristics

The relationships between potential erosion rates and sub-basin characteristics like slope, surface runoff, fraction of vegetation cover have been investigated to gain a better understanding of the controls of sediment yield. The modeled annual erosion rates seem to have weak relationship with the slope (Figure 4.10 (a)). But a comparison between the soil erosion maps and slope map shows that high erosion are more likely to occur in high-gradient mountains and hills. The weak relationship can be explained by the small variation of slopes due to the smoothing effect of average value. The relationship between annual erosion rates and vegetation is weak for the same reason. The influence of vegetation cover on erosion rates can be seen more clearly on a monthly basis. Figure 4.10 (b) shows that the monthly erosion rates in the rainy seasons (from April to October) decrease with the fraction of vegetation cover. The erosion rates are controlled by the seasonality of vegetation which intercepts precipitation to the soil. The modeled erosion rates show a significant positive relationship with the surface runoff. In addition, the erosion rates are influenced by the underlying geology. The Zhujiang basin has large area of shales and granites. Shales weather more rapidly under the subtropical climate. When shales are weathered, soils rich in clays and high mineral contents will form. In the Zhujiang basin, shales yield red soils, latosols and yellow soils which are favorable to agriculture. These soils are widely distributed in the basin, especially in mountains the hills in the upper and middle reaches. The effect of bedrock is reflected in soil erodibility k. Therefore, shales have higher k and is more susceptible to erosion. The area with greater coverage of shales has higher erosion rates (0.87 mm a^{-1}). In contrast, the granites weather more slowly and the erosion rates in granite-dominated area (0.73 mm a^{-1}) are generally lower than those in shale-dominated area.

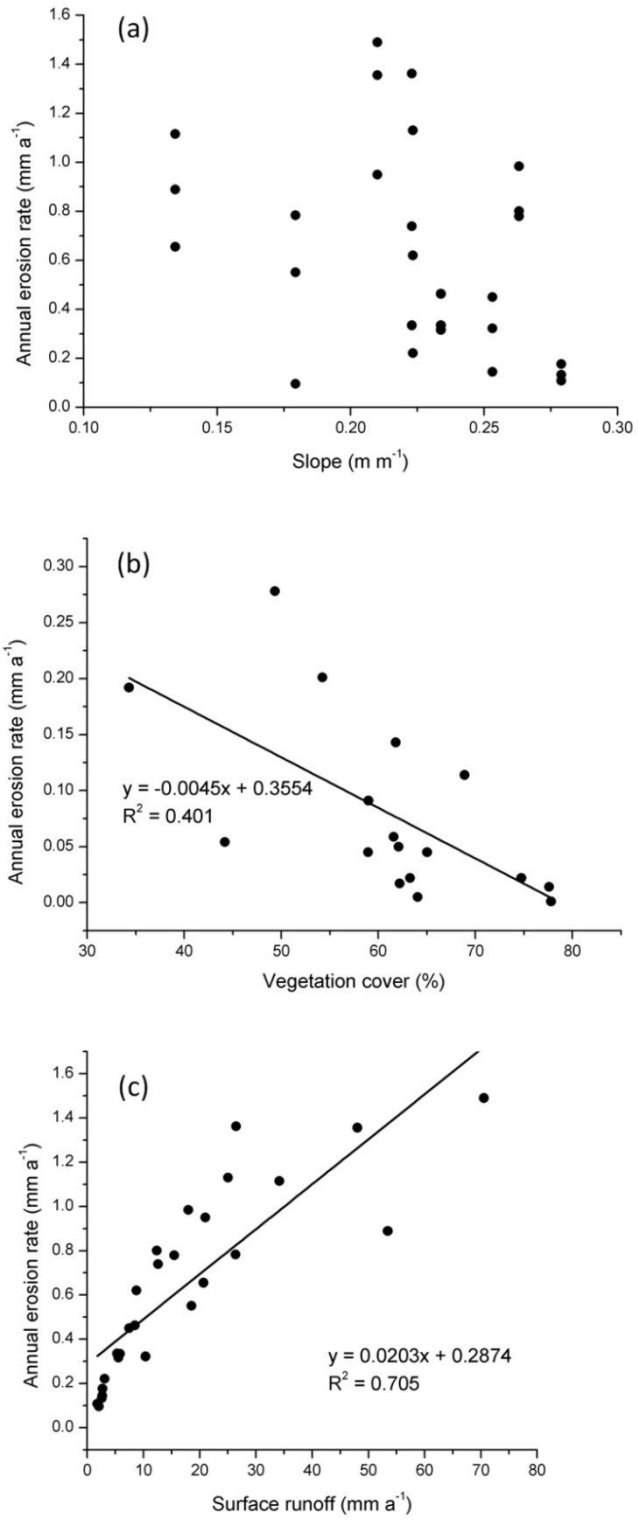

Figure 4.10 Relationship between modeled erosion rates and sub-basin characteristics: (a) slope; (b) vegetation cover; (c) surface runoff

4.4 Summary

This chapter estimates the monthly and annual soil erosion rates using Thorne's erosion model, with the surface runoff calculated in Chapter 3 as model input. Basin wide erosion rates in the rainy season (from April to September) range from 0 to 0.34 mm $month^{-1}$, average 0.09-0.11 mm $month^{-1}$. More than 70% of the gross erosion occurred in the rainy season. The similarity of temporal patterns of erosion rates in the nine sub-basins indicates that the temporal pattern of erosion is controlled by seasonality. Annual erosion rates for the entire basin in 1984, 1990 and 2004 are 0.65 mm a^{-1}, 0.75 mm a^{-1} and 0.52 mm a^{-1}, respectively. The model predicts a gross erosion of approximately twice as much as the measured sediment load. The monthly erosion rates are found to be associated with the fraction of vegetation cover, surface runoff and the underlying geology. High erosion rates are concentrated in area with steep slope and high precipitation while lower erosion rates are mostly found in the central area.

Chapter 5 Modeling sediment yield in the Zhujiang (Pearl River) basin

Reliable estimates of sediment delivered to river channels and sediment export from the drainage basin are essential in water resources analyses, modeling and engineering (Lane et al., 1997). Sediment load (t a^{-1}) from a basin is the total quantity of sediment moving out of the basin in a given time period. Sediment yield (t km^{-2} a^{-1}) is the total amount of sediment per unit area removed from the basin in a given period of time. It is a 'watershed wide' measurement of soil erosion, transport and deposition (Lane et al., 1997). Sediment yield maps can be used to indicate the regional variability of sediment sources within a drainage basin and the temporal changes in the relative contributions of parts of the catchment (Lu and Higgitt, 1998). The detached sediment is transported downslope primarily by flowing water (Walling, 1988). The efficiency of this transport process is usually represented by the concept of basin sediment delivery ratio (SDR) which is the fraction of gross eroded soil that is delivered to the outlet of the area drained (Walling, 1983; Ferro and Minacapilli, 1995). Thus, SDR represents the integrated capacity of a basin for storing and transporting eroded soil, ranging from 0 to 1. In the long term, an ephemeral or permanent stream is expected to transport all of the eroded particles to the outlet. Studies show that SDR is influenced by a wide range of factors, including drainage area, watershed characteristics as described by relief and stream length, sediment source and its proximity to the stream, transport system, texture of eroded material and land cover. (Walling 1988). Numerous models have been developed to calculate SDR. The classical SDR for a basin provides a lumped approach to sediment transport in the basin, but sediment is generated from source areas in the basin where sediment delivery characteristics are distinct. Recent studies of the sediment delivery process suggest that the relationship between area specific sediment yield and basin area is complex and non-linear (De Vente et al., 2007). Some SDR models are based on the drainage area and the distance referred to as SDR-area and SDR-distance curves respectively, e.g. Renfro's model (1975) and Vanoni

(2006). Slope, gradient, relief-length ratio and particle size have also been taken into account. These models are usually derived from statistical analysis of sediment data related to basin and climate parameters. The application of this type of models is limited by their requirement of large amount of data at local extent. So it can hardly apply to this study. Other SDR models have been based on the rainfall-runoff factors for small scale catchments, such as SWAT (Arnold et al., 1996). It cannot be used in the current study since the Zhujiang River basin is very large (4.5×10^5 km^2). Additionally, sediment data is point data, only available at the stream outlet of the nine sub-basins, even the smallest of which covers an area of 1.55×10^4km^2. The SDR-area based models calibrated using this existing sediment data can not reveal the spatial variation of sediment yield in sub-basins. Faced with such limitations, the solution is to develop a spatially distributed SDR model.

5.1 Modeling Sediment Delivery Ratio (SDR)

In this study, the spatially distributed model developed by Ferro was used. It is one of the most widely used SDR models that are spatially distributed. For modeling the within-basin variability of the sediment delivery processes, Ferro and Minacapilli (1995) proposed a sequential approach. Basically, their approach follows the sediment mass in a Lagrangian scheme and applies appropriate delivery factors to each sequential modeling morphological unit (Novotny and Chesters, 1989). Neglecting the channel sediment delivery component, Ferro and Minacapilli (1995) proposed to calculate the sediment delivery ratio SDR_i of each morphological unit i into which the basin is divided. It is assumed that the sediment particles travel along the paths of the surface runoff water. The runoff was routed from the hillslopes to the stream network. SDR is a function of the travel time t of the eroded particles along the flow path, from the area in question to the nearest stream reach. It can be calculated using the following equation:

$$SDR = e^{(-\beta t)} \tag{5.1}$$

where β is a coefficient lumping together the effects of roughness and runoff (Ferro, 1997). The sensitivity of SDR to β is watershed-specific (Ferro, 1997).

This concept was applied to catchment studies at a fine scale by Jain and Kothyari (2000). They divided a specific basin into grids instead of morphological unit and calculated the travel time for each grid. In this hypothesis, the travel time is the time (hr) from the i th overland cell to the nearest channel cell down the flow path. It is assumed that the sediment takes the same time as the runoff to reach the stream network. So the travel time for cells located in a flow path to the nearest channel can be estimated if the lengths and velocities for the flow paths are known. It is expressed as the integration of all travel time through each individual cell along the flow path:

$$t_i = \sum_{i=1}^{N_p} \frac{l_i}{v_i} \tag{5.2}$$

where l_i is the length of segment i in the flow path and is equal to the side or diagonal of a cell depending on the flow direction, v_i is the flow velocity for the cell i (m s^{-1}) and N_p is the number of cells traversed from cell i to the nearest channel. The flow direction from one cell to its neighboring cell is determined using an eight direction (D8) flow model in a grid-based GIS analysis, which chooses the direction of the steepest descent (ESRI, 2009).

Cell velocity v_i (m s^{-1}) is considered to be a function of the slope of cell and land cover characteristics:

$$v_i = d_i \sqrt{s_i} \tag{5.3}$$

where s_i is the slope of cell i (m m^{-1}), d_i is a coefficient for cell i related to land cover and the effect is measured by Manning's roughness coefficient and hydraulic radius. A coefficient map for different land cover types (Figure 5.1) can be obtained by matching the recommended values (Hann et al., 1994) to the land cover map from Global Land Cover 2000 Project (GLC 2000). Flow velocity can be calculated based on this coefficient map (Figure 5.2). The advantage of this SDR model is that it takes into account the effect of distance from stream, influence of land cover and slope along individual flow paths.

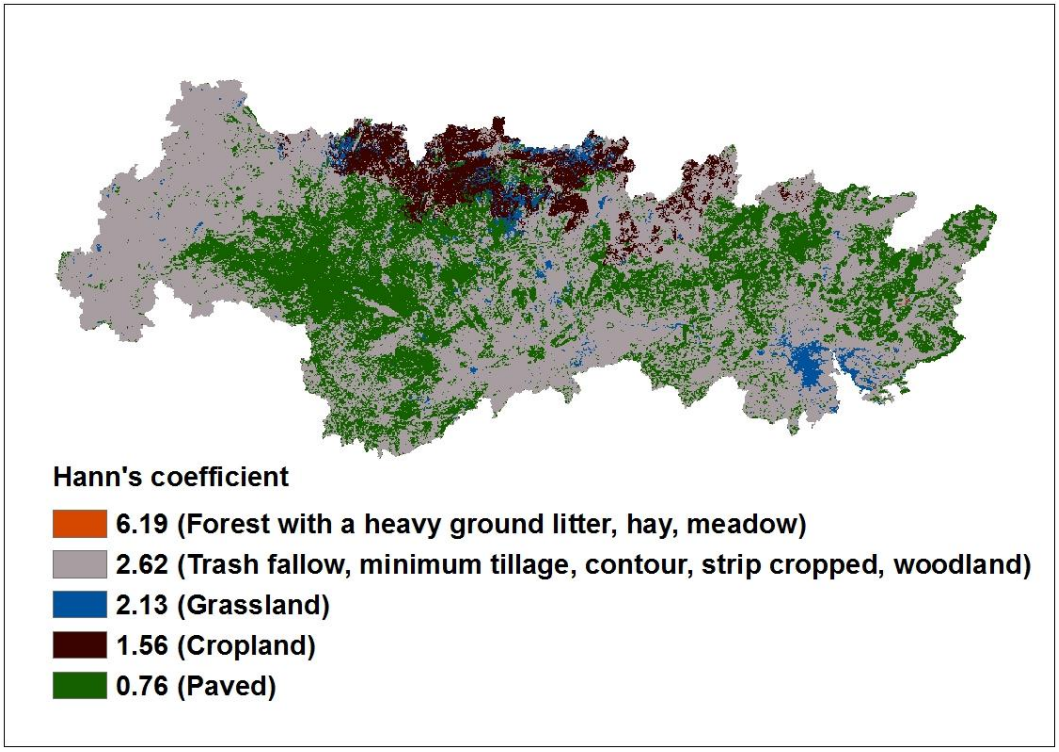

Figure 5.1 Coefficient d_i for flow velocity computation

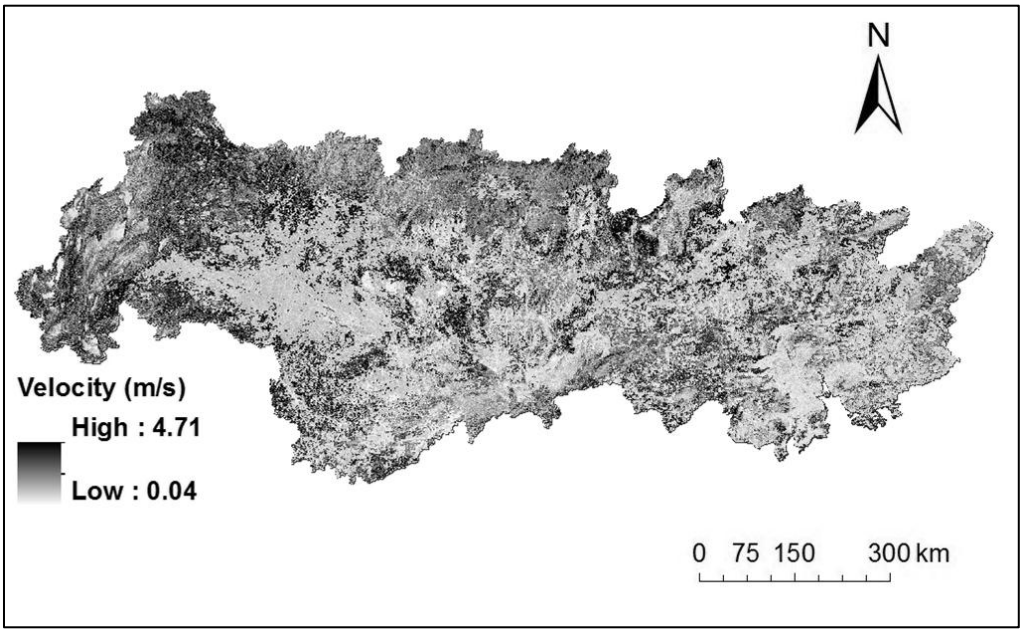

Figure 5.2 Flow velocity v_i

To calculate travel time for each cell, an indirect method was used. Flow length was estimated using the Flow Length tool in ArcGIS and an inverse velocity grid as a weighting factor to convert the length to time (Smith and

Maidment, 1995). The approach to calculate l_i is shown in Figure 5.2 (Yang et al., 2012). It should be noted that the concept of flow length in ArcGIS is different from l_i. Flow length tool in ArcGIS estimates the distance from any cell in the watershed to the outlet, which is the remotest point. In contrast, l_i refers to the distance from any cell to the nearest river channel cell (shown as shaded cells in Figure 5.3). Therefore flow path should end once the flow reaches a river channel cell. In order to end the flow path, flow direction was first identified by the D8 model based on DEM data. The flow direction codes of the river channel cells were then changed to 255 to be treated as flow sink (Devita and Long, 2005) (Figure 5.3). Once the flow path was identified using the modified flow direction, l_i can be calculated as the flow length of the corresponding cell using ArcGIS. Figure 5.4 shows the travel time of the Zhujiang River basin using the above method. The travel time for channel pixels are 0 and the values approaching unity near streams.

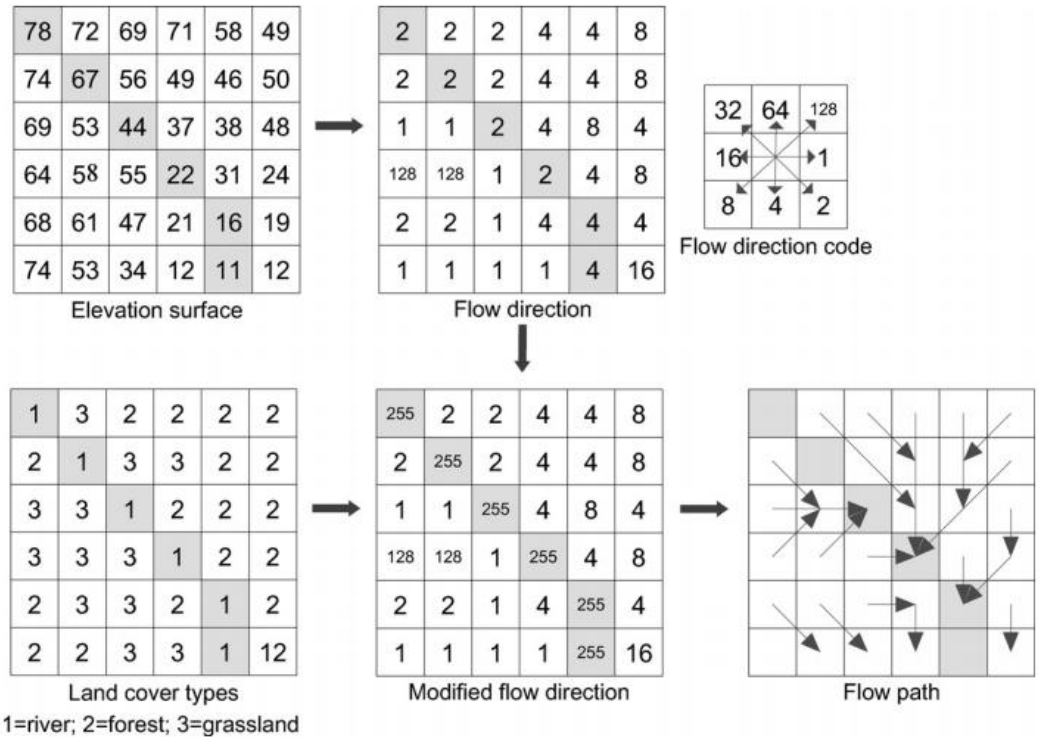

Figure 5.3 Graphic representation of the approach to identify flow path (Yang et al., 2012)

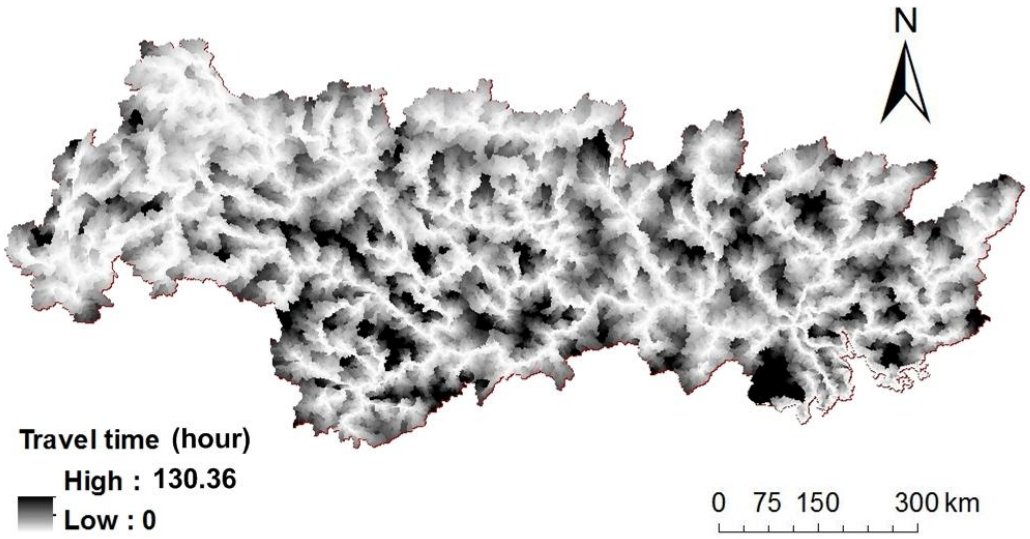

Figure 5.4 Travel time for each cell in the Zhujiang basin

To estimate β, the sensitivity of SDR to β was tested. In this study, β was considered constant. Sensitivity analysis of SDR to β shows that mean SDR for the sub-basins varies by approximately 20% when β varies from 0.1 to 0.5 with an increment of 0.1. β is assumed to be 0.3 for this study because this value produced smallest mean relative square error between modeled and measured sediment yield.

Spatially distributed SDR has been calculated for each cell in the basin using Equation (5.1) (Figure 5.5). It can be seen that any two locations that are equidistant from the basin outlet may have different travel time and delivery ratios due to differences in flow path length and slope. So the travel time does not follow concentric zones. The spatial patterns suggest increasing travel time and decreasing sediment delivery ratios with increasing distance from the stream network. This is easily explained by the equation which assumes that SDR has an inverse relationship with travel time. In the Zhujiang basin, high delivery ratios (SDR>0.6) are found in 12.1% of the basin, mostly located in the steep sub-basins like Nanpanjiang and Hongshuihe basin. The sediment delivery ratio is lower than 0.2 in 71.0% of the basin area, mostly found in the low-relief, flat-terrain area. The highest values of SDR (1.0) are in the river channel pixels. In addition, SDR

values are generally higher at the upper reaches than at the middle and lower reaches. The SDR values do not show a clear relationship with the vegetation cover SDR tends to be influenced more significantly by the character of the drainage system than by land cover (Novotny and Chesters, 1989). The average SDR for the entire Zhujiang basin is 0.184. This means that a substantial proportion of eroded particles (81.6%) have been deposited on the slopes. The modeled sediment delivery ratio of 0.184 for the Zhujiang river basin is close to the value of 0.23 for the upper Yangtze River estimated by Wang et al. (2007).

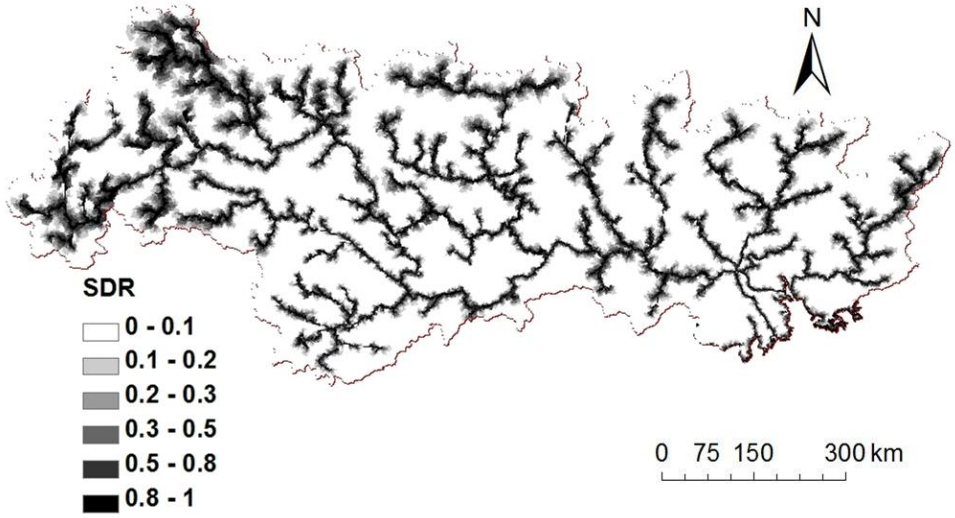

Figure 5.5 Spatial distribution of Sediment Delivery Ratio (SDR) for the Zhujiang basin

5.2 Modeled annual and monthly sediment yield

The basin has been discretized into grid cells and the sediment yield for each cell can be calculated by the following equation:

$$SY_i = SDR_i \times E_i \times d_i \tag{5.4}$$

where SY_i is the sediment yield (t km^{-2} a^{-1}) of the i th cell, SDR_i is the sediment delivery ratio, E_i is the erosion rate (mm a^{-1}) and d_i is soil density (kg m^{-3}) of the cell. The total sediment yield for a certain area can be obtained by summing up the sediment yield for all cells:

$$SY = \sum_{i=1}^{N} SY_i \tag{5.5}$$

where SY is the sediment yield of a specific area, N is the number of cells in the area. Spatially distributed annual sediment yields have been calculated by coupling sediment delivery ratios and annual erosion rates using equation (5.4). The sediment yield for the year 1984, 1990 and 2004 is 168 t km^{-2} a^{-1}, 201 t km^{-2} a^{-1}, 138 t km^{-2} a^{-1}, respectively. It is much lower than the upper Yangtze river (524 t km^{-2} a^{-1}) which is also a subtropical monsoon river basin (Lu and Higgitt, 1999). The observed sediment yield measured by MWRC is 161.86 t km^{-2} a^{-1}, 178.81 t km^{-2} a^{-1} and 64.81 t km^{-2} a^{-1}, respectively. Modeling result of annual sediment yield is fine for 1984 and 1990 but significantly overestimated for 2004 (Figure 5.6). Monthly sediment yield has been modeled and compared with the observation. Results show that in the rainy season modeled sediment yield tends to be underestimated (Figure 5.6). The models produced less variation of sediment yield than shown in the observed data. This may be partly due to the critical value we set for the monthly erosion rate in each cell. Although this approach avoid abnormally high values of erosion rates, it is also likely to reduce some peak values that did exist. It can be seen that in the dry season, modeled sediment yield is higher than the observed. This indicates that the critical value is not the only reason for the error of the model. Correlation analysis has been done between the observed monthly sediment yield and rainfall. The Pearson correlation coefficient is 0.71 for 1984 and 0.70 for 1990, suggesting that sediment yield is significant influenced by rainfall. In contrast, the correlation coefficient between the observed monthly sediment yield and modeled surface runoff is only 0.35 for 1984 and 0.43 for 1990. Better results would be expected if this relationship is more significant. It suggests that the error in estimating monthly sediment yield is very likely to be caused by the error in surface runoff modeling. As is discussed in Chapter 3, the surface runoff model does not take actual soil moisture into account. The soil water storage capacity should be dynamic and change over time. Therefore, it can be expected that modeled surface runoff will show stronger relations with the sediment yield and model errors will

be reduced if actual soil moisture is included, because rainfall influences the actual soil moisture and further influences the water storage capacity. Moreover, errors in modeling the mean sediment yield of the entire basin may cause overestimation in one region and underestimation in another. In order to better interpret the modeling results, spatial variation of modeled and observed sediment yield will be discussed in the following section.

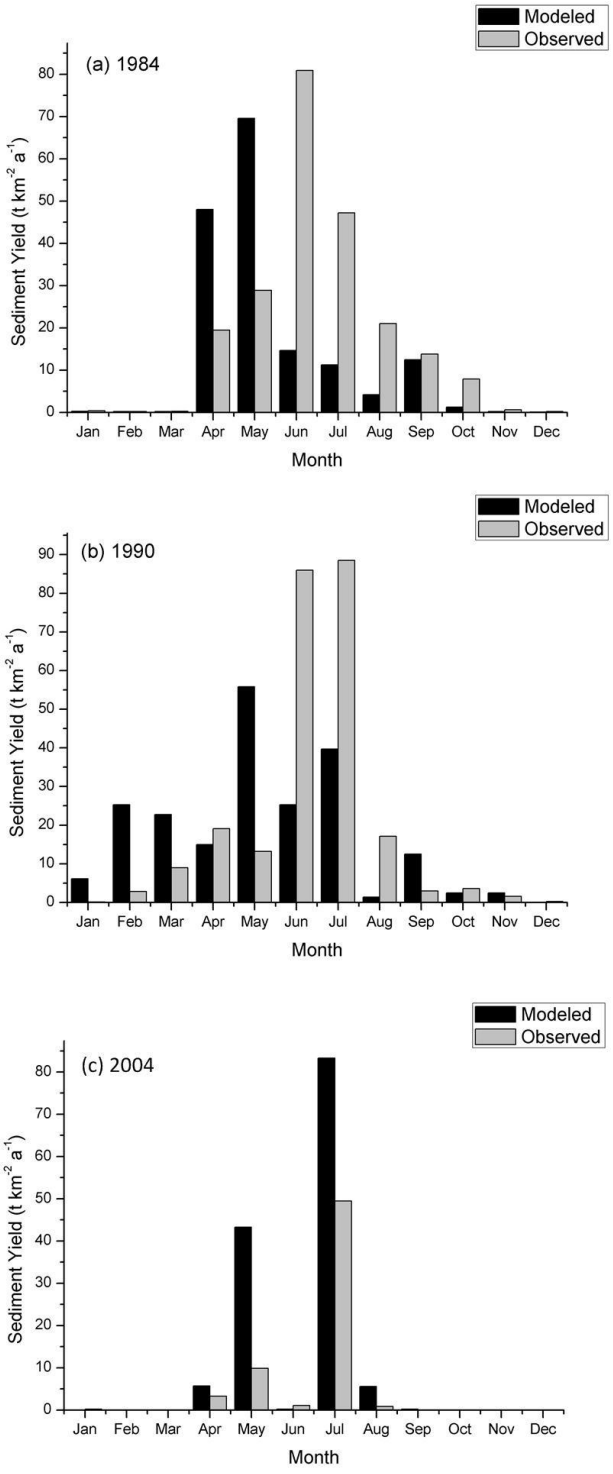

Figure 5.6 Temporal distribution of sediment yield in the Zhujiang Basin in 1984 (a), 1990 (b) and 2004 (c)

5.3 Modeled sub-basin sediment yield and sediment load

The spatially distributed annual sediment yield is presented in Figure 5.7. The modeled sediment yield exhibits an overall trend of decreasing downstream along the Zhujiang river. Although the precipitation and surface runoff are larger downstream, the largest sediment yield occurs in the upstream area, especially above the Qianjiang station (Figure 5.7). This result is consistent with the assumption of the model that not just surface runoff plays a significant role in the movement of soil particles, but that the sediment yield is also substantially affected by the other factors. Another area with high sediment yield is the lower Xijiang basin (near Gaoyao station). As part of the Pearl River Delta Economic Zone, this area is highly populated, cultivated and industrialized. Slope is not significantly correlated with sediment yield, leaving vegetation cover rather than topography as the main factor controlling sediment yield in the lower Xijiang basin. The decrease of sediment yield toward lower reaches possibly reflects the predominance of slope erosion as compared to channel erosion.

The mean sediment yield for the sub-basins was calculated using equation (5.5). The observed sediment yield data are from MWRC. In this study, the observed sediment yield is calculated by deducting the observed sediment load at the gauging station which is then divided by the incremental catchment area. It may give a negative value because sediment may have been deposited many times before it reaches the river, where further deposition may occur on flood plains, in lakes or in broad river sections upstream of the gauging stations (Jansson, 1988; Lu et al., 2003). However, the sediment yield estimated by coupling the Thornes model and SDR model always give a positive value because the major concern of the Thornes erosion model is how much eroded soil has been delivered into the channel and model only slope erosion. The channel erosion and delivery process are not included in the model. The disparity between gross erosion and sediment load suggests that a substantial amount of sediment is stored within the upstream catchment or reservoirs before the gauging stations.

Figure 5.8 shows that the modeling results of the 9 sub-basins of the Zhujiang basin are generally reasonable compared to the observed sub-basin

sediment yields except at stations with negative values. Deposition occurred in the Xunjiang basin (Dahuangjiangkou station) and the Xijiang basin (Wuzhou station). The deposition in the Xunjiang basin is mainly caused by the gentle slope (Figure 4.1), which contributes to the lowest SDR among all the sub-basins. The deposition in the Xijiang basin (Wuzhou station) can be attributable to the wide coverage of forests holding soil in place. In the other sub-basins where modeled and measured sediment yields are positive, the sediment yields in the Nanpanjiang and Hongshuihe for 1984 and 1990 have been underestimated. The reason for the underestimation may be the serious rock desertification in this area. Area under rock desertification accounts for 16.4% of the basin at upper reaches (Zhang and Yang, 2009). The rock desertification has been associated with slope farming and is exacerbated by irrational human activities, including fuel gathering and bush fires (Yuan, 1997). This phenomenon can hardly be fully reflected in the Thornes erosion model. Therefore, the modeled erosion rate and sediment yield in the Nanpanjiang and Hongshuihe basin are lower than the observed. In 2004, however, the model sediment yields before Wuzhou are much higher than the observed, particularly in the Hongshuihe basin. The estimated erosion rates in these sub-basins in 2004 decrease only slightly compared to those in 1984 and 1990. The reduction in observed sediment yield cannot be totally explained by the change in erosion rates. Therefore it is concluded that the bad performance in modeling sediment yield at the upper and middle reaches in 2004 is due to the disturbance of human activities on the natural river systems, including reservoir constructions, water diversion and hydropower generation. Reservoirs can trap substantial amount of sediment, which subsequently reduced sediment delivery to the river system. The influence of reservoirs in the upper reaches of Zhujiang has been reported (Zhang et al., 2012). Detailed information of several major reservoirs in the Zhujiang basin is listed in Table 5.2. Part of the reservoirs and dams in the basin are shown in Figure 5.9. Two large reservoirs have been built in the Hongshuihe basin before 2004. The Tianshengqiao reservoir was completed in 1989 and Yantan reservoir was completed in 1991. Located downstream of the reservoir, Qianjiang station has witnessed a dramatic decrease of average

sediment load from 64.41 Mt a^{-1} during 1981-1991 to 21.16 Mt a^{-1} during 1992-2002. And sediment yield measured at Gaoyao station decreased by 18% in the same period (Dai et al., 2007). In addition to the impact of the reservoir, the hydropower station has significantly influenced the downstream sediment yield. The Longtan hydropower station has been found to retain large amounts of sediment since it started to intercept water flow in 2003. The sediment load observed at Qianjiang station dropped to 4.36 Mt in 2004, lower than the minimum sediment load before 2004. There are numerous reservoirs and hydropower stations in the Beijiang basin. The construction of the Feilaixia reservoir was started in 1994 and put to use for power generation in 1999. But contrary to our expectation that the modeled sediment yield may be higher than the measured, the model performance at Shijiao station is fine. This can be explained by the finding of Zhang et al. (2012) that the sediment load change at the Shijiao station is the result of rainfall variation rather than the influence of reservoirs. Apart from activities to decrease sediment yield, humans may also increase natural sediment by road construction, deforestation and mining. The approach of coupling the Thornes erosion model and SDR model work well in the Zhujiang basin but the limitation of this approach is that it cannot model the delivery process and the disturbance of human activities mentioned above.

Table 5.1 Information of the major reservoirs and hydropower stations in the Zhujiang basin (Dai et al., 2007; Zhang et al., 2012)

Name	Location	Construction time	Storage capacity (10^8 m^3)
Tianshenqiao	Upstream to Qianjiang station	1984-1989	102.57
Longtan	Upstream to Qianjiang station	2003-2009	272.7
Yantan	Upstream to Qianjiang station	1985-1992	33.5
Feilaixia	Upstream to Shijiao station	1994-1999	13.36

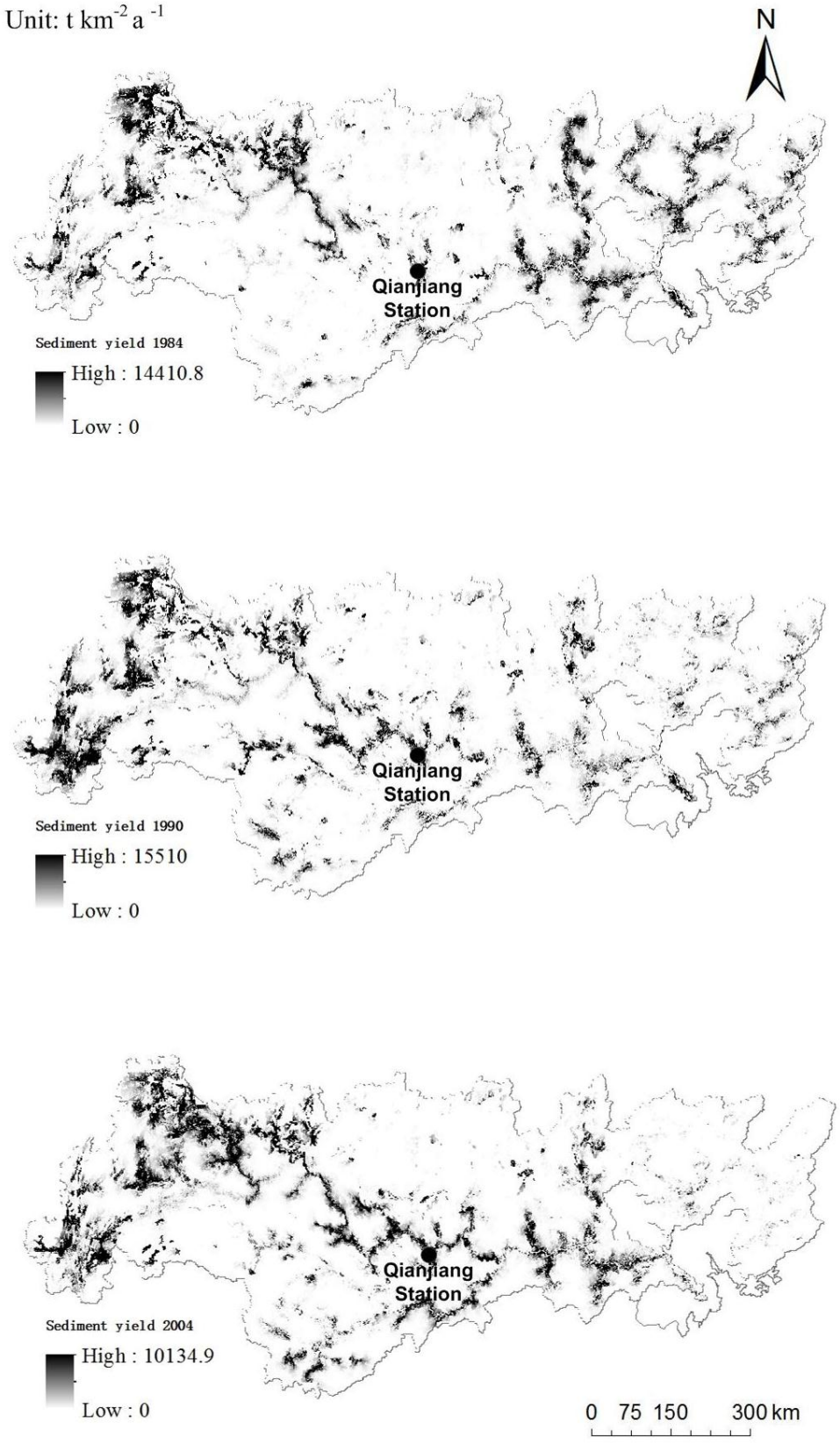

Figure 5.7 Spatial distribution of sediment yield in 1984, 1990 and 2004

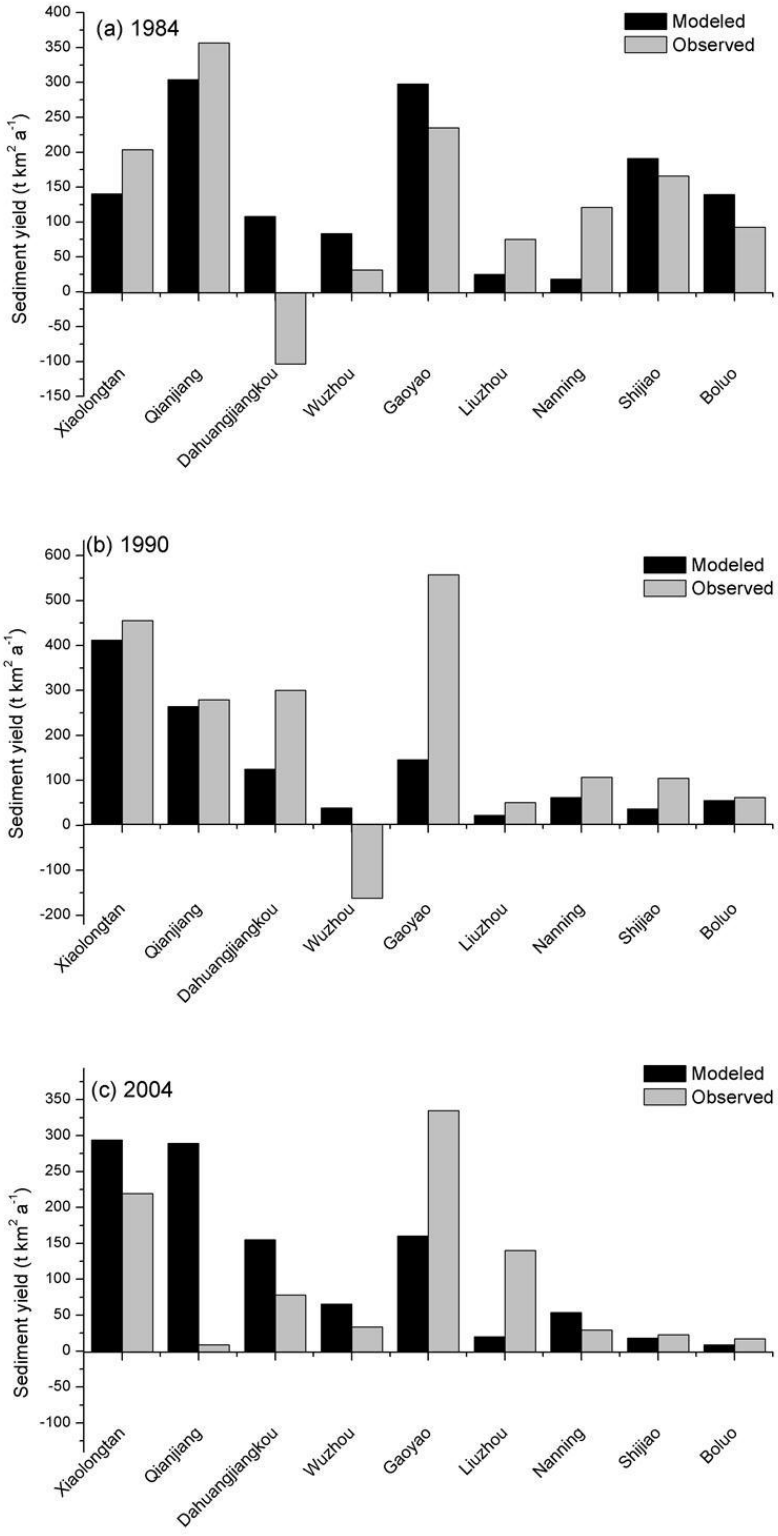

Figure 5.8 Modeled and observed sediment yield in the sub-basins of Zhujiang river basin in 1984 (a), 1990 (b) and 2004 (c)

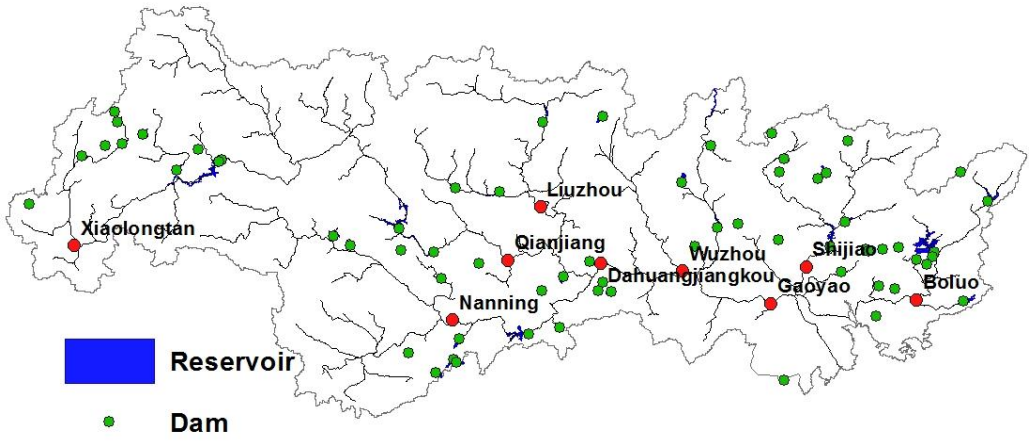

Figure 5.9 Reservoirs and dams in the Zhujiang Basin (modified from GWSP, 2011)

Correlation analysis has been done to gain a better understanding of the controlling factors of the sediment yield in the Zhuijang basin. Results show that there is no correlation between the modeled sediment yield and drainage area. This is contrary to the traditional sediment yield model which holds that sediment yield decreases with the drainage area due to the increased opportunity for sediment storage as drainage area increases. The significance of lithology has been emphasized by some researchers, for example, for the Yellow River and the Tana River (Ludwig and Probst, 1996). But in the Zhujiang basin, the difference in rock and soil erodibility is not as significant as to result in such great spatial variation of sediment yield. Elevation and maximum elevation in each sub-basin are found to be positively correlated with the annual sediment yield at 95% significance level, which is consistent with previous findings that topography exert the major controls on sediment yield (e.g. Milliman and Syvitski, 1992; Probst and Amiotte-Suchet, 1992). Other variables such as slope, relief, rainfall, and vegetation cover, are not correlated with the modeled annual sediment yield for the nine sub-basins. It indicates that the scatter of annual sediment yield is caused by the natural diversity in the basin. The spatial pattern of the sediment yield is possibly influenced by a group of factors. However, for the modeled monthly sediment yields of each sub-basins, rainfall and vegetation cover do

show some degree of association. The Pearson correlation coefficients between sediment yield and potential controlling factors for the sub-basins in 1990 are shown in Table 5.3 as an example. It can be seen that rainfall exerts a greater control on monthly sediment yields than the vegetation cover. It can be seen from the modeling results that topography is a dominant controlling factor for sediment yield in the Zhujiang basin, with rainfall and vegetation cover being the second-order influences.

Table 5.3 Pearson correlation coefficients between monthly sediment yield and potential controlling variables for the sub-basins of the Zhujiang

Station	Rainfall	Vegetation cover
Xiaolongtan	0.653*	- 0.313
Qianjiang	0.898*	0.309
Dahuangjiangkou	0.835*	- 0.234
Wuzhou	0.581*	- 0.588*
Gaoyao	0.542*	- 0.653*
Liuzhou	0.817*	0.042
Nanning	0.810*	0.284
Shijiao	0.503	- 0.422
Boluo	0.542*	- 0.173

Note: Numbers with * means that correlation is significant at the 0.05 level

Sediment loads SL (t a^{-1}) in the sub-basins are calculated by summing the sediment load in each cell, expressed as:

$$SL = \sum_{i=1}^{M} SY_i \cdot A_i \tag{5.6}$$

where SY_i is the sediment yield in i th cell (t km^{-2} a^{-1}), A_i is the area of the cell. Regarding the worse model performance in 2004 than in 1984 and 1990 due to disturbance of human activities, Table 5.2 presents the modeled sediment loads of the Zhujiang basin only in 1990. The total sediment load in 1990 is 90.70 Mt, with more than 90% coming from the Xijiang, 2.8% from the Beijiang and 3.0% from the Dongjiang. Most of the sediment in the main channel of the Xijiang is from Nanpanjing and Hongshuihe. The Xijiang (Wuzhou) contributes least to the total sediment of the Xijiang. The sediment loads generated at the upper reaches of the Zhujiang are higher than those at the lower reaches, which indicates that the basin may be supply-limited rather than transport-limited.

Table 5.2 Sediment load of sub-basins in 1990

River	Station	Modeled sediment load (Mt)	Percentage (%)
Nanpanjiang	Xiaolongtan	9.11	10.05
Hongshuihe	Qianjiang	43.54	48.01
Xunjiang	Dahuangjiangkou	7.84	8.65
Xijiang	Wuzhou	7.06	7.79
Xijiang	Gaoyao	9.09	10.03
Liujiang (Tributary)	Liuzhou	1.71	1.89
Yujiang (Tributary)	Nanning	7.06	7.79
Beijiang	Shijiao	2.54	2.80
Dongjiang	Boluo	2.73	3.01

5.4 Validation of modeled sediment yield

Model validation is required to determine whether a model is applicable. A number of quantitative statistics for model evaluation has been reviewed by Moriasi et al. (2007) and three evaluation metrics are recommended for assessing the accuracy in watershed modeling. The Nash–Sutcliffe model efficiency coefficient (NSE) determines the relative magnitude of residual variance compared to the measured variance, with 1.0 being the optimal value (Nash and Sutcliffe, 1970). The RMSE-observations standard deviation ratio (RSR) standardizes RMSE using the observations standard deviation and combines both an error and index and the additional information (Legates and McCabe, 1999). Lower RSR represents better model performance. The third metric, percent bias (PBIAS) measures the average tendency of the modeled values to be larger or smaller than their observed ones (Gupta et al., 1999). The optimal value of PBIAS is 0, with low values indicating accurate model simulation. Table 5.3 presents general model evaluation guidelines based on performance ratings for the recommended statistics.

Model evaluation of annual sediment yield was done for all the sub-basins (excluding the negative sediment yield at certain stations). For the year 1984, the

model performance is "good" to "very good" with *NSE* being 0.716, *RSR* 0.532 and *PBIAS* 6.37%. The values of the three metrics are 0.331, 0.818 and 41.4% for 1990. This major disagreement lies in the Gaoyao station where the modeled sediment yield is 145.81 t km^{-2} a^{-1} while the observed is 557.45 t km^{-2} a^{-1}. The model performance improves to "good" to "very good" without values at Gaoyao station. For the year 2004, $NSE = -0.34$, $RSR = 1.158$ and $PBIAS = -22.67\%$, suggesting unsatisfactory performance. The great difference between modeled and measured sediment yield in 2004 is mainly due to the limitation in modeling human activities and delivery process, as discussed in section 5.3. Additionally, accuracy of the model is influenced by the resolution of the data. The coarsest resolution of the dataset used in this study is 0.25 degree, equivalent to about 25 km in the study area. So local variation may be smoothed out, leading to greater errors. This effect is more obvious in small sub-basins. Moreover, model accuracy is influenced by errors associated with its data source and generation technique. In summary, the approach coupling the Thornes erosion model and sediment delivery model is acceptable in estimating sediment yield in the Zhujiang basin, considering that no field calibration for model parameters has been involved.

Table 5.3 General performance ratings for recommended statistics (Moriasi et al., 2007)

Performance rating	NSE	RSR	PBIAS (%)
Very good	0.75 < NSE ≤1.00	0.00< RSR ≤0.50	PBIAS<±15
Good	0.65 < NSE ≤0.75	0.50< RSR ≤0.60	±15≤PBIAS≤±30
Satisfactory	0.50 < NSE ≤0.65	0.60< RSR ≤0.70	±30≤PBIAS≤±55
Unsatisfactory	NSE ≤0.55	RSR > 0.70	PBIAS≥±55

5.5 Summary

This chapter investigates the sediment yield in the Zhujiang basin using a travel-time based Sediment Delivery Ratio (SDR) model. The overall SDR for the Zhujiang basin is 0.184. High delivery ratios (SDR>0.6) are found in 12.1% of the basin and low values (SDR<0.2) are found in 71.0% of the basin. The sediment yield in 1984, 1990 and 2004 is estimated to be 168 t km^{-2} a^{-1}, 201 t km^{-}

^{2} a^{-1}, 138 t km^{-2} a^{-1} respectively.. The modeled annual sediment yield exhibit an overall trend of decreasing downstream along the Zhujiang river, suggesting the predominance of slope erosion as compared to channel erosion. Correlation analysis shows that the modeled monthly sediment yield is influenced by topography, rainfall, vegetation cover and also reservoirs.

Chapter 6 Conclusion

6.1 Overview of the study

Rivers play a critical role in transporting eroded soil from mountains to lowlands and the oceans. Soil erosion is a complex natural process that can be significantly accelerated by human activities. Intensified soil erosion in a drainage basin not only reduces soil productivity but also causes problems for rivers by increasing sediment delivered to rivers, such as disruption of river ecosystems, siltation of reservoirs and morphological changes in the coast. Soil erosion and sediment dynamics in river basins is thus a great concern. The Zhujiang (Pearl River) the second largest river in China draining a large area of the country. The high precipitation and gradient in the basin provide favorable conditions for soil erosion. In addition, like most of the rivers in China, the Zhujiang has undergone strong disturbance by human activities in the past decades. Soil erosion has become one of the major environmental problems in the Zhujiang basin, especially in the upper reaches of the river. Therefore, it is necessary to gain an understanding of the soil erosion and sediment dynamics of the Zhujiang basin. In view of the difficulty of applying expensive and time consuming field-based methods at such a large spatial scale, this study utilizes a modeling framework of estimating soil erosion rates and sediment yields in different years in the Zhujiang basin by coupling spatially distributed models of erosion and sediment delivery. Erosion rates were estimated using the Thornes model in combination with Carson and Kirkby's surface runoff model based on global environmental datasets. Modeling was done in a GIS environment at 1-km spatial resolution and at monthly time steps. The relationship between modeled erosion rates and basin characteristics, the controlling factors for sediment yield in the Zhujiang basin as well as model performance has been investigated. In the following sections, the main findings of the study, their implications, limitations of this study and recommendations for future study are summarized.

6.2 Main findings of the study and the implications

Monthly surface runoff has been modeled with Carson and Kirkby's model (1972) based on monthly data of rainfall, the number of rainy days, soil moisture content at field capacity, soil bulk density, AET/PET ratio and effective hydrological depth. Influenced by the East Asian monsoon, the division between dry and wet seasons is evident, with approximately 80% rainfall in the wet seasons. Basin-wide surface runoff in the summer months of June, July and August is generally higher than in other months. The monthly surface runoff in 2004 has a greater temporal variation possibly due to greater variation of rainfall. In January, when the rainfall is generally low, the surface runoff increases from the western to the eastern part of the basin. In July, a large amount of surface runoff is generated in the Nanpanjiang and Hongshuihe basin because of low water storage capacity. The greater runoff in the Xunjiang is associated with higher precipitation. Surface runoff in July peaks in the southeastern corner of the Xijiang basin, which is quite close to the Zhujiang River Delta where the AET/PET ratio is low due to large area of urban and built-up land despite a high temperature. Monthly surface runoff was summed to obtain annual surface runoff. The annual mean surface runoff for the entire basin is 21.21mm in 1984, 19.35 mm in 1990 and 7.07 mm in 2004. The spatial pattern of annual surface runoff is similar to that in July, with greatest runoff generated in the eastern and southwestern area. The exponential nature of the Carson and Kirby's model result in significant spatial and temporal variation in annual surface runoff.

The monthly erosion rates were estimated using the Thornes model which comprises a runoff component, a sediment transport component and a vegetation cover component. The fraction of vegetation cover in the Zhujiang basin remained almost unchanged from 1984 to 1990 while from 1990 to 2004 it increased in 35% of the basin. For the three years studied, the modeled basin-wide erosion rates in the rainy season (from April to September) range from 0.00 to 0.34mm $month^{-1}$, average 0.09 - 0.11 mm $month^{-1}$. More than 70% of the gross erosion occurred in the rainy seasons. The temporal patterns of monthly erosion rates at the nine sub-basins are generally similar. It indicates that the temporal pattern of

erosion is controlled by seasonality. Monthly erosion rates were summed to calculate annual erosion rates. The annual mean erosion rates for the entire basin in 1984, 1990 and 2004 are 0.65 mm a^{-1}, 0.75 mm a^{-1} and 0.52 mm a^{-1}, about 1.5-2 times as much as the overall global average. The erosion rates in each sub-basin ranges from 0.11mm a^{-1} to 1.49 mm a^{-1}. Approximately 70 % of the basin has experienced low to medium erosion and the other 30% is under high to severe intensity of erosion. High erosion rates are concentrated in area with steep slopes and high precipitation, including the mountainous Nanpnajiang and Hongshuihe basin in the upper reaches and the high-gradient mountains and hills in the middle reaches. Lower erosion rates are mostly found in the central area like Liujiang basin. The soil erosion in the Xijiang basin is more severe than that in Dongjiang and Beijang basin. The gross erosion of the basin is approximately 400 Mt a^{-1} in 1984 and 1990, equivalent to 2.3 times the long-term sediment yield. This figure decreased to 294 Mt a^{-1} despite denser vegetation in 2004. The disparity between gross erosion and sediment load suggests that a substantial amount of sediment is stored within the upstream catchment or reservoirs before the gauging stations. Semi-quantitative validation shows that the modeled erosion rates are generally consistent with published values. The monthly erosion rates is negatively correlated with the fraction of vegetation cover and positively correlated with the surface runoff. In addition, the erosion rates are influenced by the underlying geology. The erosion rates in granite-dominated area (0.73 mm a^{-1}) are generally lower than those in shale-dominated area (0.87 mm a^{-1}).

The spatially distributed sediment delivery ratio (SDR) model developed by Ferro and Minacapilli (1995) is used to calculate the capacity of the Zhujiang basin for storing and transporting eroded soil. The SDR model takes into account the effect of distance from the stream network, influence of land cover and slope along individual flow paths. The average SDR for the entire Zhujiang basin is 0.184. High delivery ratios (SDR>0.6) are found in 12.1% of the basin, mostly located in the steep sub-basins like Nanpanjiang and Hongshuihe basin. The sediment delivery ratio is lower than 0.2 in 71.0% of the basin area, mostly found in the low-relief, flat-terrain area. The sediment yield in 1984, 1990 and 2004

calculated by coupling sediment delivery ratios and annual erosion rates is 168 t km^{-2} a^{-1}, 201 t km^{-2} a^{-1}, 138 t km^{-2} a^{-1} respectively.. The modeling result is fine for 1984 and 1990 but overestimated for 2004. The modeled annual sediment yield exhibit an overall trend of decreasing downstream along the Zhujiang river. Large sediment yield occurs mostly along the upper reaches, especially above the Qianjiang station. The decrease of sediment yield toward lower reaches possibly reflects the predominance of slope erosion as compared to channel erosion. Correlation analysis indicates that the modeled monthly sediment yield is influenced by various factors, with topography being a dominant controlling factor, and rainfall and vegetation cover being the second-order influences. The Xijiang is found to contribute most to the total sediment load of the Zhujiang basin. Most of the sediment in the main channel of the Xijiang is from Nanpanjing and Hongshuihe. The Xijiang (Wuzhou) contributes least to the total sediment of the Xijiang. The sediment loads generated at the upper reaches of the Zhujiang are higher than those at the lower reaches, suggesting that the basin may be supply-limited rather than transport-limited.

Model evaluation based on quantitative statistics suggests good performance in modeling sub-basin sediment yields in 1984 and 1990 but unsatisfactory for 2004. The disagreement is largely due to the limitation in modeling delivery process and disturbance of human activities, particularly the construction of reservoirs. The approach of coupling the Thornes erosion model and sediment delivery model is acceptable for the Zhujiang basin considering that no calibration has been done. It is expected that calibrating model parameters would improve model accuracy.

6.3 Limitation of the study and recommendations for the future work

Erosion rates and sediment yields were satisfactory modeled using the proposed low-data demanding, spatially distributed models in this study and a better understanding of the basin-wide sediment dynamics has been achieved. However, some of the limitations need to be addressed in future studies.

Recent development and increased availability of geospatial datasets in

combination with GIS techniques have provided an opportunity for spatially distributed modeling at large temporal and spatial scales, facilitating fast and easy data acquisition. However, the coverage and resolution of certain datasets is still limited. For example, the land cover data from GIMMS used in this study is at 0.25 degree. Local variation is smoothed out at such a coarse resolution, increasing the uncertainty of the model results based on this dataset. This influence is more obvious in a small area. Model accuracy is also influenced by errors associated with the data sources and generation techniques. In addition, incompatibility issues are associated with combining different types of data at differing scales and resolutions (Gotway and Young, 2002). Therefore, a need for finer resolution and more reliable datasets should be emphasized.

The surface runoff model applied in this study is very sensitive to the soil water storage capacity. However, the actual influence of soil moisture on the water storage capacity of soil is not considered in the runoff model. Attempts can be made to include the actual soil moisture. The soil erosion model and sediment delivery model is very simple. The inclusion of potential influencing factors and processes on sediment dynamics may improve the model accuracy. The Thornes model estimates only slope erosion and the SDR model is based on the assumption that little anthropogenic disturbance is involved in the sediment delivery process. So the next step should be increasing complexity of the model by taking bank and channel erosion and human activities into account. This study investigates the erosion and sediment yields only in 1984, 1990 and 2004 for comparison in different periods due to time limitation. Another possible step in future could be modeling the sediment dynamics for each year since 1950s, when the field sediment data is available. Time series analysis can be done to reveal the temporal variation and controlling factors of erosion on a long-term basis. Furthermore, the response of soil erosion and sediment yield to the land use/cover change over time can be explored based on remote sensing image. With more information about the complex anthropogenic effects in the basin, such as the amount of sediment trapped in the reservoirs, a sediment budget can be constructed as part of future work.

Model calibration and validation are extremely important. This study used recommended values from literature for model parameters, including moisture content and effective hydrological depth which the results are very sensitive to. To decrease the uncertainty in model parameters, field-based calibration should be done. Validation of model requires a comparison between the observed and modeled values. However, observed data is available at only nine stations in this study. Regarding the large spatial scale of the Zhujiang, field-based erosion data and sediment yield data at more gauging stations, as well as information on their corresponding drainage sub-basins are required. In summary, finer resolution and reliable datasets, inclusion of more processes and field data to obtain more accurate estimation represent possible future work for this study.

References

Abbott, M. B., Bathurst, J. C., Cunge, J. A., et al. 1986. An introduction to the European Hydrological System—Systeme Hydrologique Europeen,"SHE", 1: History and philosophy of a physically-based, distributed modelling system. Journal of Hydrology, 87, 45-59.

Abbott, M. B.and Refsgaard, J. C. 1996. Distributed hydrological modelling, Springer.

Aksoy, H.and Kavvas, M. L. 2005. A review of hillslope and watershed scale erosion and sediment transport models. CATENA, 64, 247-271.

Ali, K. F. and De Boer, D. H. 2010. Spatially distributed erosion and sediment yield modeling in the upper Indus River basin. Water Resources Research, 46, W08504.

Ali, K. F. and De Boer, D. H. 2003. Construction of sediment budgets in large-scale drainage basins: the case of the upper Indus River, in Erosion Prediciton of Ungauged Basins (PUBs): Integrating Methods and Techniques, edited by D. H. De Boer et al., IAHS Publ., 279, 206-215.

Andersen, J., Refsgaard, J. C.and Jensen, K. H. 2001. Distributed hydrological modelling of the Senegal River Basin — model construction and validation. Journal of Hydrology, 247, 200-214.

Anh Luu, T. 2009. Regional scale soil erosion modeling for onservation planning using remote sensing and GIS techniques - A case study in the centre of Himalayan Ranges, viewed 01 April 2013. < http://www.fig.net/pub/vietnam/papers/>.

Arnell, N. 1996. Global warming, river flows and water resources. Wiley, New York

Arnold, J. G., Williams, J. R., Srinivasan, R. and King. K. W. 1996. SWAT: Soil and Water Assessment Tool. Temple Texas: USDA–ARS Grassland Soil and Water Research Laboratory.

Atucha, A., Merwin, I. A., Brown, M. G., et al. 2012. Soil erosion, runoff and nutrient losses in an avocado (Persea americana Mill) hillside orchard under different groundcover management systems. Plant and Soil, 1-14.

Bakker, M. M., Govers, G., van Doom, A., et al. 2008. The response of soil erosion and sediment export to land-use change in four areas of Europe: The importance of landscape pattern. Geomorphology, 98, 213-226.

Beasley, D.B., L.F. Huggins, and E.J. Monke. 1980. ANSWERS: A Model for. Watershed Planning. Transactions of the ASAE 23(4):938-944.

Beck, M. B. 1987. Water quality modeling: A review of the analysis of uncertainty. Water Resources Research, 23, 1393-1442.

Beven, K. 1989. Changing ideas in hydrology — The case of physically-based models. Journal of Hydrology, 105, 157-172.

Beven, K. 1995. Linking parameters across scales: Subgrid parameterizations and scale dependent hydrological models. Hydrological Processes, 9, 507-525.

Beven, K. 1997. TOPMODEL: A critique. Hydrological Processes, 11, 1069-1085.

Blaszczynski, J. 2001. Regional sheet and rill soil erosion prediction with the RUSLE-GIS Interface, Bureau of Land Management Resource Notes No. 46, viewed 1st April 2013. <http://www.blm.gov/nstc/resourcenotes/respdf/RN46.pdf>.

Boardman, J., Ligneau, L., de Roo, A., et al. 1994. Flooding of property by runoff from agricultural land in northwestern Europe. Geomorphology, 10, 183-196.

Boughton, W. 2004. The Australian water balance model. Environmental Modelling & Software, 19, 943-956.

Brown, M. E., Pinzón, J. E., Didan, K., et al. 2006. Evaluation of the consistency of long-term NDVI time series derived from AVHRR, SPOT-Vegetation, SeaWiFS, MODIS, and Landsat ETM+ sensors. Geoscience and Remote Sensing, IEEE Transactions on, 44, 1787-1793.

Bryan, R. B. 2000. Soil erodibility and processes of water erosion on hillslope. Geomorphology, 32, 385-415.

Carson, M. A.and Kirkby, M. J. 1972. Hillslope form and process, Cambridge University Press Cambridge.

Chen, C. H., 1993. An available measure for promoting the recovery of degraded land productivity. Improving Degraded lands: Promising Experiences from South China, Bishop museum press, Honolulu.

Chen, Y. D., Zhang, Q., Lu, X., et al. 2011. Precipitation variability (1956–2002) in the Dongjiang River (Zhujiang River basin, China) and associated large-scale circulation. Quaternary International, 244, 130-137.

Chen, Y. Q. D., Zhang, Q. A., Xu, C. Y., et al. 2010. Multiscale streamflow variations of the Pearl River basin and possible implications for the water resource management within the Pearl River Delta, China. Quaternary International, 226, 44-53.

Chiew, F. H. S. 2010. Lumped Conceptual Rainfall-Runoff Models and Simple Water Balance Methods: Overview and Applications in Ungauged and Data Limited Regions. Geography Compass, 4, 206-225.

Chiew, F., Peel, M., Western, A., et al. 2002. Application and testing of the simple rainfall-runoff model SIMHYD. Mathematical models of small watershed hydrology and applications, 335-367.

Chin, D. A. 2000. Water-resources engineering, Prentice Hall.

Chu, Z. X., Zhai, S. K., Lu, X. X., et al. 2009. A quantitative assessment of human impacts on decrease in sediment flux from major Chinese rivers entering the western Pacific Ocean. Geophysical Research Letters, 36, L19603.

Clark, E.H. 1985. The off-site costs of soil erosion. Journal of Soil and Water Conservation 40, 19 – 22.

Critchley, W. 1991. Water harvesting : a manual for the design and construction of water harvesting schemes for plant production, FAO.

Croke, B. F., Andrews, F., Jakeman, A. J., et al. 2006. IHACRES Classic Plus: A redesign of the IHACRES rainfall-runoff model. Environmental Modelling & Software, 21, 426-427.

Crutzen, P. 2006. The “Anthropocene”. In: EHLERS, E. & KRAFFT, T. (eds.) Earth System Science in the Anthropocene. Springer Berlin Heidelberg.

Dai, S. B., Yang, S. L. and Cai, A. M. 2007. Variation of sediment discharge of the Pearl River Basin from 1955 to 2005. Acta Geographica Sinica, 62 (5): 545-554 (in Chinese).

Dai, S. B.and Lu, X. X. Sediment load change in the Yangtze River (Changjiang): A review. Geomorphology.

Davie, T. 2002. Fundamentals of hydrology. Routledge fundamentals of physical geography. Abingdon, Oxon: Routledge.

De Roo, A. P. J., Wesseling, C. G.and Van Deursen, W. P. A. 2000. Physically based river basin modelling within a GIS: the LISFLOOD model. Hydrological Processes, 14, 1981-1992.

De Roo, A., Wesseling, C. G., Jetten, V. G., et al. 1996. LISEM: a physically-based hydrological and soil erosion model incorporated in a GIS. IAHS Publication, 235, 395-403.

De Vente, J., Poesen, J., Arabkhedri, M., et al. 2007. The sediment delivery problem revisited. Progress in Physical Geography, 31, 155-178.

Dedkov, A. P.and Mozzherin, V. I. 1992. Erosion and sediment yield in mountain regions of the world. Erosion, debris flows and environment in mountain regions, 209, 29-36.

DeVita, S.H., Long, J.A. 2005. GIS-based Soil Erosion and Sediment Delivery Model for the Fairchild Creek Watershed, Ontario.

Eckhardt, K.and Ulbrich, U. 2003. Potential impacts of climate change on groundwater recharge and streamflow in a central European low mountain range. Journal of Hydrology, 284, 244-252.

ESRI 2009. ArcGIS Desktop Help 9.3, viewed 1st May 2013.< http://webhelp.esri.com/arcgiSDEsktop/9.3/index.cfm?TopicName=Determining_flow_direction>.

Eswaran, H., R. Lal and P.F. Reich. 2001. Land degradation: an overview. In: Bridges, E.M., I.D. Hannam, L.R. Oldeman, F.W.T. Pening de Vries, S.J. Scherr, and S. Sompatpanit (eds.). Responses to Land Degradation. Proc. 2nd. International Conference on Land Degradation and Desertification, Khon Kaen, Thailand. Oxford Press, New Delhi, India.

Evans, R. 2002. An alternative way to assess water erosion of cultivated land – field-based measurements: and analysis of some results. Applied Geography, 22, 187-207.

FAO, ISRIC and ISSCAS 2009. Harmonized World Soil Database (version 1.1). FAO, Rome, Italy and IIASA, Laxenburg, Austria.

Feng, X., Suoyan, G.and Zengxiang, Z. 2002. Soil erosion in China based on the 2000 national remote sensing survey. Journal of Geographical Sciences, 12, 435-442.

Fernandez, C., Wu, J. Q., McCool, D. K., et al. 2003. Estimating water erosion and sediment yield with GIS, RUSLE, and SEDD. Journal of Soil and Water Conservation, 58, 128-136.

Ferro, V. 1997. Further remarks on a distributed approach to sediment delivery. Hydrological Sciences Journal, 42, 633-647.

Ferro, V.and Minacapilli, M. 1995. Sediment delivery processes at basin scale. Hydrological Sciences Journal, 40, 703-717.

Ferro, V.and Porto, P. 2000. Sediment Delivery Distributed (SEDD) Model. Journal of Hydrologic Engineering, 5, 411-422.

Fischer, T., Gemmer, M., Lüliu, L., et al. 2011. Temperature and precipitation trends and dryness/wetness pattern in the Zhujiang River Basin, South China, 1961–2007. Quaternary International, 244, 138-148.

Folland, C. K., Rayner, N. A., Brown, S. J., et al. 2001. Global temperature change and its uncertainties since 1861. Geophysical Research Letters, 28, 2621-2624.

Foster, G. R. 1982. Modeling the erosion process. In Hydrology Modeling of Small Watersheds. American Society of Agricultural Engineers, eds. Haan, C. T., Johnson, H. P. and Brakensiek, D.L., 297-380.AWAE, St. Joseph, Michigan, USA.

Fournier, F. 1972. Soil conservation. Nature and Environment Series, Council of Europe.

García-Ruiz, J. M. 2010. The effects of land uses on soil erosion in Spain: A review. CATENA, 81, 1-11

Garnier, J., Billen, G., Hannon, E., et al. 2002. Modelling the Transfer and Retention of Nutrients in the Drainage Network of the Danube River. Estuarine, Coastal and Shelf Science, 54, 285-308.

Gemmer, M., Fischer, T., Jiang, T., et al. 2010. Trends in Precipitation Extremes in the Zhujiang River Basin, South China. Journal of Climate, 24, 750-761.

Global Water System Project 2011. Global Reservoir and Dam (GRanD) Database, retrieved 5th Jun, 2013. < http://www.gwsp.org/products/grand-database.html >.

Gotway, C. A.and Young, L. J. 2002. Combining incompatible spatial data. Journal of the American Statistical Association, 97, 632-648.

Govers, G., Takken, I.and Helming, K. 2000. Soil roughness and overland flow. Agronomie, 20, 131-146.

Gupta, A.and Ping, C. 2002. Sediment movement on steep slopes to the Mekong River: An application of remote sensing. International Association of Hydrological Sciences, Publication, 399-406.

Gupta, H., Sorooshian, S.and Yapo, P. 1999. Status of Automatic Calibration for Hydrologic Models: Comparison with Multilevel Expert Calibration. Journal

of Hydrologic Engineering, 4, 135-143.

Gutteridge, H., Davey, 1991. Integrated Quantity/Quality Modelling—Stage 3, Gutteridge. Haskins and Davey, for Department of Water Resources, Sydney, 102.

Gutteridge, H., Davey, Ernst, et al. 1991. Rural Water Commission Future Management Review: Options Paper, Gutteridge, Haskins and Davey.

Haan, C. T., Barfield, B. J.and Hayes, J. C. 1994. Design Hydrology and Sedimentology for Small Catchments, Academic Press.

Harrison, C. G. A. 2000. What factors control mechanical erosion rates? International Journal of Earth Sciences, 88, 752-763.

He, X., Li, Z., Hao, M., et al. 2003. Down-scale analysis for water scarcity in response to soil–water conservation on Loess Plateau of China. Agriculture, Ecosystems & Environment, 94, 355-361.

He, X., Zhou, J., Zhang, X., et al. 2006. Soil erosion response to climatic change and human activity during the Quaternary on the Loess Plateau, China. Regional Environmental Change, 6, 62-70.

Herweg, K. 1996. Field manual for assessment of current erosion damage. Soil Conservation Research Programme, Ethiopia and Center for Development and Environment, University of Berne, Switzerland.

Houghton, R. A. 1999. The annual net flux of carbon to the atmosphere from changes in land use 1850–1990*. Tellus B, 51, 298-313.

Hoyos, N. 2004. Spatial and temporal patterns of soil erosion potential in a mountainous tropical watershed, central Andean Cordillera of Colombia. 3136953 Ph.D., University of Florida.

Huang, Z., Ouyang, Z., Li, F., et al. 2010. Response of runoff and soil loss to reforestation and rainfall type in red soil region of southern China. Journal of Environmental Sciences, 22, 1765-1773.

International Water Management Institute (IWMI) 2008. World Water and

Climate Atlas, viewed 1st March, 2013. < http://www.iwmi.cgiar.org/resources/world-water-and-climate-atlas/ >.

IPCC (International Panel on Climate Change) 2007: Climate Change 2007: The Physical Science Basis. Contribution of Working Group I to the Fourth Assessment Report of the Intergovernmental Panel on Climate Change [Solomon, S., D. Qin, M.

Jain, M. K.and Kothyari, U. C. 2000. Estimation of soil erosion and sediment yield using GIS. Hydrological Sciences Journal, 45, 771-786.

Jain, S., Kumar, S.and Varghese, J. 2001. Estimation of Soil Erosion for a Himalayan Watershed Using GIS Technique. Water Resources Management, 15, 41-54.

Jansson, M. B. 1988. A global survey of sediment yield. Geografiska Annaler. Series A. Physical Geography, 81-98.

Jiongxin, X. 2005. Precipitation–vegetation coupling and its influence on erosion on the Loess Plateau, China. CATENA, 64, 103-116.

Johanson, R.C., Imhoff, J.D., and Davis, H.H., Jr. 1980, User's manual for hydrological simulation program - Fortran (HSPF): Environmental Research Laboratory, EPA-600/9-80-015, Athens, Ga., April 1980.

Kao, S.-J.and Liu, K.-K. 1996. Particulate Organic Carbon Export from a Subtropical Mountainous River (Lanyang Hsi) in Taiwan. Limnology and Oceanography, 1749-1757.

Karydas, C., Sekuloska, T.and Silleos, G. 2009. Quantification and site-specification of the support practice factor when mapping soil erosion risk associated with olive plantations in the Mediterranean island of Crete. Environmental Monitoring and Assessment, 149, 19-28.

Kemp, D. D. 1998. The Environment Dictionary, Routledge.

Kinnell, P. I. A.and Risse, L. M. 1998. USLE-M: Empirical Modeling Rainfall Erosion through Runoff and Sediment Concentration. Soil Sci. Soc. Am. J.,

62, 1667-1672.

Kirkby, M. J., Le Bissonais, Y., Coulthard, T. J., et al. 2000. The development of land quality indicators for soil degradation by water erosion. Agriculture, Ecosystems & Environment, 81, 125-135.

Knisel, W. G., 1980. CREAMS: A Fieldscale Model for Chemical, Runoff, and Erosion from Agricultural Management Systems, USDA, Science and Education Administration, Conservation Report No. 26, Washington, D.C.

Knox, J. C. 1985. Responses of floods to Holocene climatic change in the upper Mississippi Valley. Quaternary Research, 23, 287-300.

Krishna Bahadur, K. C. 2009. Mapping soil erosion susceptibility using remote sensing and GIS: a case of the Upper Nam Wa Watershed, Nan Province, Thailand. Environmental Geology, 57, 695-705.

Laflen, J. M., Elliot, W., Flanagan, D., et al. 1997. WEPP-predicting water erosion using a process-based model. Journal of Soil and Water Conservation, 52, 96-102.

Lajczak, A., Jansson, M.B. 1993. Suspended sediment yield in the Baltic drainage basin. Nordic Hydrology 24, 31 –52.

Lancelot, C., Martin, J. M., Panin, N., et al. 2002. The North-western Black Sea: A Pilot Site to Understand the Complex Interaction Between Human Activities and the Coastal Environment. Estuarine, Coastal and Shelf Science, 54, 279-283.

Lane, L. J., Hernandez, M.and Nichols, M. 1997. Processes controlling sediment yield from watersheds as functions of spatial scale. Environmental Modelling & Software, 12, 355-369.

Le Bissonnais, Y., Cerdan, O., Lecomte, V., et al. 2005. Variability of soil surface characteristics influencing runoff and interrill erosion. CATENA, 62, 111-124.

Legates, D. R.and McCabe, G. J. 1999. Evaluating the use of “goodness-of-fit”

Measures in hydrologic and hydroclimatic model validation. Water Resources Research, 35, 233-241.

Legesse, D., Vallet-Coulomb, C.and Gasse, F. 2003. Hydrological response of a catchment to climate and land use changes in Tropical Africa: case study South Central Ethiopia. Journal of Hydrology, 275, 67-85.

Leprieur, C., Kerr, Y. H., Mastorchio, S., et al. 2000. Monitoring vegetation cover across semi-arid regions: Comparison of remote observations from various scales. International Journal of Remote Sensing, 21, 281-300.

Li, D. Q. and Yao, S. X. 1998. Theory and practice of soil and water conservat ion and sustainable development. Cartology Press of Guangdong Province, Guangzhou, China, 2-149 (in Chinese with English abstract).

Li, R., Shangguan, Z.P., Liu, B.Y., Zheng, F.L., Yang, Q.K. 2009. Advances of soil erosion research during the past 60 years in China. Science of Soil and Water Conservation 7 (5), 1-6 (in Chinese).

Lin, C. Y., Lin, W. T.and Chou, W. C. 2002. Soil erosion prediction and sediment yield estimation: the Taiwan experience. Soil and Tillage Research, 68, 143-152.

Liu, X. T., Yan, B. X. 2009. Soil erosion and food security in Northeast China. Chinese Journal of Soil and Water Conservation 1, 17-19 (in Chinese).

Liu,Y. Q. and Chen, C. M. 2007. Temporal variation of precipitation during flood season in the Pearl River Basin. Pearl River, (4), 47-51, (in Chinese).

López-Vicente, M.and Navas, A. 2010. Relating soil erosion and sediment yield to geomorphic features and erosion processes at the catchment scale in the Spanish Pre-Pyrenees. Environmental Earth Sciences, 61, 143-158.

Lu, X. X., Ashmore, P. and Wang, J. 2003. Sediment yield mapping in a large river basin: the Upper Yangtze, China. Environmental Modelling & Software, 18, 339-353.

Lu, X. X.and Higgitt, D. L. 1998. Recent changes of sediment yield in the Upper

Yangtze, China. Environmental Management, 22, 697-709.

Lu, X. X.and Higgitt, D. L. 1999. Sediment yield variability in the Upper Yangtze, China. Earth Surface Processes and Landforms, 24, 1077-1093.

Ludwig, W.and Probst, J. L. 1996. A global modelling of the climatic, morphological, and lithological control of river sediment discharges to the oceans. Erosion and Sediment Yield: Global and Regional Perspectives, 21-28.

Macklin, M. G., Benito, G., Gregory, K. J., et al. 2006. Past hydrological events reflected in the Holocene fluvial record of Europe. CATENA, 66, 145-154.

Maeda, E. E., Pellikka, P. K. E., Siljander, M., et al. 2010. Potential impacts of agricultural expansion and climate change on soil erosion in the Eastern Arc Mountains of Kenya. Geomorphology, 123, 279-289.

Manning, Z. Chen, M. Marquis, K.B. Averyt, M.Tignor and H.L. Miller (eds.) 2007. Climate Change 2007: The Physical Science Basis. Cambridge University Press, Cambridge, United Kingdom and New York, NY, USA.

Marston, R. 2008. Land, Life, and Environmental Change in Mountains. Annals of the Association of American Geographers, 98, 507-520.

Matin, M. A.and Bourque, C. P. A. 2013. Influence of Vegetation Cover on Regional Evapotranspiration in Semi-Arid Watersheds in Northwest China.

McCarney-Castle, K. 2011. Simulating anthropogenic and climatic influences on fluvial sediment load in the southeastern U.S. and Central Europe. BiblioLabsII, South Carolina.

McManus, J. n.d. Soil erosion and reservoirs, viewed 1st March, 2013. < http://www.st-andrews.ac.uk/~rab/st-a_www_files/gl3025.html>.

Meade, R. H. 1982. Sources, Sinks, and Storage of River Sediment in the Atlantic Drainage of the United States. Journal of Geology, 90, 235-252.

Meade, R. H. 1994. Suspended sediments of the modern Amazon and Orinoco rivers. Quaternary International, 21, 29-39.

Meade, R. H., T. R. Yuzyk & T. J. Day, 1990. Movement and storage of sediment in rivers of the United States and Canada. In Wolman, M. G. & H. C. Riggs (eds), The Geology of North America, Vol. 0-1. SurfaceWater Hydrology, Geological Society of America, Boulder, Colorado: 255-280.

Merritt, W. S., Letcher, R. A.and Jakeman, A. J. 2003. A review of erosion and sediment transport models. Environmental Modelling & Software, 18, 761-799.

Meybeck, M. 2001. River basin under anthropocene conditions. In: B. von Bodungen, K. Turner (eds) Science and Integrated Basin Management. Dahlem workshop series, Wiley, 307-329.

Meyer, C.and Flanagan, D. 1992. Application of case-based reasoning concepts to the WEPP soil erosion model. AI applications, 6.

Meyer, L. D., Bauer, A., Heil, R. D. 1985. Experimental Approaches for Quantifying the Effect of Soil Erosion on Productivity. In: Follett, R. F., Stewart, B. A., Ballew, I. Y., eds., Soil Erosion and Crop Productivity. American Society of Agronomy, Crop Science Society of America and Soil Science Society of America Publishers, Madison, WI, USA. 213–234

Michael, A., Schmidt, J., Enke, W., et al. 2005. Impact of expected increase in precipitation intensities on soil loss—results of comparative model simulations. CATENA, 61, 155-164.

Milliman, J. D.and Syvitski, J. P. M. 1992. Geomorphic/tectonic control of sediment discharge to the ocean: The importance of small mountainous rivers. Journal Name: Journal of Geology; (United States); Journal Volume: 100:5, Medium: X; Size: Pages: 525-544.

Ministry of Water Resources Conservancy (MWRC) 2003. Introduction to the water and soil conservation projects of the Zhujiang, viewed 1st April 2013, < http://www.mwr.gov.cn/ztbd/zjsyhy/20031209/27898.asp> (in Chinese).

Ministry of Water Resources Conservancy (MWRC) 2004. Soil and water conservation monitoring bulletin of the Zhujiang basin, viewed 1st February

2013, < http://www.pearlwater.gov.cn/ztzl/stbczt/jcjky/t20060627_14363.htm> (in Chinese).

Ministry of Water Resources Conservancy (MWRC) 2009. Bulletin of Chinese River Sediment (BCRS). Beijing: China Waterpub, viewed 1st February 2013, <http://www.mwr.gov.cn/xygb/hlnsgb/index.aspx> (in Chinese).

Mitasova, H., Hofierka, J., Zlocha, M., et al. 1996. Modelling topographic potential for erosion and deposition using GIS. International Journal of Geographical Information Systems, 10, 629-641.

Mohamed Rinos, M. H., Aggarwal, S. P. and De Silva, R.P. 1997. Application of Remote Sensing and GIS on soil erosion assessment at Bata River. Basin, India. The 18th Asian Conference on Remote Sensing, Kuala Lumpur, Malaysia, 20-24 October 1997.

Mohammad, A. G.and Adam, M. A. 2010. The impact of vegetative cover type on runoff and soil erosion under different land uses. CATENA, 81, 97-103.

Morgan, R. P. C., Martin, L.and Noble, C. A. 1987. Soil Erosion in the United Kingdom: A Case Study from Mid-Bedfordshire, Silsoe College.

Morgan, R. P. C., Morgan, D. D. V.and Finney, H. J. 1984. A predictive model for the assessment of soil erosion risk. Journal of Agricultural Engineering Research, 30, 245-253.

Morgan, R. P. C., Quinton, J. N., Smith, R. E., et al. 1998. The European Soil Erosion Model (EUROSEM): a dynamic approach for predicting sediment transport from fields and small catchments. Earth Surface Processes and Landforms, 23, 527-544.

Morgan, R. P. C.and Duzant, J. H. 2008. Modified MMF (Morgan–Morgan–Finney) model for evaluating effects of crops and vegetation cover on soil erosion. Earth Surface Processes and Landforms, 33, 90-106.

Moriasi, D., Arnold, J., Van Liew, M., et al. 2007. Model evaluation guidelines for systematic quantification of accuracy in watershed simulations. Transactions

of the ASABE, 50, 885-900.

Mukundan, R., Pradhanang, S. M., Schneiderman, E. M., et al. 2013. Suspended sediment source areas and future climate impact on soil erosion and sediment yield in a New York City water supply watershed, USA. Geomorphology, 183, 110-119.

Musy, A. 2001. Hydrology. Ecole Polytechnique Fédérale, Lausanne, Suisse.

Nash, J.and Sutcliffe, J. 1970. River flow forecasting through conceptual models part I—A discussion of principles. Journal of Hydrology, 10, 282-290.

National Aeronautics and Space Administration (NASA) n.d. Measuring Vegetation (NDVI&EVI), viewed 1st April 2013. < http://earthobservatory.nasa.gov/Features/MeasuringVegetation/measuring_vegetation_2.php>.

National Aeronautics and Space Administration (NASA), 2012. Global Land Data Assimilation System Version 1 (GLDAS-1). Retrieved from <http://disc.sci.gsfc.nasa.gov/services/grads-gds/gldas>.

National Aeronautics and Space Administration (NASA) and Japan Aerospace Exploration Agency (JAXA), 1998. Tropical Rainfall Measuring Mission Project (TRMM) Version 7. Retrieved from: <http://trmm.gsfc.nasa.gov/>.

National Bureau of Statistics of China, 2001. 2000 Chinese census, viewed 1st February 2013, <http://www.stats.gov.cn/tjgb/rkpcgb/qgrkpcgb/t20020404_16769.htm> (in Chinese).

National Bureau of Statistics of China, 2011. 2010 Chinese census, viewed 1st February 2013, < http://www.stats.gov.cn/tjgb/rkpcgb/qgrkpcgb/t20110429_402722510.htm> (in Chinese).

NEARING, #160, A., M., et al. 2004. Expected climate change impacts on soil erosion rates: A review, Ankeny, IA, ETATS-UNIS, Soil and Water Conservation Society.

NEARING, #160and A., M. 2001. Potential changes in rainfall erosivity in the U.S. with climate change during the 21[st] century, Ankeny, IA, ETATS-UNIS, Soil and Water Conservation Society.

Nearing, M. A., Romkens, M. J. M., Norton, L. D., et al. 2000. Measurements and Models of Soil Loss Rates. Science, 290, 1300-1301.

Nearing, M., Lane, L.and Lopes, V. L. 1994. Modeling soil erosion. Soil erosion research methods, 2, 127-156.

Nijssen, B., O'Donnell, G., Hamlet, A., et al. 2001. Hydrologic Sensitivity of Global Rivers to Climate Change. Climatic Change, 50, 143-175.

Novotny, V.and Chesters, G. 1989. Delivery of sediment and pollutants from nonpoint sources: A water quality perspective. Journal of Soil and Water Conservation, 44, 568-576.

Ontario Ministry of Agriculture, Food and Rural Affairs Factsheet, viewed 1st April. < http://www.omafra.gov.on.ca/english/engineer/facts/12-051.htm#t2>.

Orellana, B., Pechlivanidis, I., McIntyre, N., et al. 2008. A Toolbox for the Identification of Parsimonious Semi-Distributed Rainfall-Runoff Models: Application to the Upper Lee Catchment. In: International Congress on Environmental Modelling and Software Integrating Sciences and Information Technology for Environmental Assessment and Decision Making.

Oyedele, J. D. 1996. Effects of Erosion on the Productivity of Selected Southwestern Nigerian Soils: [Dissertaion]. Department of Soil Science, Obafemi Awolowo University, Ile-Ife, Nigeria.

Pan, M. H., Wu, Y. Q., Ren, P. P., Dong, Y. F. and Jiang, Y. 2010. Estimating soil erosion in the Dongjiang River Basin based on USLE. Journal of Natural Resources, 25 (12): 2154-2164 (in Chinese).

Pearl River Water Resources Committee (PRWRC) 1991. The Zhujiang Archive, vol. 1. Guangdong Science and Technology Press, Guangzhou (in Chinese).

Pearl River Water Resources Committee (PRWRC), n.d. Brief introduciton to the Zhujiang, viewed 1st February 2013, <http://www.pearlwater.gov.cn/zjgk/> (in Chinese).

Perrin, C., Michel, C.and Andréassian, V. 2001. Does a large number of parameters enhance model performance? Comparative assessment of common catchment model structures on 429 catchments. Journal of Hydrology, 242, 275-301.

Piégay, H., Walling, D. E., Landon, N., et al. 2004. Contemporary changes in sediment yield in an alpine mountain basin due to afforestation (the upper Dr?me in France). CATENA, 55, 183-212.

Pimentel, D.and Kounang, N. 1998. Ecology of Soil Erosion in Ecosystems. Ecosystems, 1, 416-426.

Pistocchi, A. 2008. An assessment of soil erosion and freshwater suspended solid estimates for continental-scale environmental modelling. Hydrological Processes, 22, 2292-2314.

Probst, J.-L.and Amiotte-Suchet, P. 1992. Fluvial suspended sediment transport and mechanical erosionin the Maghreb (North Africa). Hydrological Sciences Journal, 37, 621-637.

Prosser, I., Land, C., Water, et al. 2001. Constructing River Basin Sediment Budgets for the National Land and Water Resources Audit, CSIRO Land and Water.

Pruski, F. F.and Nearing, M. A. 2002. Climate-induced changes in erosion during the 21st century for eight U.S. locations. Water Resources Research, 38, 1298.

Pruski, F.F. and M.A. Nearing. 2002. Runoff and soil loss responses to changes in precipitation: a computer simulation study. Journal of Soil and Water Conservation. 57(1):7-16.

Pu, L. J., Bao, H. S., Peng, B. Z. and Higgitt, D. L. 1998. Distribution and assessment of soil and land degradation in subtropical China——A case

study of Dongxi River Basin, Fujian Province. Pedosphere, 8(3): 201-210.

Purevdorj, T. S., Tateishi, R., Ishiyama, T., et al. 1998. Relationships between percent vegetation cover and vegetation indices. International Journal of Remote Sensing, 19, 3519-3535.

Ramankutty, N., Graumlich, L., Achard, F., et al. 2006. Global Land-Cover Change: Recent Progress, Remaining Challenges. In: LAMBIN, E. & GEIST, H. (eds.) Land-Use and Land-Cover Change. Springer Berlin Heidelberg.

Renard, K. G., Foster, G. R., Weesies, G. A., et al. 1997. Predicting soil erosion by water: a guide to conservation planning with the revised universal soil loss equation (RUSLE). Agriculture Handbook (Washington).

Renfro, G. 1975. Use of erosion equations and sediment delivery ratios for predicting sediment yield. Present and prospective technology for predicting sediment yields and sources, 33-45.

Renschler, C. S., Mannaerts, C.and Diekkrüger, B. 1999. Evaluating spatial and temporal variability in soil erosion risk—rainfall erosivity and soil loss ratios in Andalusia, Spain. CATENA, 34, 209-225.

Reuter, H. I., Nelson, A.and Jarvis, A. 2007. An evaluation of void‐filling interpolation methods for SRTM data. International Journal of Geographical Information Science, 21, 983-1008.

Rompaey, A., Krasa, J., Dostal, T., et al. 2003. Modelling sediment supply to rivers and reservoirs in Eastern Europe during and after the collectivisation period. In: KRONVANG, B. (ed.) The Interactions between Sediments and Water. Springer Netherlands.

Ruddiman, W. 2003. The Anthropogenic Greenhouse Era Began Thousands of Years Ago. Climatic Change, 61, 261-293.

Saavedra, C.P. and Mannaerts, C.M, 2005. Comparison of sediment delivery ratio concepts for medium - sized catchments in the Bolivian Andes: abstract. In:

EGU 2005 : European Geosciences Union : general assembly abstract book, Vienna, Austria, 24-29 April 2005. Geophysical Research Abstracts, 7(2005)09140,1.

Schmidt, J. 1991. A mathematical Model to Simulate Rainfall Erosion. Catena Supplement, Vol. 19, pp. 101-109.

Sharma, A., Tiwari, K.and Bhadoria, P. B. S. 2011. Effect of land use land cover change on soil erosion potential in an agricultural watershed. Environmental Monitoring and Assessment, 173, 789-801.

Shen, H. J. and Wang, Y. Y, 2004. Preliminary analysis on the major sources, spatial and temporal variation of sediment in the Pearl River. Pearl River, 2:39-42 (in Chinese).

Shrestha, D. P. 1997. Assessment of soil erosion in the Nepalese Himalaya: a case study in Likhu Khola Valley, Middle Mountain Region. Land Husbandry, 2, 59-80.

Smith, P., Maidment, D. 1995. Hydrologic Data Development System, in CRWR Online Report 95-1. Center for Research in Water Resources, University of Texas.

Smith, R., Goodrich, D., Woolhiser, D., et al. 1995. KINEROS-A kinematic runoff and erosion model. Computer models of watershed hydrology., 697-732.

Stone, R. P., and Hilborn, D. 2000. Universal Soil Loss Equation (USLE),

Sun, X. X., Zhang, J. X. and Liu, Z. J. 2008. Vegetation cover annual changes based on MODIS/TERRA NDVI in the three gorges reservoir area. The International Archives of the Photogrammetry, Remote Sensing and Spatial Information Sciences, Vol.XXXVII. Part B7, Beijing, 2008.

Syvitski, J. P. M. 2003. Supply and flux of sediment along hydrological pathways: research for the 21st century. Global and Planetary Change, 39, 1-11.

Syvitski, J. P. M., Peckham, S. D., Hilberman, R., et al. 2003. Predicting the

terrestrial flux of sediment to the global ocean: a planetary perspective. Sedimentary Geology, 162, 5-24.

Syvitski, J. P. M., Vörösmarty, C. J., Kettner, A. J., et al. 2005. Impact of Humans on the Flux of Terrestrial Sediment to the Global Coastal Ocean. Science, 308, 376-380.

Syvitski, J. P. M.and Saito, Y. 2007. Morphodynamics of deltas under the influence of humans. Global and Planetary Change, 57, 261-282.

Thornes, J. 1985. The ecology of erosion. Geography, 70, 222-235.

Thornes, J. B. 1990. The interaction of erosional and vegetational dynamics in land degradation: spatial outcomes. Vegetation and erosion. Processes and environments., 41-53.

Tian, Y. C., Zhou, Y. M., Wu, B. F., et al. 2009. Risk assessment of water soil erosion in upper basin of Miyun Reservoir, Beijing, China. Environmental Geology, 57, 937-942.

Tim, U. 1996. Emerging technologies for hydrologic and water quality modeling research. Transactions of the ASAE, 39, 465-476.

Trimble, S. W. 1999. Decreased Rates of Alluvial Sediment Storage in the Coon Creek Basin, Wisconsin, 1975-93. Science, 285, 1244-1246.

Trimble, S. W.and Crosson, P. 2000. U.S. Soil Erosion Rates--Myth and Reality. Science, 289, 248-250.

ts06f/ts06f-anh-3671.pdf >.

Tucker, C. J. 1979. Red and photographic infrared linear combinations for monitoring vegetation. Remote Sensing of Environment, 8, 127-150.

Tucker, C. J., Pinzon, J. E., Brown, M. E., et al. 2005. An extended AVHRR 8 - km NDVI dataset compatible with MODIS and SPOT vegetation NDVI data. International Journal of Remote Sensing, 26, 4485-4498.

Tucker, C.J., Pinzon, J.E. and Brown, M.E. 2004. Global Inventory Modeling and Mapping Studies, NA94apr15b.n11-VIg, 2.0, Global Land Cover Facility,

University of Maryland, College Park, Maryland, Aril May 1994.

UCLouvain team and ESA team, 2010. GlobCover 2009 (Global Land Cover Map). Retrieved from: < http://due.esrin.esa.int/globcover/>.

UNESCO-IHE Institute for Water Education, n.d. Rainfall runoff modeling, viewed 1st March 2013. < http://www.ihe.nl/Flood-Management-Education-Platform/Flood-Modelling-for-Management2/3.1-Rainfall-Runoff-Modelling >

University Of Michigan, 4 November 2004. People Cause More Soil Erosion Than All Natural Processes. Science Daily, viewed 3rd April 2013, <http://www.sciencedaily.com- /releases/2004/11/041103234736.htm>.

USGS, 2008. SRTM 90m Digital Elevation Database v4.1. Retrieved from: <http://glovis.usgs.gov/>.

van Lieshout, A., n.d. Chapter 12: Erosion modeling, viewed 1st March 2013. < ftp://ftp.itc.nl/pub/ilwis/pdf/appch12.pdf>.

Van Oost, K., Govers, G.and Desmet, P. 2000. Evaluating the effects of changes in landscape structure on soil erosion by water and tillage. Landscape Ecology, 15, 577-589.

Vanoni, V. A. 2006. Sedimentation Engineering, ASCE, American Society of Civil Engineers.

Vcrstraeten, G., Poesen, J. 1999. The nature of small-scale flooding, muddy floods and retention pond sedimentation in central Belgium. Geomorphology. 29,275-292.

Veihmeyer, F.and Hendrickson, A. 1931. The moisture equivalent as a measure of the field capacity of soils. Soil Science, 32, 181-194.

Vieux, B. E. 2003. Review of Mathematical Models of Large Watershed Hydrology by Vijay P. Singh and Donald K. Prevert. Journal of Hydraulic Engineering, 130, 89-90.

Viney, N. R.and Sivapalan, M. 1999. A conceptual model of sediment transport:

application to the Avon River Basin in Western Australia. Hydrological Processes, 13, 727-743.

Wall, G. J., Coote, D. R., Pringle E. A. and Shelton, I. J.1997. RUSLEFAC — Revised Universal Soil Loss Equation for Application in Canada: A Handbook for Estimating Soil Loss from Water Erosion in Canada. Research Branch, Agriculture and Agri-Food Canada. Ottawa.

Walling, D. E, Webb, B. W. 1996. Erosion and sediment yield: a global overview In Erosion and Sediment Yield: Global and Regional Perspectives, edited by D. E. Walling and B. W. Webb, IAHS Publ., 236, 76-84.

Walling, D. E. 1983. The sediment delivery problem. Journal of Hydrology, 65, 209-237.

Walling, D. E. 1988. Erosion and sediment yield research — Some recent perspectives. Journal of Hydrology, 100, 113-141.

Walling, D. E. 1999. Linking land use, erosion and sediment yields in river basins. Hydrobiologia, 410, 223-240.

Walling, D. E. 2006. Human impact on land–ocean sediment transfer by the world's rivers. Geomorphology, 79, 192-216.

Wan, Y., Han, T. D., Duan, C. Q., Shi, Z. T., Si, T. Q. and Wang, J. P. 2005. Soil-water loss subareas and regional characteristics and development in Yunnan Province. Journal of Desert Research, 25 (3): 442-447 (in Chinese).

Wang, G., Jiang, H., Xu, Z., et al. 2012. Evaluating the effect of land use changes on soil erosion and sediment yield using a grid-based distributed modelling approach. Hydrological Processes, n/a-n/a.

Wang, J. J., Lu, X. X.and Zhou, Y. 2007. Retrieval of suspended sediment concentrations in the turbid water of the Upper Yangtze River using Landsat ETM. Chinese Science Bulletin, 52, 273-280.

Wei, W., Chen, L., Fu, B., et al. 2009. Responses of water erosion to rainfall extremes and vegetation types in a loess semiarid hilly area, NW China.

Hydrological Processes, 23, 1780-1791.

Wei, X., Shen, C., Li, N., et al. 2010. Apparent ages of suspended sediment and soil erosion of the Pearl River (Zhujiang) drainage basin. Chinese Science Bulletin, 55, 1547-1553.

Wei, X. and Wang, F. 2006. Riverine carbon fluxes and soil erosion in the Zhujiang (Pearl) River Drainage Basin, South China. Chinese Journal of Geochemistry, 25, 276-276.

Wei, X. G. 2003. Study on riverine carbon flux and erosion of Zhujiang (Pearl) river drainage basin. PhD thesis, Chinese Academy of Science, Beijing.

Weng, Q. 2002. Land use change analysis in the Zhujiang Delta of China using satellite remote sensing, GIS and stochastic modelling. Journal of Environmental Management, 64, 273-284.

Wheater, H. S. 2002. Progress in and prospects for fluvial flood modelling. Philosophical Transactions of the Royal Society of London. Series A:

Wheater, H. S., Jakeman, A. J.and Beven, K. J. 1993. Progress and directions in rainfall-runoff modelling. In: JAKEMAN, A. J., BECK, M. B. & MCALLEN, M. J. (eds.) Modelling Change in Environmental Systems. John Wiley.

Wilkinson, B. H.and McElroy, B. J. 2007. The impact of humans on continental erosion and sedimentation. Geological Society of America Bulletin, 119, 140-156.

Williams, J. R. 1975. Sediment-yield prediction with universal equation using runoff energy factor. Present and prospective technology for predicting sediment yields and sources, 40, 244-252.

Wischmeier, W.and Smith, D. 1978. Predicting rainfall erosion losses: a guide to conservation planning. Agriculture handbook USDA (

Withers, B.and Vipond, S. 1974. Irrigation: design and practice, BT Batsford Ltd.

Wolman, M. G.and Schick, A. P. 1967. Effects of construction on fluvial

sediment, urban and suburban areas of Maryland. Water Resources Research, 3, 451-464.

Woolhiser, D.A., Smith, R.E. and Goodrich, D.C. 1990. KINEROS, A Kinematic Runoff and Erosion Model: Documentation and User Manual. U.S. Department of Agriculture, Agricultural Research Service, ARS-77, 130.

Xia, H. P. 1999. Study on the floods, soil erosion and reforestation project of the Yangtze basin and Zhujiang basin. Tropical Geography, 19, 124-129.

Xu, Y. Q., Shao, X. M., Kong, X. B., et al. 2008. Adapting the RUSLE and GIS to model soil erosion risk in a mountains karst watershed, Guizhou Province, China. Environmental Monitoring and Assessment, 141, 275-286.

Xu, Z.and Liu, C. Q. 2007. Chemical weathering in the upper reaches of Xijiang River draining the Yunnan–Guizhou Plateau, Southwest China. Chemical Geology, 239, 83-95.

Yan, B., Fang, N. F., Zhang, P. C., et al. 2013. Impacts of land use change on watershed streamflow and sediment yield: An assessment using hydrologic modelling and partial least squares regression. Journal of Hydrology, 484, 26-37.

Yang, A., Wang, H., Tang, K., et al. 2002. Soil erosion characteristics and control measures in China. In: Proceedings of 12th International Soil Conservation Organization Conference, 26-31.

Yang, D., Kanae, S., Oki, T., et al. 2003. Global potential soil erosion with reference to land use and climate changes. Hydrological Processes, 17, 2913-2928.

Yang, M., Li, X. Z., Hu, Y. M., et al. 2012. Assessing effects of landscape pattern on sediment yield using sediment delivery distributed model and a landscape indicator. Ecological Indicators, 22, 38-52.

Yazidhi, B. 2003. A comparative study of soil erosion modelling in Lom Kao-Phetchabun, Thailand. M.Sc. thesis, ITC, Enschede.

Young, R.A., Onstad, C.A., Bosch, D.D. and Anderson, W.P. 1987. AGNPS: Agricultural Non-Point Source pollution model: A large watershed analysis tool. USDA, ARS Conservation Research Report, 35: 77.

Yuan, D.X. 1997. Rock desertification in the subtropical karst of south China, viewed 1st May 2013. < http://www.karst.edu.cn/desert/rockdesert.htm>.

Zhang, L., O'Neill, A. L.and Lacey, S. 1996. Modelling approaches to the prediction of soil erosion in catchments. Environmental Software, 11, 123-133.

Zhang, Q., Xu, C.-Y., Chen, X., et al. 2012. Abrupt changes in the discharge and sediment load of the Pearl River, China. Hydrological Processes, 26, 1495-1508.

Zhang, S. 1999. Analysis on benefits of soil-water conservation in The middle reaches of the Yellow River. Huanghe Press, Zhengzhou (in Chinese).

Zhang, S. R., Lu, X. X., Higgitt, D. L., et al. 2007. Water chemistry of the Zhujiang (Pearl River): Natural processes and anthropogenic influences. Journal of Geophysical Research-Earth Surface, 112.

Zhang, S. R., Lu, X. X., Higgitt, D. L., et al. 2008. Recent changes of water discharge and sediment load in the Zhujiang (Pearl River) Basin, China. Global and Planetary Change, 60, 365-380.

Zhang, X. C.and Nearing, M. A. 2005. Impact of climate change on soil erosion, runoff, and wheat productivity in central Oklahoma. CATENA, 61, 185-195.

Zhang, X. J. and Yang, D. S., 2009. Analysis of the reasons for the rock-desertification and the countermeasures in the upper Zhujiang river. Proceedings of the 13th Cross-Strait Water Resources Conference. Taizhong, 23-24 November 2009.

Zhang, X., Drake, N.and Wainwright, J. 2002. Scaling land surface parameters for global-scale soil erosion estimation. Water Resources Research, 38, 1180.

Zhao, W., Jiao, E., Wang, M.G., and Meng, X. 1992. Analysis on the variation of

sediment yield in the Sanchuanhe river basin in the 1980s. International Journal of Sediment Research 7:1-19.

Zhu, Y. M. 2007. The Impact of climate change & human activity on water, Ph.D. thesis, National University of Singapore, Singapore.

Zhu, Z. 1990. Hydrogenic sediments–paleosol sequences and climatic-tectonic cycles. Loess Quaternary Geological Globbal Change 1:62–70 (in Chinese).

Zhuo, L. 1993. The effects of forest in controlling gully erosion. Journal of Sediment Research, 1, 2.